

**CORRELATION BETWEEN MERCURY INJECTION AND  
CENTRIFUGE CAPILLARY PRESSURE  
MEASUREMENT FOR SANDSTONES**

**by**

**Mabkhout Al-Dousari**

ARTHUR LAKES LIBRARY  
COLORADO SCHOOL OF MINES  
GOLDEN, CO 80401

ProQuest Number: 10794430

All rights reserved

INFORMATION TO ALL USERS

The quality of this reproduction is dependent upon the quality of the copy submitted.

In the unlikely event that the author did not send a complete manuscript and there are missing pages, these will be noted. Also, if material had to be removed, a note will indicate the deletion.



ProQuest 10794430

Published by ProQuest LLC (2018). Copyright of the Dissertation is held by the Author.

All rights reserved.

This work is protected against unauthorized copying under Title 17, United States Code  
Microform Edition © ProQuest LLC.

ProQuest LLC.  
789 East Eisenhower Parkway  
P.O. Box 1346  
Ann Arbor, MI 48106 – 1346

A thesis submitted to the Faculty and Board of Trustees of the Colorado School of Mines in partial fulfillment of the requirement for the degree of Master of Science (Petroleum Engineering).

Golden, Colorado

Date 27<sup>th</sup> April 1999

Signed: Mabkhout AL-Dousari  
Mabkhout M. AL-Dousari

Approved: Ramona M. Graves  
Dr. Ramona M. Graves  
Thesis Advisor

Golden, Colorado

Date April 27, 1999

Craig W. Van Kirk  
Dr. Craig W. Van Kirk  
Professor and Head,  
Department of  
Petroleum Engineering

## ABSTRACT

Controversy surrounds the development of a usable correlation between mercury injection and centrifuge capillary pressure measurements. The centrifuge method uses an oil-water system, while the mercury injection method uses mercury and nitrogen. In this research, an empirical correlation was developed that adapts curves produced by the mercury injection (gas-mercury) method to centrifuge (liquid-liquid). The correlation was achieved by using the same sandstone plugs for both measurement methods. To yield reliable data, careful core preparation was a priority in this research.

Twelve cylindrical sandstone plugs were prepared for capillary pressure measurement. The plugs were fired at 800°C. Permeability and porosity were measured using the Pressure Decay Profile Permeameter (PDPK) and the Core Measurement System (CMS-300). Centrifuge experiments were performed first, due to the destructive nature of the mercury injection method. Plugs were carefully cleaned between the two sets of experiments.

An appropriate firing procedure was devised for this research. It was found that firing the plugs at temperatures up to 800°C and using a step function over seven hours

was appropriate for stabilizing the plug matrix. This procedure was needed to insure consistency of properties in both tests.

It was concluded that a capillary pressure curve obtained by the mercury injection method can be corrected to represent curves produced from centrifuge measurement.

The correlation is as follows:

- Divide the pressure from mercury injection curve by 48.
- Increase the saturation for the mercury injection curve by 8 units.

The above procedure gave a close match with a low percentage error in the empirical correlation. The average percent error was 1.6. Capillary pressure curves from mercury injection need to be transformed to curves from centrifuge since the centrifuge is more representative of the reservoir fluid.

## TABLE OF CONTENTS

ABSTRACT .....	iii
LIST OF FIGURES .....	viii
LIST OF TABLES .....	xii
ACKNOWLEDGMENT .....	xiv
Chapter 1. INTRODUCTION .....	1
Chapter 2. LITERATURE REVIEW .....	4
2.1 The Meaning and Importance of Capillary Pressure .....	4
2.2 Historical Background .....	7
2.3 Forces Between Rock-Fluid and Fluid-Fluid .....	8
2.3.1 Wettability .....	8
2.3.2 Interfacial Tension .....	9
2.4 Effect of Firing on Rock Properties .....	9
2.5 Mercury Injection Method .....	11
2.6 Centrifuge Method .....	12
2.7 Previous Investigation on Conversion Factor .....	12
Chapter 3. EXPERIMENTAL PROCEDURE .....	16
3.1 Core Preparation .....	16

3.2 Firing Procedure .....	19
3.3 Centrifuge Method .....	20
3.4 Mercury Injection Method .....	24
3.4.1 Calibration of Mercury Injection Apparatus ...	24
3.4.2 Capillary Pressure Measurement .....	26
Chapter 4. RESULTS and DISCUSSION .....	30
4.1 Centrifuge Method .....	30
4.2 Mercury Injection Method .....	31
4.3 Capillary Pressure Correlation .....	33
4.4 Error in Correlation .....	49
4.5 Validation of Conversion Method .....	52
Chapter 5. CONCLUSIONS and RECOMMENDATIONS .....	54
5.1 Conclusions .....	54
5.2 Recommendations .....	55
NOMENCLATURE .....	56
REFERENCES .....	59
APPENDICES .....	62
Appendix A: Calculation Procedure for Centrifuge Method .....	60
Appendix B: Centrifuge Raw Data .....	73
Appendix C: Capillary Pressure Curve from Centrifuge and Mercury Injection .....	80

Appendix D: Correlation Attempts .....	105
Appendix E: Accuracy Plots .....	118

## LIST OF FIGURE

Figure Number	Page
3.1.1 Comparative Study Between Twin Plugs .....	18
3.3.1 Simplified Centrifuge Schematic .....	20
3.4.1 Capillary Pressure Cell for Mercury Injection .....	25
3.4.2 Mercury Injection Calibration Curve .....	27
3.4.3 Permeability Comparisons Before and After Centrifuge .....	28
4.3.1 Centrifuge and Mercury Injection Correlation for Plug K1 .....	37
4.3.2 Centrifuge and Mercury Injection Correlation for Plug K3 .....	38
4.3.3 Centrifuge and Mercury Injection Correlation for Plug K4 .....	39
4.3.4 Centrifuge and Mercury Injection Correlation for Plug K5 .....	40
4.3.5 Centrifuge and Mercury Injection Correlation for Plug K6 .....	41
4.3.6 Centrifuge and Mercury Injection Correlation for Plug K9 .....	42
4.3.7 Centrifuge and Mercury Injection Correlation for Plug K10 .....	43
4.3.8 Centrifuge and Mercury Injection Correlation for Plug K13 .....	44
4.3.9 Centrifuge and Mercury Injection Correlation for Plug K14 .....	45
4.3.10 Centrifuge and Mercury Injection Correlation for Plug K15 .....	46
4.3.11 Centrifuge and Mercury Injection Correlation for Plug K16 .....	47
4.3.12 Centrifuge and Mercury Injection Correlation for Plug K17 .....	48

4.4.1	Correlation Error Plot for all Plugs excluding K9, K14, and K15 .....	50
4.4.2	Correlation Error Plot for all Plugs .....	51
4.5.1	Samples of Capillary Pressure Comparisons from Sabatiers (1994) .....	53
C-1	Centrifuge Capillary Pressure Curve for Plug K1 .....	81
C-2	Centrifuge Capillary Pressure Curve for Plug K3 .....	82
C-3	Centrifuge Capillary Pressure Curve for Plug K4 .....	83
C-4	Centrifuge Capillary Pressure Curve for Plug K5 .....	84
C-5	Centrifuge Capillary Pressure Curve for Plug K6 .....	85
C-6	Centrifuge Capillary Pressure Curve for Plug K9 .....	86
C-7	Centrifuge Capillary Pressure Curve for Plug K10 .....	87
C-8	Centrifuge Capillary Pressure Curve for Plug K13 .....	88
C-9	Centrifuge Capillary Pressure Curve for Plug K14 .....	89
C-10	Centrifuge Capillary Pressure Curve for Plug K15 .....	90
C-11	Centrifuge Capillary Pressure Curve for Plug K16 .....	91
C-12	Centrifuge Capillary Pressure Curve for Plug K17 .....	92
C-13	Mercury Injection Capillary Pressure Curve for Plug K1 .....	93
C-14	Mercury Injection Capillary Pressure Curve for Plug K3 .....	94
C-15	Mercury Injection Capillary Pressure Curve for Plug K4 .....	95
C-16	Mercury Injection Capillary Pressure Curve for Plug K5 .....	96
C-17	Mercury Injection Capillary Pressure Curve for Plug K6 .....	97
C-18	Mercury Injection Capillary Pressure Curve for Plug K9 .....	98

C-19	Mercury Injection Capillary Pressure Curve for Plug K10 .....	99
C-20	Mercury Injection Capillary Pressure Curve for Plug K13 .....	100
C-21	Mercury Injection Capillary Pressure Curve for Plug K14 .....	101
C-22	Mercury Injection Capillary Pressure Curve for Plug K15 .....	102
C-23	Mercury Injection Capillary Pressure Curve for Plug K16 .....	103
C-24	Mercury Injection Capillary Pressure Curve for Plug K17 .....	104
D-1	Sample K1 Testing Conversion Factor 8.7 .....	106
D-2	Sample K3 Testing Conversion Factor 8.7 .....	106
D-3	Sample K4 Testing Conversion Factor 8.7 .....	107
D-4	Sample K5 Testing Conversion Factor 8.7 .....	107
D-5	Sample K6 Testing Conversion Factor 8.7 .....	108
D-6	Sample K9 Testing Conversion Factor 8.7 .....	108
D-7	Sample K10 Testing Conversion Factor 8.7 .....	109
D-8	Sample K13 Testing Conversion Factor 8.7 .....	109
D-9	Sample K14 Testing Conversion Factor 8.7 .....	110
D-10	Sample K15 Testing Conversion Factor 8.7 .....	110
D-11	Sample K16 Testing Conversion Factor 8.7 .....	111
D-12	Sample K17 Testing Conversion Factor 8.7 .....	111
D-13	Sample K1 Testing Conversion Factor 14.1 .....	112
D-14	Sample K3 Testing Conversion Factor 14.1 .....	112
D-15	Sample K4 Testing Conversion Factor 14.1 .....	113

D-16	Sample K5 Testing Conversion Factor 14.1 .....	113
D-17	Sample K6 Testing Conversion Factor 14.1 .....	114
D-18	Sample K9 Testing Conversion Factor 14.1 .....	114
D-19	Sample K10 Testing Conversion Factor 14.1 .....	115
D-20	Sample K13 Testing Conversion Factor 14.1 .....	115
D-21	Sample K14 Testing Conversion Factor 14.1 .....	116
D-22	Sample K15 Testing Conversion Factor 14.1 .....	116
D-23	Sample K16 Testing Conversion Factor 14.1 .....	117
D-24	Sample K17 Testing Conversion Factor 14.1 .....	117
E-1	Accuracy Plots at 2.5 psi Excluding Plugs K9, K14 and K15 .....	119
E-2	Accuracy Plots at 5 psi Excluding Plugs K9, K14 and K15 .....	120
E-3	Accuracy Plots at 10 psi Excluding Plugs K9, K14 and K15 .....	121
E-4	Accuracy Plots at 15 psi Excluding Plugs K9, K14 and K15 .....	122
E-5	Accuracy Plots at all Pressures .....	123
E-6	Accuracy Plots at 2.5 psi Including all Plugs .....	124
E-7	Accuracy Plots at 5 psi Including all Plugs .....	125
E-8	Accuracy Plots at 10 psi Including all Plugs .....	126
E-9	Accuracy Plots at 15 psi Including all Plugs .....	127
E-10	Accuracy Plots at all Pressure Including all Plugs .....	128

## LIST OF TABLES

Table Number	Page
3.1.1 Plug Dimensions Permitted by Each Apparatus .....	17
3.3.1 Plugs Data at the Start of Centrifuge Experiments .....	22
3.4.1 Volume of Brine Displaced by Oil During Centrifuge in (cc) .....	29
4.2.1 Entry Pressure and $Sw_i$ for Mercury Injection .....	32
4.3.1 Interfacial Tension and Contact Angles .....	34
B-1 Centrifuge Raw Data for Sample K1 .....	68
B-2 Centrifuge Raw Data for Sample K3 .....	69
B-3 Centrifuge Raw Data for Sample K4 .....	70
B-4 Centrifuge Raw Data for Sample K5 .....	71
B-5 Centrifuge Raw Data for Sample K6 .....	72
B-6 Centrifuge Raw Data for Sample K9 .....	73
B-7 Centrifuge Raw Data for Sample K10 .....	74
B-8 Centrifuge Raw Data for Sample K13 .....	75
B-9 Centrifuge Raw Data for Sample K14 .....	76
B-10 Centrifuge Raw Data for Sample K15 .....	77
B-11 Centrifuge Raw Data for Sample K16 .....	78

B-12 Centrifuge Raw Data for Sample K17 ..... 79

## ACKNOWLEDGMENT

I would like to thank my thesis advisor, Professor Ramona M. Graves, and the members of this thesis committee, Professor Robert S. Thompson and Professor Mark G. Miller for their support. I would like to acknowledge the help of Dr. Graves. She gave me the motivation to research this thesis.

Gratitude is extended to the industry support of centrifuge experimentation from Marathon Oil Company of Littleton, Colorado, especially Dr. Teresa Monger-McClure for approving the work. Also, special thanks for Hiemi K. Haines and Gary R. Kennedy for performing the centrifugal experimental work. My greatest appreciation to my employer, Kuwait University, for its scholarship and financial support throughout my study.

Special thanks goes to my family, for their support and continuous inspiration.

## CHAPTER 1

### INTRODUCTION

“Two or more immiscible fluids in a porous media, such as reservoir rock, give rise to capillary forces. Because of the interfacial tension existing at the boundary between the fluids, the interface is curved and there is a pressure difference across the interface. This pressure difference is called capillary pressure” (Brown, 1951).

Although the absolute magnitude of the capillary pressure in most petroleum reservoirs is usually not large, the effects are extremely important. Together with gravity, it controls the original distribution of the fluid saturation within the reservoir; particularly the distribution of connate water. By virtue of capillary pressure and gravity effects on the shapes of the fluid interfaces within the pore spaces, they control in large measure the relative freedom of movement of the fluid present in the reservoir. They are important factors in influencing the behavior of fluids in the production processes. Capillary curves are valuable aids for exploration and development. In exploration programs the data can be used to upgrade prospects or define areas for further exploratory efforts. Capillary pressure curves are necessary to reservoir simulation and enhanced oil recovery.

There are many methods used to measure capillary pressure. This research considered the mercury injection method and the centrifugation method. Mercury injection method was developed by Purcell in 1949. It is a rapid and reliable test which uses mercury and nitrogen to obtain capillary pressure curves. Mercury injection is a destructive test and does not use reservoir fluids. Hassler and Brunner (1944) presented the centrifuge technique. Although it takes several days to produce a complete curve, it has the capability of using reservoir fluids to obtain capillary pressure curves.

In this thesis a correlation was developed to convert measurements taken by mercury injection to measurements taken with the centrifuge.

Sandstone cores were used because of their less complex structure and to avoid changes in the matrix structure due to drying of the cores, which can occur in limestone. The cores have different ranges of permeability, from a few millidarcies up to one darcy. A technique was devised to restore cores to their original state after the centrifuge test, making sure to not alter the core pore structure. Next, the mercury injection method was used to obtain capillary pressure curves. Finally, a correlation relating the capillary pressure and the fluid saturation between the two methods was developed.

The correlation developed converts between gas-liquid system (mercury injection) and liquid-liquid system (centrifuge). The correlation makes it possible to convert from the mercury injection method, which has the advantages of rapid data collection and the

capability of using irregular shape samples, to the reliable more realistic centrifuge method.

A literature review and previous investigation are in Chapter 2. Procedures for preparing the cores and operating the different apparatus used are in Chapter 3. Result and discussion are found in Chapter 4. Chapter 4 also contains the method of conversion devised in this work. Conclusions and recommendations for future work can be found in Chapter 5. Raw data and calculation procedures for centrifuge can be found in Appendices A and B respectively. Capillary pressure curves from both methods can be found in Appendix C. Appendix D includes the various conversion factors attempted.

## CHAPTER 2

### LITERATURE REVIEW

#### 2.1 The Meaning and Importance of Capillary Pressure

Two or more immiscible fluids in a porous media, such as reservoir rock, give rise to capillary forces. Because of the interfacial tension existing at the boundary between the fluids, the interference is curved, and there is a pressure difference across the interface. This pressure difference is called capillary pressure and can be defined as:

$$P_c = P_{oil} - P_{water}$$

Alternately, capillary pressure can also be defined in a generalized expression as:

$$P_c = \frac{2\sigma \cos \theta}{r}$$

where  $\sigma$  is the interfacial tension of the system,  $\theta$  is the contact angle and  $r$  is the average pore throat radius for a capillary tube model.

The magnitude of the capillary pressure between two immiscible fluids that together fill a porous medium depends upon several factors. From various papers and the Advance Rock and Fluid Properties (508) class by Dr. Graves (1996), the following were found to be the affecting factors:

1. Textural properties of the medium,
2. Wettability of the medium,
3. Interfacial tension between the fluids,
4. Fluid densities,
5. Respective saturation of the fluids,
6. Manner in which these saturation were attained,
7. Hysteresis.

For a given pair of immiscible fluids in a particular sample of the reservoir rock, the capillary pressure is a unique function of the fluid saturation, provided the saturation of the fluid which wets the rock has previously been decreased unidirectionally from an initially complete saturation. Similarly, for a given pair of fluids at a particular saturation that has been achieved by a previous decrease of saturation of the wetting fluid, the capillary pressure depends upon the textural properties and wettability of the reservoir rock.

Although the absolute magnitude of the capillary pressure in most petroleum reservoirs is usually not large, the effects are extremely important. Together with gravity, it controls the original distribution of the fluid saturation within the reservoir, particularly the distribution of connate water. By virtue of their effects on the shapes of the fluid interfaces within the pore spaces, they control the relative freedom of movement of fluid present in the reservoir and are important factors in influencing the behavior and distribution of fluids in the production processes.

Capillary curves are valuable aids for exploration and development. In exploration programs the data can be used to upgrade prospects or define area for further exploratory efforts. Regional studies on values calculated from capillary pressure, like pore-throat sorting (PTS) and reservoir grade (RG) (Jennings 1987), can be constructed in much the same fashion as stratigraphic studies and can be integrated into geological, geophysical and engineering models. Pore throat sorting (PTS) is a number that measure the sorting of the pore throats within a rock sample. The number ranges from 1.0 (perfect sorting) to 8.0 (essentially no sorting). Reservoir grade (RG) indicates the reservoir quality of a rock and ranges from 0 (best quality) to 100 (lowest quality). For field development, capillary pressure data can be used to locate economic oil-water contacts, to calculate oil columns, or to determine if reservoir tilting is a function of hydrodynamics, capillary pressure, or both. Stratigraphic traps are significantly influenced by capillary pressure, and understanding the concept of a capillary pressure release valve can help

exploit this type of traps. With the increasing interest in enhanced recovery programs, capillary pressure derived from permeability can provide an inexpensive yet valuable source of data.

## **2.2 Historical Background.**

In 1941, Leverett introduced the concept of capillary pressure for oil industry use and presented general concepts on capillarity in porous media that are still used today. He also proposed a dimensionless capillary pressure function, the "Leverett J Function", as a method for normalizing capillary pressure data for porous media with similar lithology. Leverett did his experiments by measuring water drainage from columns of unconsolidated sands. A number of other, more convenient, techniques for measuring drainage capillary pressures have been proposed since Leverett's initial work. Hassler and Brunner (1944) presented the centrifuge technique and a methodology for converting the average saturation to the saturation at a given position in the core. McCullough (1944) developed the porous-plate technique. Purcell (1949) presented the mercury-injection technique as another method for rapidly obtaining drainage capillary pressure data. Brown (1951) proposed a dynamic capillary pressure measurement technique, while

Calhoun (1949) reported on a vapor-pressure-lowering technique for measurements at high capillary pressures.

The centrifuge, mercury-injection, and porous-plate techniques are now the most commonly used. For this research, only the mercury injection method and the centrifuge method were used.

### **2.3 Forces Between Rock-Fluid and Fluid-Fluid**

There are many factors that could influence the capillary pressure within the rock. The following section details the rock fluid forces of wettability and interfacial tension.

#### **2.3.1 Wettability**

Surface forces, or wetting, are defined as the tendency of one fluid to spread or adhere to a solid surface in the presence of other immiscible fluids. If the oil/brine/solid system is water wet, water will occupy the small pores and spread or adhere to the majority of the solid surface. In an oil wet system, the oil occupies the small pores and contacts the majority of the rock surface. The solid surface in petroleum systems is reservoir rock. Since wettability is of a varying degree, firing the cores will insure a strongly water wet system

### **2.3.2 Interfacial Tension**

Interfacial tension (IFT) is a fundamental thermodynamic property of a fluid-fluid interface. Interfaces in a porous hydrocarbon reservoir occur when two immiscible fluids, water and oil, are put in contact with one another. A region of limited solubility will exist between the two phases. A water molecule at the oil-water interface has a force acting on it from the overlaying oil molecule as well as the force from the underlying water molecules. The interface forces are unbalanced and are termed “interfacial tension”. The lower the IFT, the more miscible the two fluids become. The IFT is high for a typical water/oil reservoir. This results in a high capillary pressure.

### **2.4 Effect of Firing on Rock Properties**

In research studies, consistent core properties are essential to the analysis and interpretation of experimental results. Core samples that are used in experiments are often fired at high temperatures to ensure strongly water wet mineral surfaces by burning off organic contaminants and by stabilizing clay minerals to reduce clay swelling and fine migration.

Prior to firing, a core must be cleaned. This is the first step in restoring wettability of the cores. In the case of reservoir cores, this would mean cleaning drilling and completion fluids from the pore spaces. Core cleaning is an important part of this research since cores will be subjected to different experiments. Al-Lawati (1995) performed extensive core cleaning and firing experiments on Berea sandstone samples with a range of permeabilities and concluded that cleaning the cores for 24 hours in a toluene extractor before firing gave the best repeatability of results.

Ma and Morrow (1991) presented an important petrological and petrophysical analysis of the effect of firing on physical properties of Berea sandstone. They concluded that firing causes complex effects on core samples including damage to mineral structure, permanent thermal expansion, increased core friability, and cracking due to thermal stress. Above  $400^{\circ}\text{C}$  ( $752^{\circ}\text{F}$ ), Berea core weight decreased, and porosity, permeability, and bulk volume increased. They recommended for their samples a firing temperature of  $800^{\circ}\text{C}$  ( $1472^{\circ}\text{F}$ ) and a firing time of six hours. It was noted that firing temperature had a much stronger influence on Berea core samples than firing time.

Al-Lawati (1995) presented an optimal firing procedure for Berea cores with permeabilities ranging from 300 to 1910 md. An unidentified low permeability sandstone also showed optimal test repeatability. The procedure consisted of firing cores to  $500^{\circ}\text{C}$  ( $950^{\circ}\text{F}$ ) using a step function increase in temperature over seven hours, then maintaining

maximum temperature for three hours. Using this firing procedure, he was able to obtain excellent repeatability in static imbibition tests.

## **2.5 Mercury Injection**

The mercury capillary pressure apparatus (Purcell 1949) was developed to accelerate the determination of the capillary pressure/saturation relationship. Mercury is normally a non-wetting fluid. The core sample is inserted in the mercury chamber and then evacuated from air. Mercury is forced into the core under pressure. The volume of mercury injected at each pressure determines the non-wetting phase saturation. This procedure is continued until the core sample is filled with mercury or the injection pressure reaches some predetermined value. Important advantages are gained by this method: (1) the time for determination is reduced to a few minutes; (2) small, irregularly shaped pieces can be used; and (3) the range of pressure investigation is increased because limitation of the other methods are removed. Disadvantages of this method are the difference in wetting properties and permanent destruction of the core sample.

## 2.6 Centrifuge Method.

Centrifuge is a method to obtain capillary pressure curves. The high acceleration in the centrifuge increases the gravitational field of force on the fluids. By rotating the sample at various constant speeds, a complete capillary pressure curve may be obtained. The speed of rotation is converted into force units in the center of the sample, and fluid saturation is read visually by the operator. The advantages of the method are the increased speed of obtaining data, compared to all the other methods except mercury injection, and it is non-destructive test. The disadvantages are that it may takes days to get a complete curve and it costs three times more than mercury injection.

## 2.7 Previous Investigation on Conversion Factors

Purcell (1949) first suggested the use of a conversion factor after he saw the difference between curves generated by mercury injection and the porous diaphragm.

The following is a derivation of the equations he used:

since,

$$P_{c(\text{Hg-gas})} = \frac{2\sigma \cos \theta}{r}$$

$$Pc_{(w-air)} = \frac{2\sigma \cos \theta}{r}$$

rearranging equation in term of radius (r),

$$r = \frac{(2\sigma \cos \theta)_{Hg-gas}}{Pc_{(Hg-gas)}} = \frac{(2\sigma \cos \theta)_{w-air}}{Pc_{(w-air)}}$$

$$\frac{Pc_{(Hg-gas)}}{Pc_{(w-air)}} = \frac{(2\sigma \cos \theta)_{Hg-gas}}{(2\sigma \cos \theta)_{w-air}}$$

simplifying,

$$\frac{Pc_{(Hg-gas)}}{Pc_{(w-air)}} = \frac{(\sigma \cos \theta)_{Hg-gas}}{(\sigma \cos \theta)_{w-air}}$$

Purcell assumed the following values:

1. Surface tension of water  $\sigma$  , 70 dynes per cm,
2. Surface tension of mercury  $\sigma$  , 480 dynes per cm,
3. Contact angle of water against solid  $\theta$  ,  $0^\circ$  ,
4. Contact angle of mercury against solid  $\theta$  ,  $140^\circ$  .

The ratio is then,

$$\frac{Pc_{(Hg-gas)}}{Pc_{(w-air)}} = \frac{-(480)(\cos 140^\circ)}{(70)(\cos 0^\circ)} = 5.25$$

Solving for  $P_{c(w-air)}$

$$P_{c(w-air)} = \frac{P_{c(Hg-gas)}}{5.25}$$

To convert from water/air capillary pressure curve to mercury/gas, divide by 5.25.

Brown (1951) later said that Purcell's factor is only theoretical and cannot be applied due to contamination in the water which make the surface tension of the water less than 70 dynes per cm. Brown gave an average values of 6.4 for limestone and 7.2 for sandstone. Purcell replied by saying the contamination is not the governing factor, pore geometry is the key component.

Omoregle (1988) discussed the factors affecting the equivalency of different capillary pressure measurement techniques. He made the following conclusions:

1. Rock samples with clays that change morphology upon drying should not be subjected to drying before capillary pressure measurement are made.
2. For intermediate wettability rock, the use of  $30^\circ$  for capillary pressure data is inadequate (for this research, sample were fired to insure strong wettability).
3. When capillary pressure data obtained with horizontal and vertical plugs samples are normalized, the horizontal permeabilities should be used for the

vertical samples, because they are more representative of average pore size and less affected by the thin laminations of low permeability strata.

Sabatier (1994) did a comparative study using different techniques and different fluid systems. He concluded that an oil-water system is not transposable with an air-mercury system.

## CHAPTER 3 EXPERIMENTAL PROCEDURE

### 3.1 Core preparation

One of the requirements of this research was to use plugs with varying permeability. Different sandstone core samples were tested using the Pressure Decay Profiler Permeameter (PDPK) to estimate permeability. Samples, which fall under the permeability range of 15-1250 md were chosen. Plugs underwent testing in three different apparatus; therefore, it is important to decide on the proper dimension of the core. There were some limitations on the plug size, for instance the Core Measurement System (CMS-300), will take only two diameters, 1 and 1.5 inches. Table 3.1.1 shows plug dimensions for different apparatus. It was decided to use 1-inch by 1-inch plugs for the CMS-300 and the centrifuge. For the mercury injection, 1/3 of the plug would be cut for use in the mercury injection apparatus. In order to make sure that this portion of the sample gave the same result as the whole plug, some additional experiments were performed. Four identical plugs were cut from Berea sandstone block with the same permeability and porosity (two sets of twin plugs). Mercury injection capillary pressure curve was determined for one of the plugs. Then the twin plug was taken and cut into

two halves. Mercury injection capillary pressure curve for the two halves were determined. The resulting three curves were almost identical. The same procedure was repeated for the other twin plugs and the results were also similar (See Figure 3.1.1).

Apparatus	Diameter (inch)	Length (inch)	Shape
CMS-300	1 and 1.5	Up to 3	Cylindrical
Centrifuge	1	1	Cylindrical
Mercury Injection	Less than 1	Up to 1.5	Irregular or Cylindrical

Table 3.1.1 Plugs dimensions permitted by each apparatus

Twenty-four cylindrical shaped plugs with a 1-inch diameter and a length of 1-inch were cut. The samples were then cleaned with toluene using a Soxhlet extractor for 24 hours. Sample porosity and permeabilities were then measured using the CMS-300 under a confining pressure of 1000 psia. Plugs were fired in an oven for seven hours with the temperature reaching up to 800°C (for procedures see Section 3.2). After firing three samples were fragile and no longer useful. Another three samples showed visible fracture

and had to be taken out due to the errors that they would create in the measurements.

Permeability and porosity of the remaining cores were then determined using CMS-300.

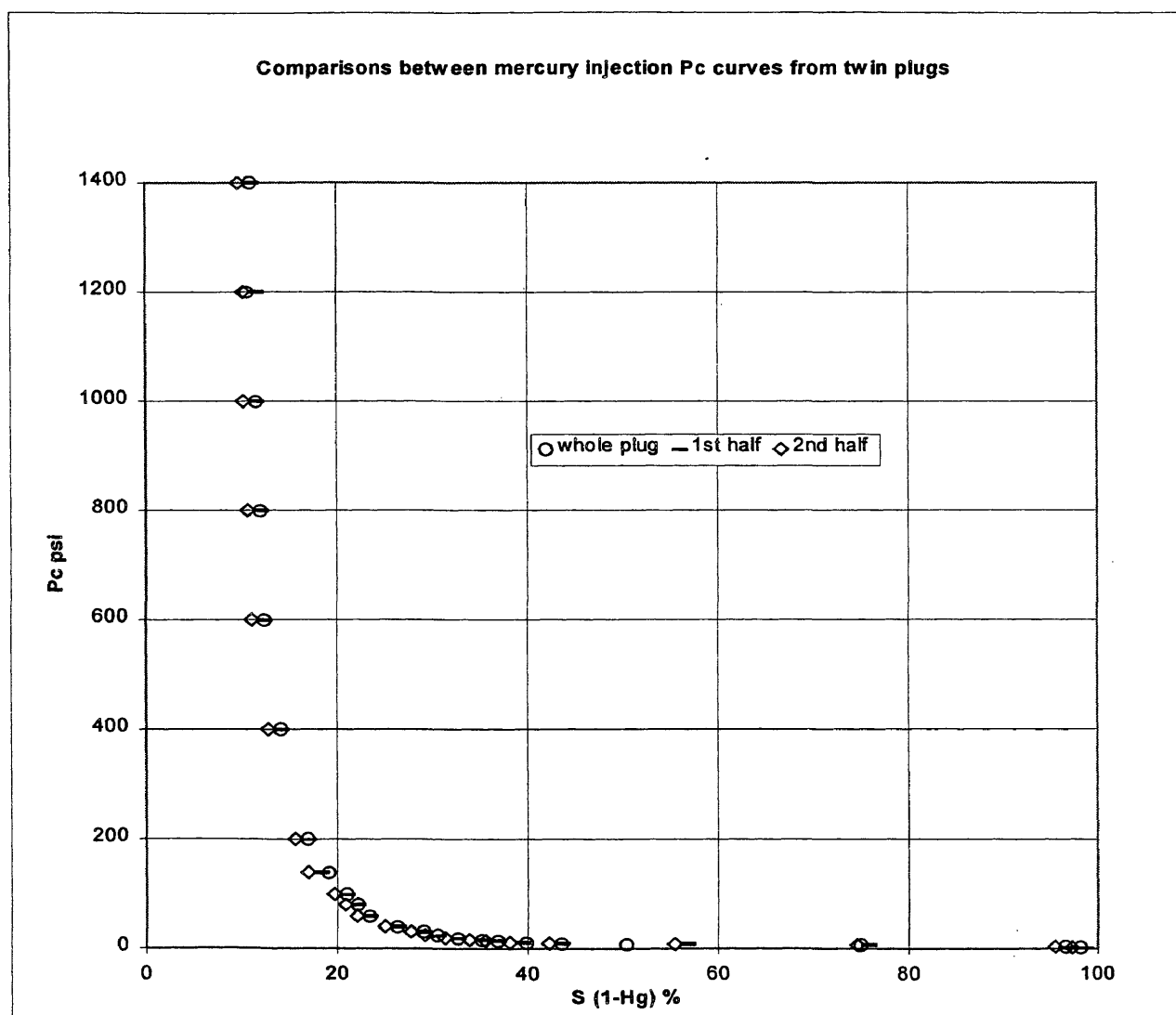


Figure 3.1.1 Comparative Study Between Twin Plugs

In centrifuge experiment, cores were saturated with brine, then oil is used to displace brine. The Soxhlet extractor was used to clean them from the oil using toluene for 24 hours. This procedure is to insure that the core was the same for mercury injection experiments. After that, plugs were prepared for the mercury injection stage.

### **3.2 Firing Procedure**

The purpose of firing the cores was to create a stable internal structure for the plugs by stabilizing the clay minerals and keeping them strongly water wet, insuring constant core properties between the different testing methods. Based on the conclusions of Section 2.4 and the Recommended Practice 40 (API 1998), the following firing procedure was established:

1. Preheat the oven for 200 °C (392 °F),
2. Place samples inside the oven for two hours,
3. Increase temperature to 350 °C (662 °F) for one hour,
4. Increase temperature by 150 °C (302 °F) every two hours,
5. Maintain a maximum temperature of 800 °C (1472 °F) for three hours,
6. Switch the oven off and let the plugs cool slowly overnight.

### 3.3 Centrifuge Method

The experimental work was performed by Gary R. Kennedy and Hiemi K. Haines at Marathon Oil Company Research laboratories in Littleton, Colorado. Experimental procedure, input data, and output data will be shown in this section. Raw data is found in Appendix B. Apparatus schematic is in Figure 3.3.1. Before the centrifugal run the plug went through the following:

1. The plug was fully saturated with brine,
2. The drainage bucket was surrounded with oil,
3. RPM was increased for the centrifuge to displace water with oil,
4. A primary drainage curve (oil displacing water) was produced.

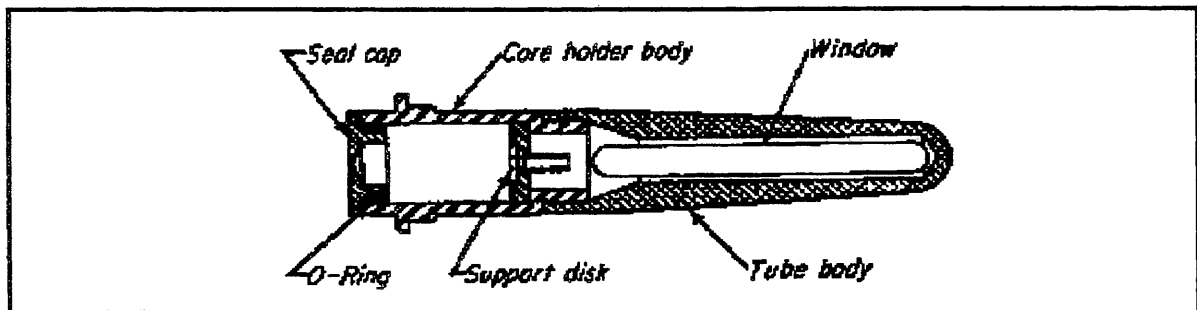


Figure 3.3.1 Simplified Centrifuge Schematic (From Amyx 1960)

The water saturation resulting from the experiment was average water saturation  $S_{w_{avg}}$ . The  $S_{w_{avg}}$  was adjusted to inlet water saturation  $S_{w_{inlet}}$  using the Rajan method. The procedure for adjusting the saturation can be found in Appendix A. The plug data at the start of centrifuge experiment are in Table 3.3.1, which include plug characterization. Volume of brine displaced by oil during centrifuge experiment at different RPM can be found in Table 3.3.2. The assumption made was that the lab condition is the same as reservoir conditions therefore, contact angle ( $\theta$ ) and IFT are the same for both conditions.

Sample	Dry weight (g)	Brine saturated weight (g)	Pore Volume (cc)	K (md)	Length (inch)	Diameter (inch)
K1	27.11	29.90	2.945	221.7	0.995	1.02
K3	25.58	28.00	2.607	135.7	0.921	1.02
K4	25.99	28.78	3.011	403.6	0.979	1.02
K5	24.63	27.36	2.954	958.2	1.040	0.97
K6	27.18	30.19	3.220	503.0	1.024	1.02
K9	22.19	24.82	2.856	111.6	0.947	0.97
K10	27.4	30.11	3.029	318.9	1.015	1.02
K13	27.33	30.18	2.876	162.5	1.004	1.02
K14	26.61	29.00	2.734	130.4	0.960	1.02
K15	23.99	26.67	2.933	657.5	0.950	1.00
K16	24.55	27.15	2.944	42.2	0.974	0.97
K17	28.55	31.22	2.811	119.2	1.020	1.02

Table 3.3.1 Plug Data at Start of Centrifuge Experiment

Sample	400 RPM	800 RPM	1200 RPM	2500 RPM	5000 RPM	8000 RPM	Final Weight (g)
K1	0	0.05	0.34	1.44	1.91	2.10	29.63
K3	0	0.02	0.13	1.10	1.61	1.80	27.78
K4	0	0.15	0.99	1.86	2.21	2.40	28.49
K5	0	0.52	1.31	2.00	2.21	2.30	27.08
K6	0	0.27	1.15	2.05	2.43	2.60	29.85
K9	0	0.32	1.10	1.82	2.10	2.20	24.52
K10	0	0.00	0.73	1.76	2.15	2.30	29.83
K13	0	0.02	0.21	1.41	1.83	1.90	29.95
K14	0	0.00	0.22	1.13	1.61	1.79	28.79
K15	0	0.08	0.81	1.81	2.21	2.26	26.42
K16	0	0.00	0.17	0.62	0.82	0.92	28.06
K17	0	0.00	0.20	1.20	1.71	1.92	31.00

Table 3.3.2 Volume of Brine Displaced by Oil During Centrifuge in (cc)

### **3.4 Mercury Injection Method.**

In this section procedure for calibration of mercury injection apparatus is shown. Detailed procedure for capillary pressure measurement using mercury injection is shown in Section 3.4.2. Comparison between permeability before and after centrifuge is shown in this section.

#### **3.4.1 Calibration of the Mercury Injection Apparatus.**

The purpose of the calibration is to determine the error that results from the compressibility of mercury, the expansion of the steel in the apparatus, and the compressibility of the air that is trapped in the apparatus. Apparatus schematic is found in Figure 3.4.1. The following is the procedure for calibration revised from PE413 laboratory manual:

1. Position the mercury pump plunger so that all mercury is pulled from the test chamber into the pump cylinder.
2. Place the top on the test chamber, open valves (0-30, 0-200), and close the atmosphere valve and nitrogen valve.
3. Turn the arrow to vacuum and turn on the vacuum pump and vacuum gauge. Allow the vacuum pump to run until the pressure stabilizes (50 to 100 millitorrs).

4. Fill test chamber with mercury to the upper reference mark. Zero the ruler and vernier and record the starting pressure in millitorr.
5. Switch the arrow to pressure. Open the atmospheric valve and raise pressure to the desired step. Turn the handle wheel clockwise until the level of mercury is back to the upper reference mark. Wait until pressure stabilizes, then record the reading on the counters in cubic centimeters (cc).
6. After atmospheric pressure is reached, switch from atmosphere valve to nitrogen valve.
7. Repeat this procedure until 2000 psi pressure is reached, making sure to close each gauge before the maximum pressure it can handle is reached.

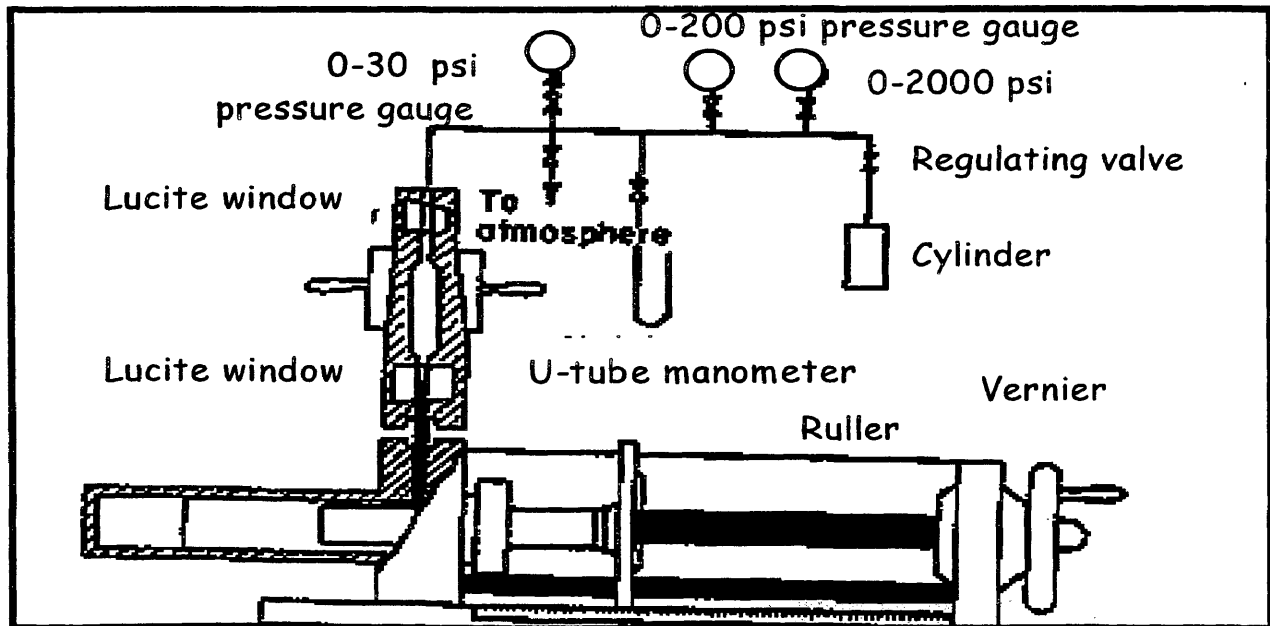


Figure 3.4.1 Capillary Pressure Cell for Mercury Injection (From Purcell 1949).

### 3.4.2 Capillary Pressure Measurement

The following are the steps required to run a mercury injection test:

1. Record the volume of mercury required for filling the test chamber. Place sample in chamber and record mercury volume. The sample bulk volume is the difference between the two volumes,
2. Reduce the pressure to the starting pressure used to calibrate the equipment,
3. Slowly increase the pressure in the test cell while watching the mercury in the upper sight window,
4. Follow the same procedure used to calibrate the instrument. Be sure the volume is stabilized before taking data.

Figure 3.4.2 is an example plot of the data obtained from the above procedure. In order to plot a capillary pressure curve, the mercury volume has to be converted to the wetting phase saturation ( $1-S_{Hg}$ ) for comparison purposes. To find the volume of mercury inside the plug, for each pressure step, subtract the mercury volume obtained during calibration of the apparatus from the volume of mercury during running of the sample. For example, a pressure of 100 psia draw 0.38 cc of mercury from the chamber, from calibration curve we see that 0.1 cc goes to steel expansion. The rest of the mercury (0.28 cc) were injected inside the plug (Figure 3.4.2).

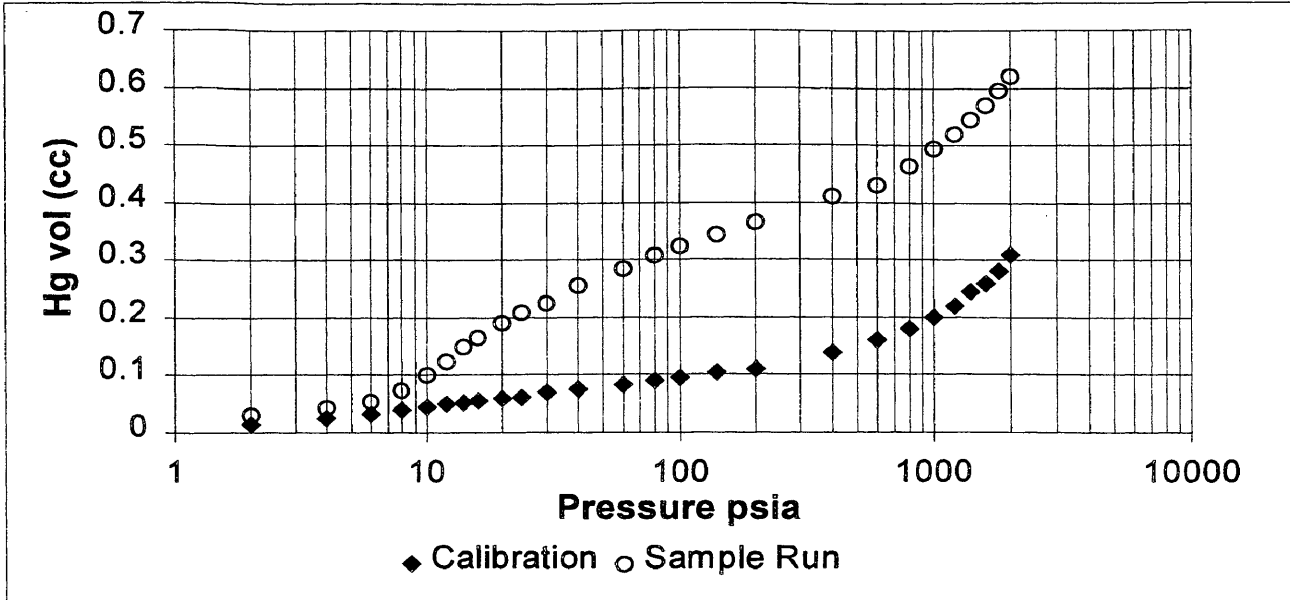


Figure 3.4.2 Mercury Injection Calibration Curve

Mercury saturation is obtained by dividing the mercury volume by the pore volume of the plug. Pore volume for the plug is obtained by the following equation:

$$PV = BV - GV$$

$$GV = \frac{Wt}{\rho g}$$

where,

$PV$  = Pore volume of the plug (cc),

$BV$  = Bulk volume of the plug (cc),

$GV$  = Grain volume of the plug in (cc),

$Wt_{dry}$  = Dry weight of the plug in (g),

$\rho_g$  = Density of sandstone in (g/cc).

In order for the capillary pressure curve to be representative of the plug for both methods constant property should be maintained. Comparisons between the plug permeability before the centrifuge run and the permeability after cleaning the plug from the centrifuge fluids were made. Figure 3.4.3 shows comparisons between those values.

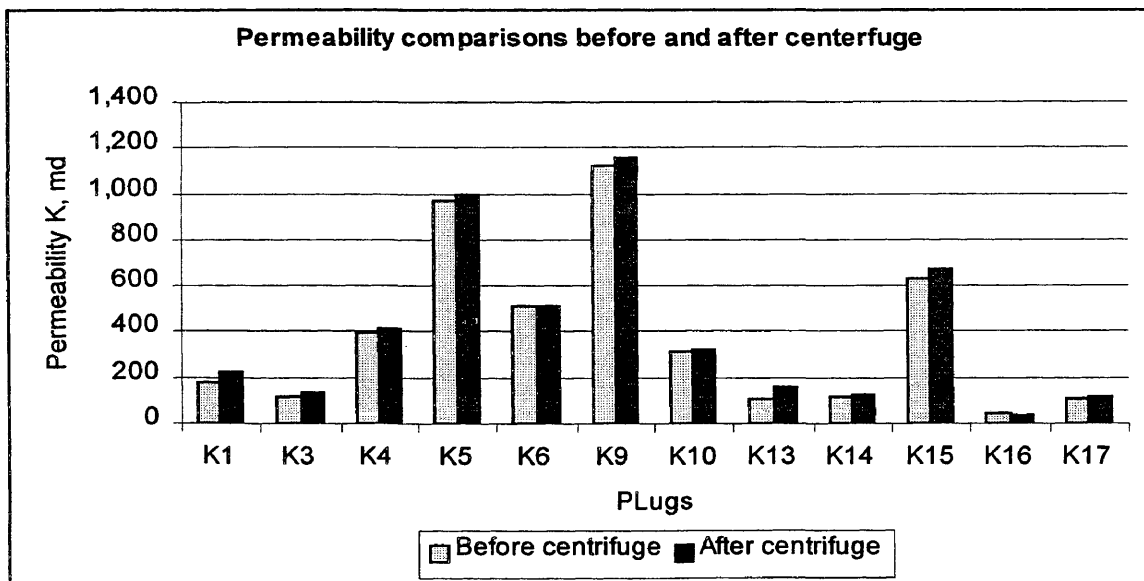


Figure 3.4.3 Permeability Comparisons Before and After Centrifuge

Sample	Permeability before centrifuge md	Permeability after centrifuge md	Difference %
K1	175	225	22
K3	115	134	14
K4	399	413	3
K5	966	998	3
K6	509	515	1
K9	1,118	1,157	3
K10	318	324	2
K13	106	162	34
K14	117	129	9
K15	632	677	7
K16	46	40	-15
K17	105	118	12

Table 3.4.1 Permeability Comparisons Before and After Centrifuge

## **CHAPTER 4**

### **RESULTS AND DISCUSSION**

The data obtained from centrifuge and the mercury injection method are discussed in this chapter. Capillary pressure data for both techniques will be plotted on the same graph. A suitable conversion method is obtained. Centrifuge data will be analyzed first, then mercury injection data will follow. A record of the attempts to reach the suitable conversion factors will be shown.

#### **4.1 Centrifuge Method**

The centrifugal experiments were performed at Marathon Oil Company Research Laboratories, since the equipment is not available at the Colorado School of Mines. The number of plugs tested by Marathon was 12, due to their time limitation. The experimental procedure is found in Section 3.1. Raw data is found in Appendix B. The calculation procedure for water saturation is in Appendix A.

A capillary pressure curve is obtained by plotting water saturation on the x-axis, and the pressure required to attain that saturation on the y-axis. Figures C-1 through C-12 in Appendix C show capillary pressure curves from the centrifuge method. The

graphs show  $Sw_i$  values ranging of 11-27 %, except plug K-16 had 60 %  $Sw_i$ , due to it's low permeability. K16 also showed a high value of  $Sw_i$  during mercury injection. Plugs with low permeability had higher entry pressure and  $Sw_i$ .

#### **4.2 Mercury Injection Method.**

Mercury injection experiments were performed on the same core after they had been cleaned. For details on core cleaning and experiment procedures see Chapter 3. Procedures for constructing a capillary pressure curve from the mercury injection method are outlined in Section 3.4. The capillary pressure for mercury curves are found in Figures C-13 through C-25 in Appendix C. These graphs were analyzed to find pore throat sorting (PTS) and reservoir grade (RG) using techniques developed by Jennings (1987). This was one of the attempts to find a relationship between the two sets of capillary pressure curves. Curves were well developed with a clear entry pressure of about 10 psi and  $Sw_i$  of 7 % (See Table 4.2.1).

Sample No.	K md	Porosity %	Sw <sub>i</sub> %	Entry Pressure psia	RG	PTS
K1	175	22.1	7	10	24	1.83
K3	115	20.5	8	9	26	2.00
K4	400	23.0	5	7	19	1.97
K5	965	23.5	5	4	22	1.85
K6	509	23.5	9	8	26	1.76
K9	1118	24.9	13	4	18	1.41
K10	318	22.3	5	8	21	1.97
K13	106	21.4	8	8	27	2.04
K14	117	21.3	19	12	23	2.18
K15	632	23.9	13	7	21	2.24
K16	46	24.7	47	7	25	2.74
K17	104	20.6	12	12	22	2.16

Table 4.2.1 Entry Pressure and Sw<sub>i</sub> for Mercury Injection

### 4.3 Capillary Pressure Correlation

This section will describe the method used to reach a suitable conversion factor. In order to correlate between curves established from two different methods, a relationship with some theoretical background must first be found. Purcell (1949) used the ratio of the interfacial tension and contact angle between the fluids in each experiment to correlate between the two curves. Details of his work can be found in Chapter 2.

Using the same principal in Section 2.7, a conversion factor based on the ratios of IFT and contact angles was found. Typical values for IFT and contact angles are in Table 4.3.1. The equation below used to convert mercury capillary pressure to centrifuge capillary pressure, both under laboratory conditions.

$$\frac{P_{c(Hg-gas)lab}}{P_{c(w-oil)lab}} = \frac{(\sigma \cos \theta)_{Hg-gas}}{(\sigma \cos \theta)_{w-oil}}$$

Assuming IFT for air-mercury system is 480 dynes/cm and the oil-water system is 48 dynes/cm and for contact angles, 140 degrees were used for air-mercury and 30 degrees the for oil-water system (Graves 1996), we can then calculate the ratio.

$$\frac{P_{c(Hg-gas)lab}}{P_{c(w-oil)lab}} = \frac{(480 \cos 140)_{Hg-gas}}{(48 \cos 30)_{w-oil}} = 8.7$$

$$P_{c(w-oil)lab} = \frac{P_{c(Hg-gas)lab}}{8.7}$$

The ratio of IFT for the fluids was found to be 8.7 for laboratory conditions. The ratio of IFT when converting from laboratory conditions (Hg-gas) to reservoir conditions (w-o) was found to be 14.1.

$$\frac{Pc_{(Hg-gas)lab}}{Pc_{(w-oil)reservoir}} = \frac{(\sigma \cos \theta)_{Hg-gas}}{(\sigma \cos \theta)_{w-oil}}$$

$$\frac{Pc_{(Hg-gas)lab}}{Pc_{(w-oil)reservoir}} = \frac{(480 \cos 140)_{Hg-gas}}{(30 \cos 30)_{w-oil}} = 14.1$$

$$Pc_{(w-oil)reservoir} = \frac{Pc_{(Hg-gas)lab}}{14.1}$$

Table 4.3.1 shows typical values for IFT and contact angles for the different fluids

System	Contact Angle $\theta$ (degrees)	Interfacial Tension $\sigma$ (dynes/cm)	$\sigma \cos \theta$
<b>Laboratory Conditions</b>			
Oil-water	30°	48	42
Air-mercury	140°	480	367
<b>Reservoir Conditions</b>			
Oil-water	30°	30	26

Table 4.3.1 Typical Interfacial Tension and Contact Angles Values  
(From Graves 1996)

A plot of capillary pressure curves using the above conversion factors can be found in Appendix D. Different empirical conversion factors were tested and it was found that dividing the pressure by 48 is the most suitable number. From those curves it was found that the conversion factor is higher than what the theory of ratios proposed. A record of this is found in Appendix D.

After applying the pressure conversion factor, there was not a saturation match between the two sets of curves, due to saturation divergence. Previous investigation (Sabatier 1994) has concluded that capillary pressure for gas-liquid systems are not transposable to a liquid-liquid system. The reason given was a different drainage system. This confirms the use of empirical correlation since the theory did not work.

The saturation divergence was taken further to find a relation between the curves. After numerous attempts, it was found that an increase of eight percent in the water saturation of mercury capillary pressure curves would result in the best fit possible. Nine plugs out of the twelve showed a match using the conversion techniques. Figures 4.3.1 through 4.3.12 show the curves from the two methods using the conversion techniques mentioned above. The other three plugs were K9, K14, and K15. The latter two plugs come from unidentified sandstone rock. K9 is a Berea sandstone plug. From the comparison plots in Appendix D, K14, and K15 are the only plugs in which the centrifuge curve is to the left of the corrected mercury injection curve (See Figures D-9, D-10). As for plug K9, the two curves do not have saturation divergence (See Figure D-

6). Since there was no apparent reason for the three plugs mismatch, it was recommended to test more plugs. Testing more plugs will help us identify the source of the mismatch whether it is the correlation or the plug themselves.

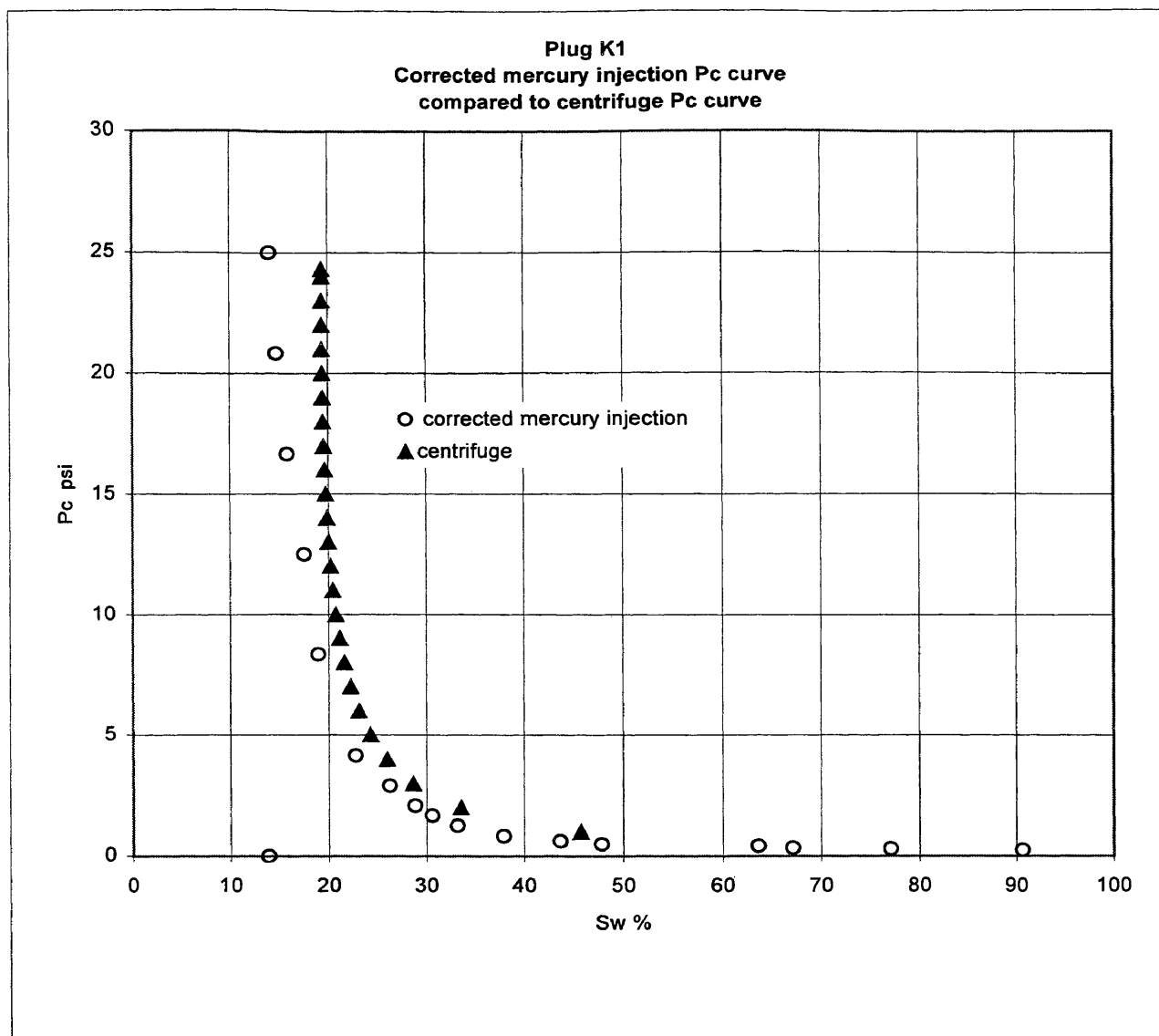


Figure 4.3.1 Sample K1 centrifuge and mercury injection correlation by dividing mercury pressure by 48 and increasing its saturation ( $1-S_{Hg}$ ) by 8%

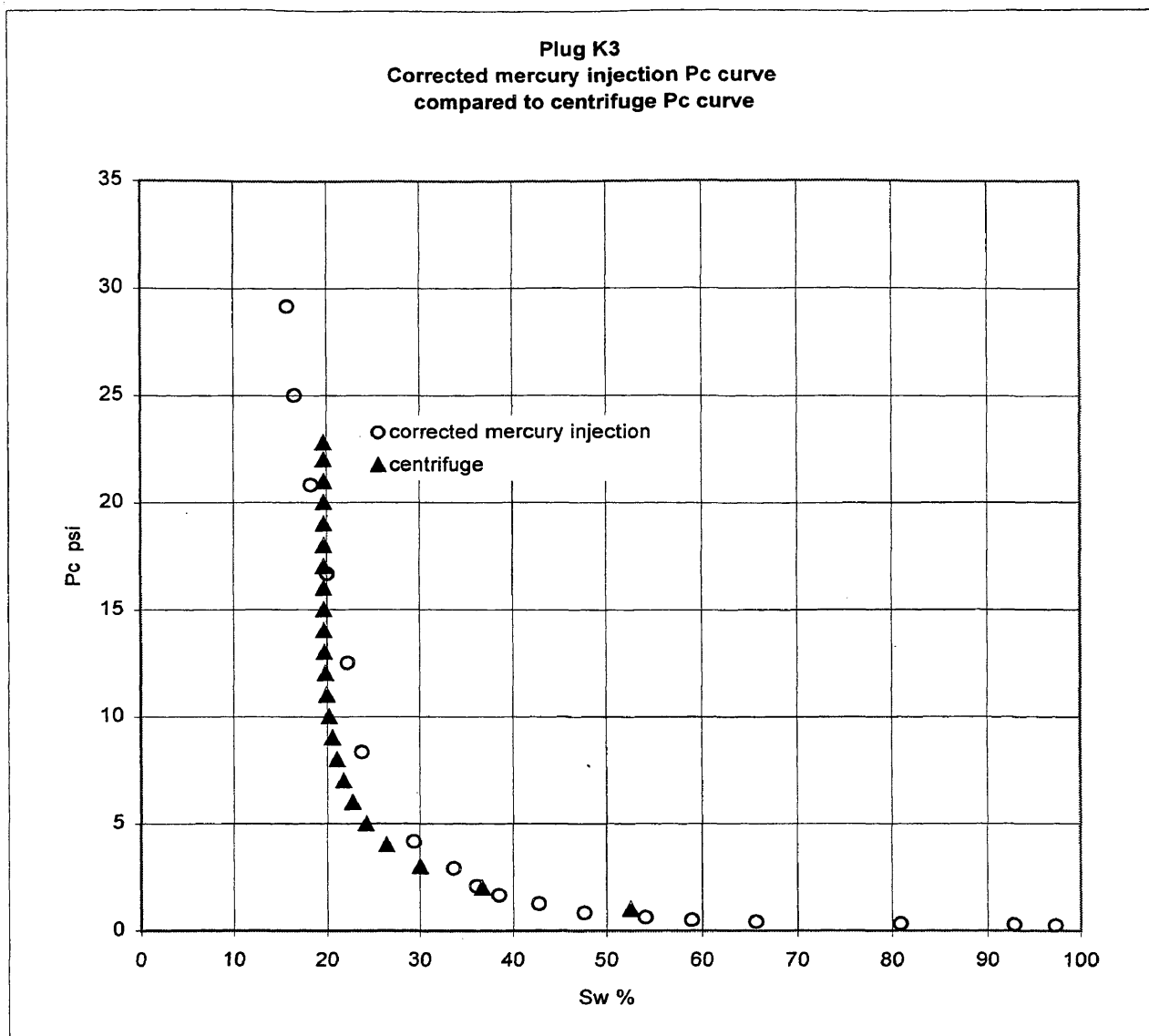


Figure 4.3.2 Sample K3 centrifuge and mercury injection correlation by dividing mercury pressure by 48 and increasing its saturation ( $1-S_{Hg}$ ) by 8%

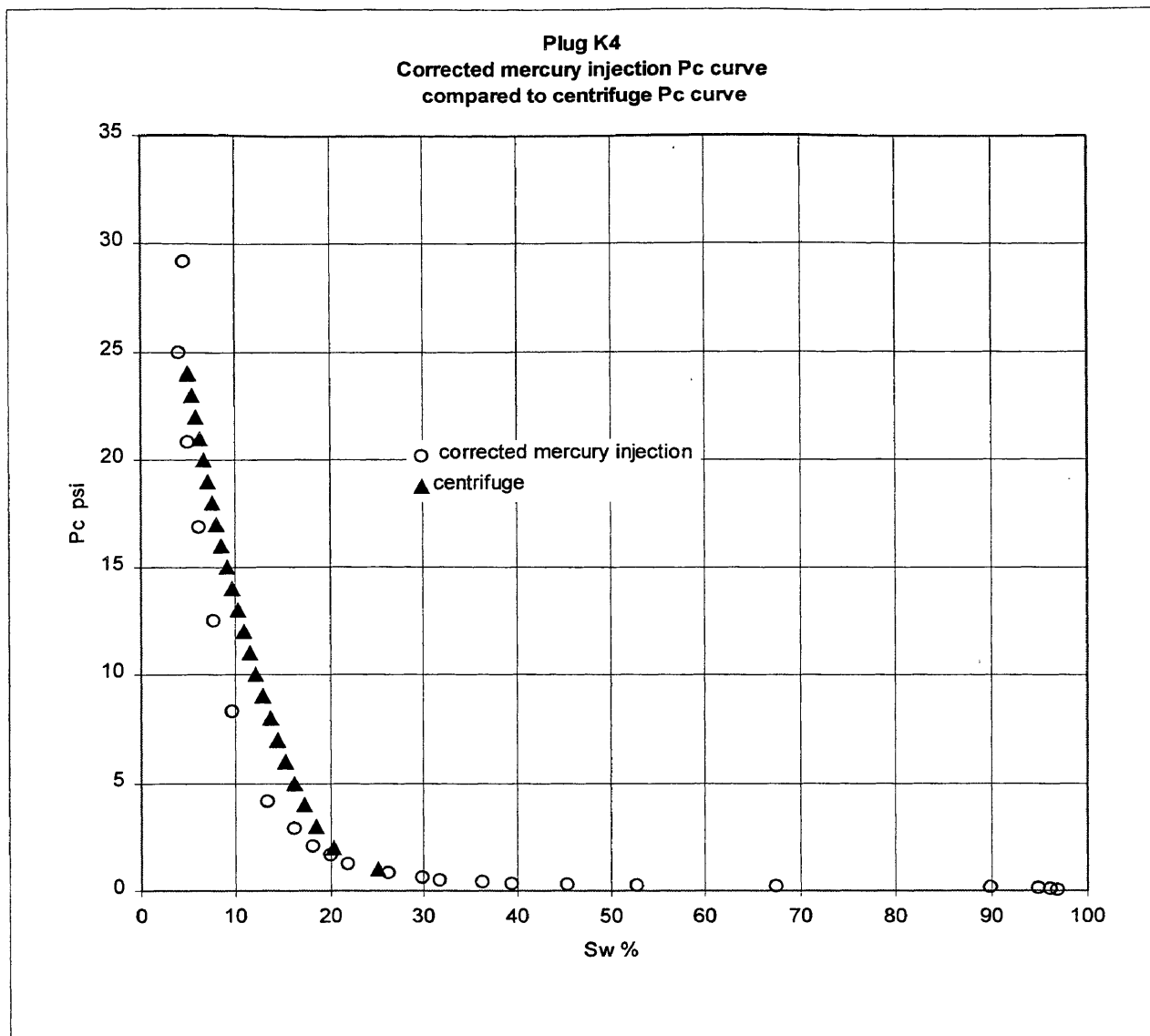


Figure 4.3.3 Sample K4 centrifuge and mercury injection correlation by dividing mercury pressure by 48 and increasing its saturation  $(1-S_{Hg})$  by 8%

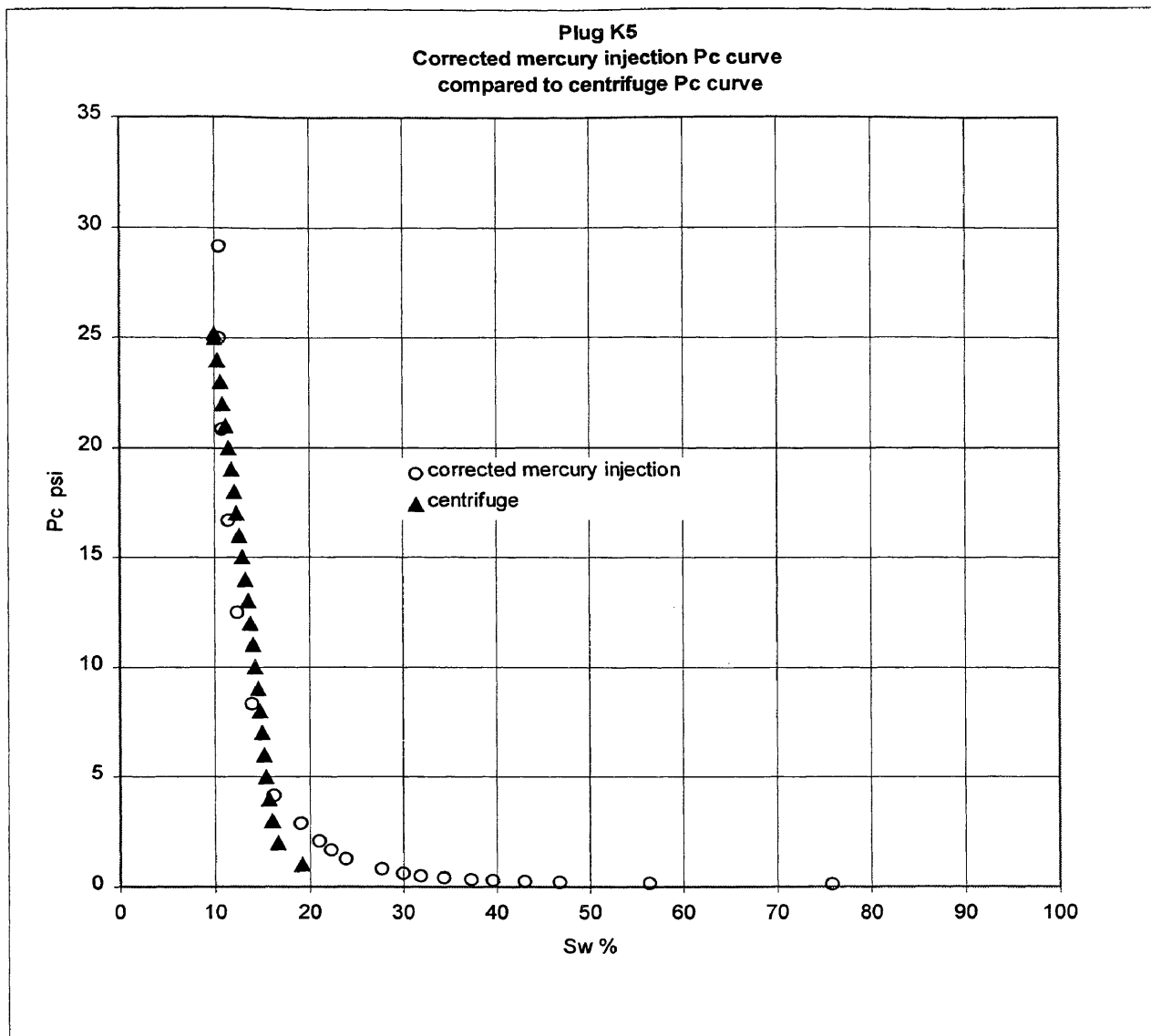


Figure 4.3.4 Sample K5 centrifuge and mercury injection correlation by dividing mercury pressure by 48 and increasing its saturation ( $1-S_{Hg}$ ) by 8%

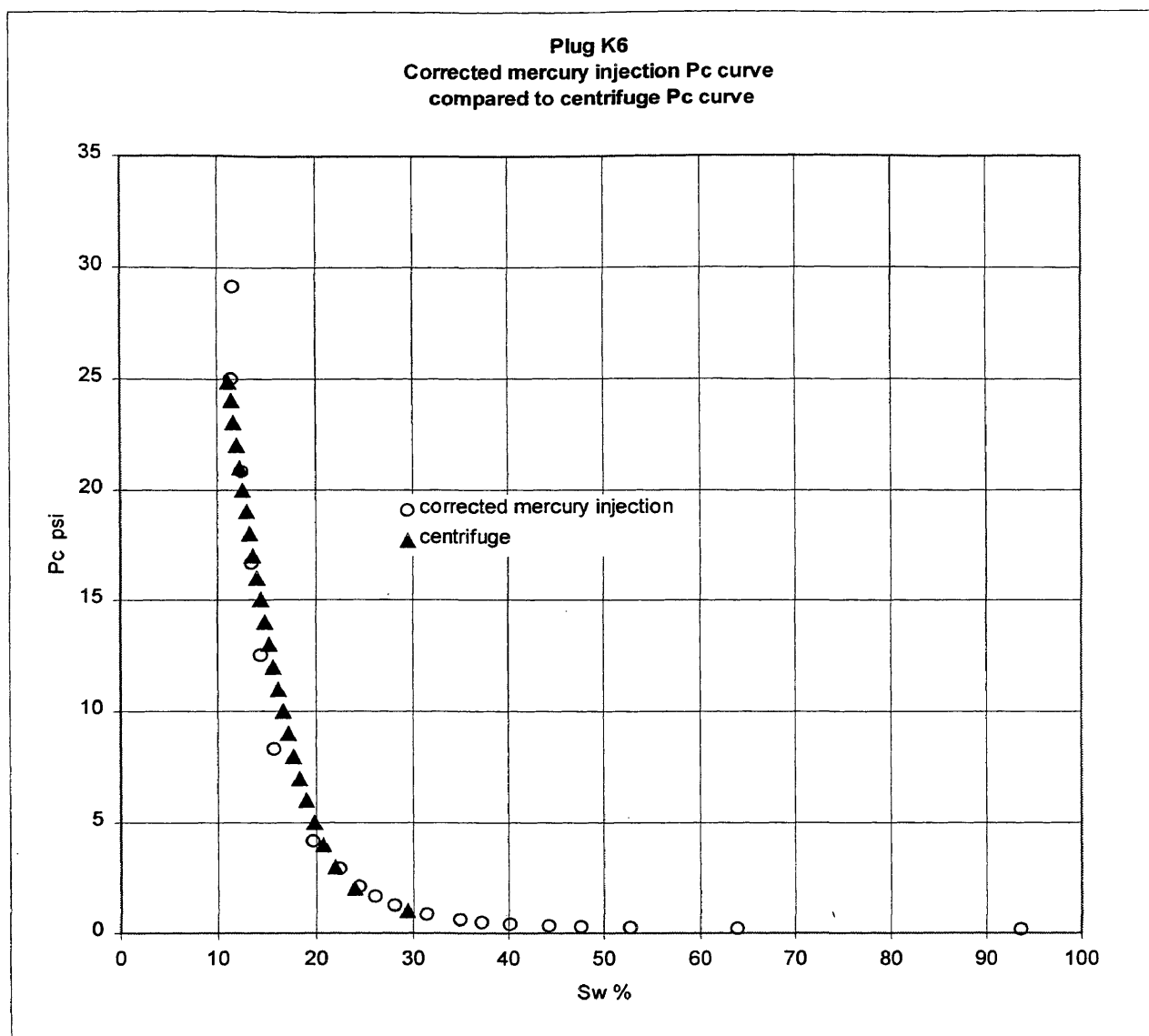


Figure 4.3.5 Sample K6 centrifuge and mercury injection correlation by dividing mercury pressure by 48 and increasing its saturation ( $1-S_{Hg}$ ) by 8%

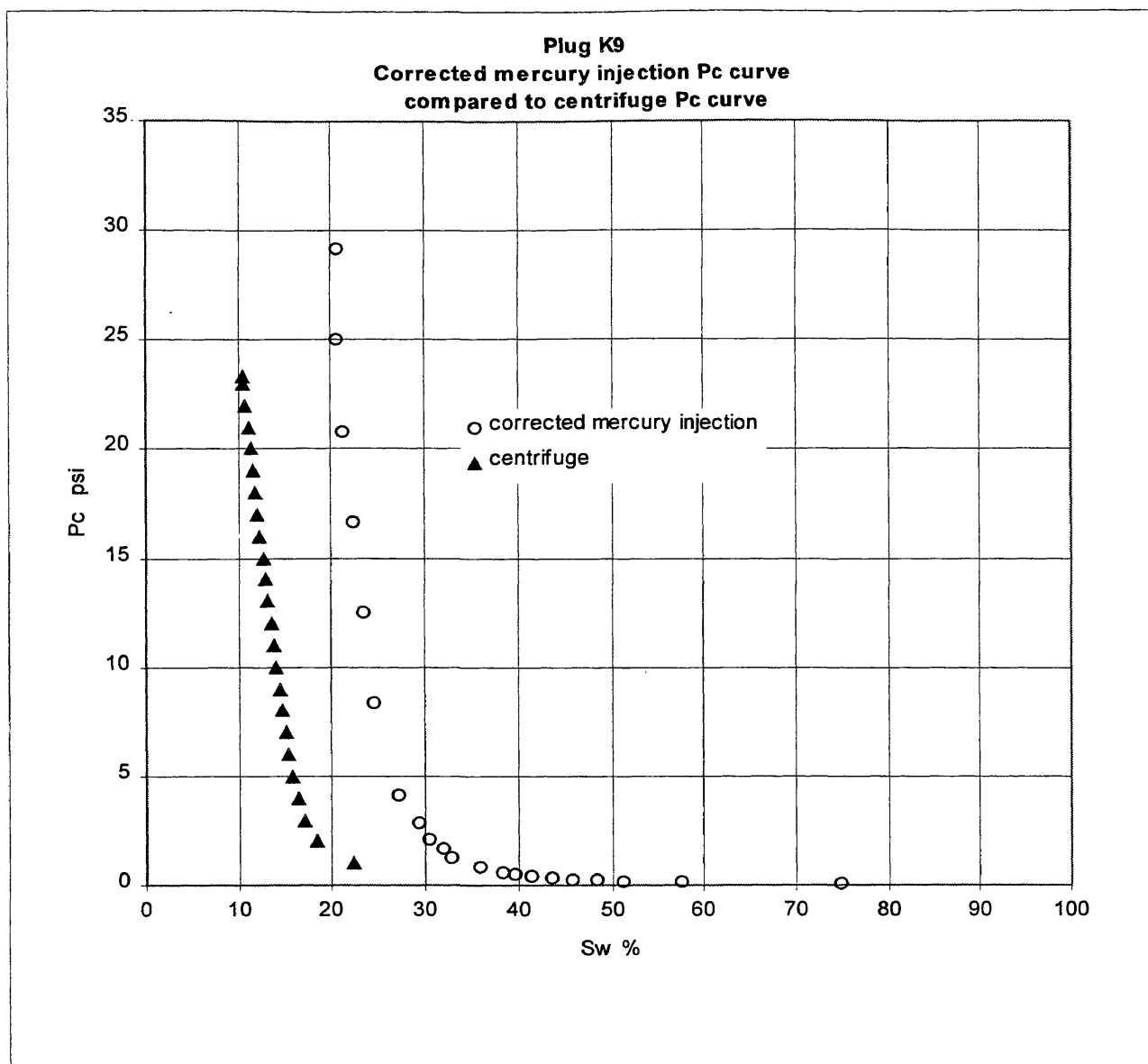


Figure 4.3.6 Sample K9 centrifuge and mercury injection correlation by dividing mercury pressure by 48 and increasing its saturation ( $1-S_{Hg}$ ) by 8%

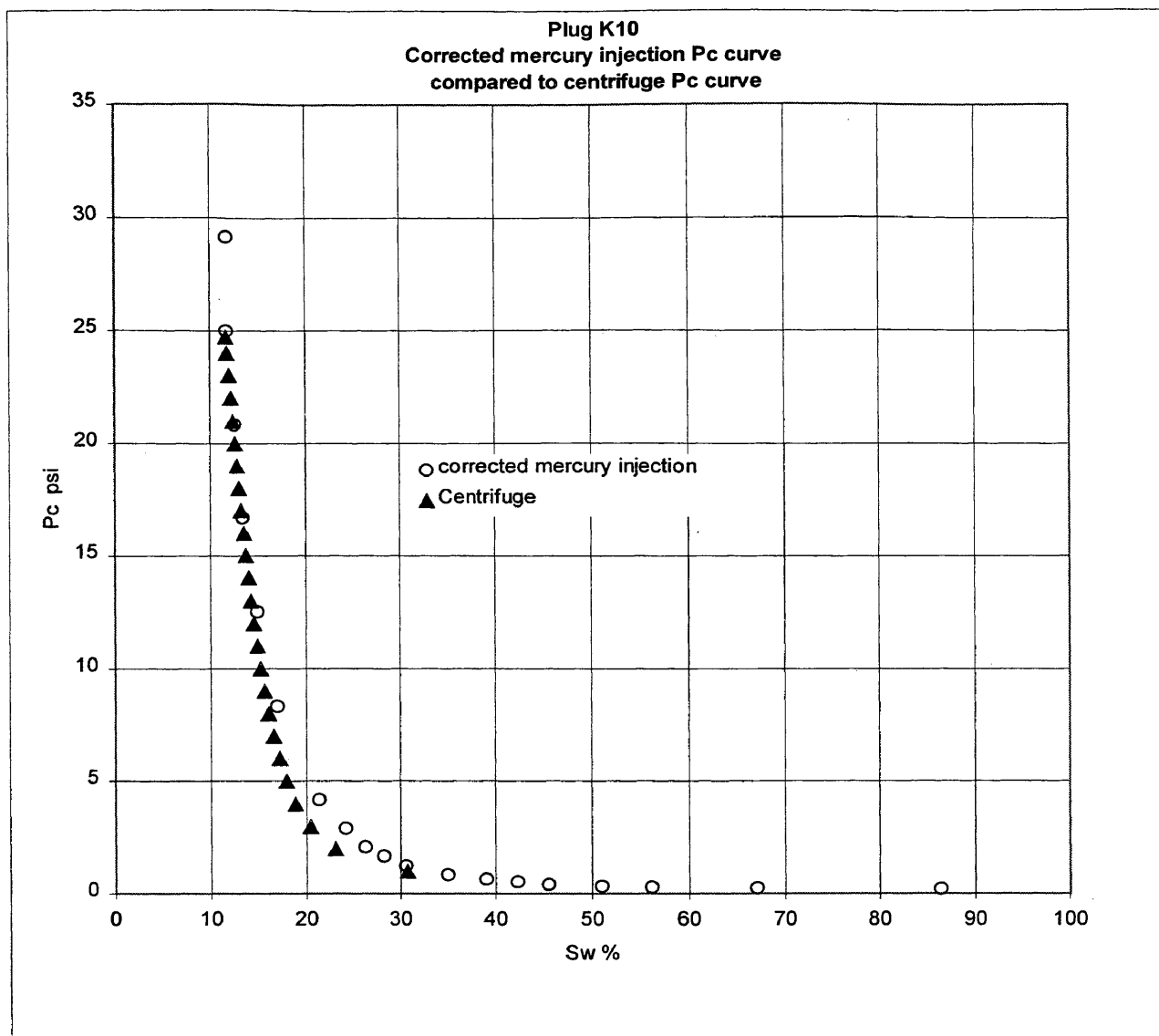


Figure 4.3.7 Sample K10 centrifuge and mercury injection correlation by dividing mercury pressure by 48 and increasing its saturation ( $1-S_{Hg}$ ) by 8%

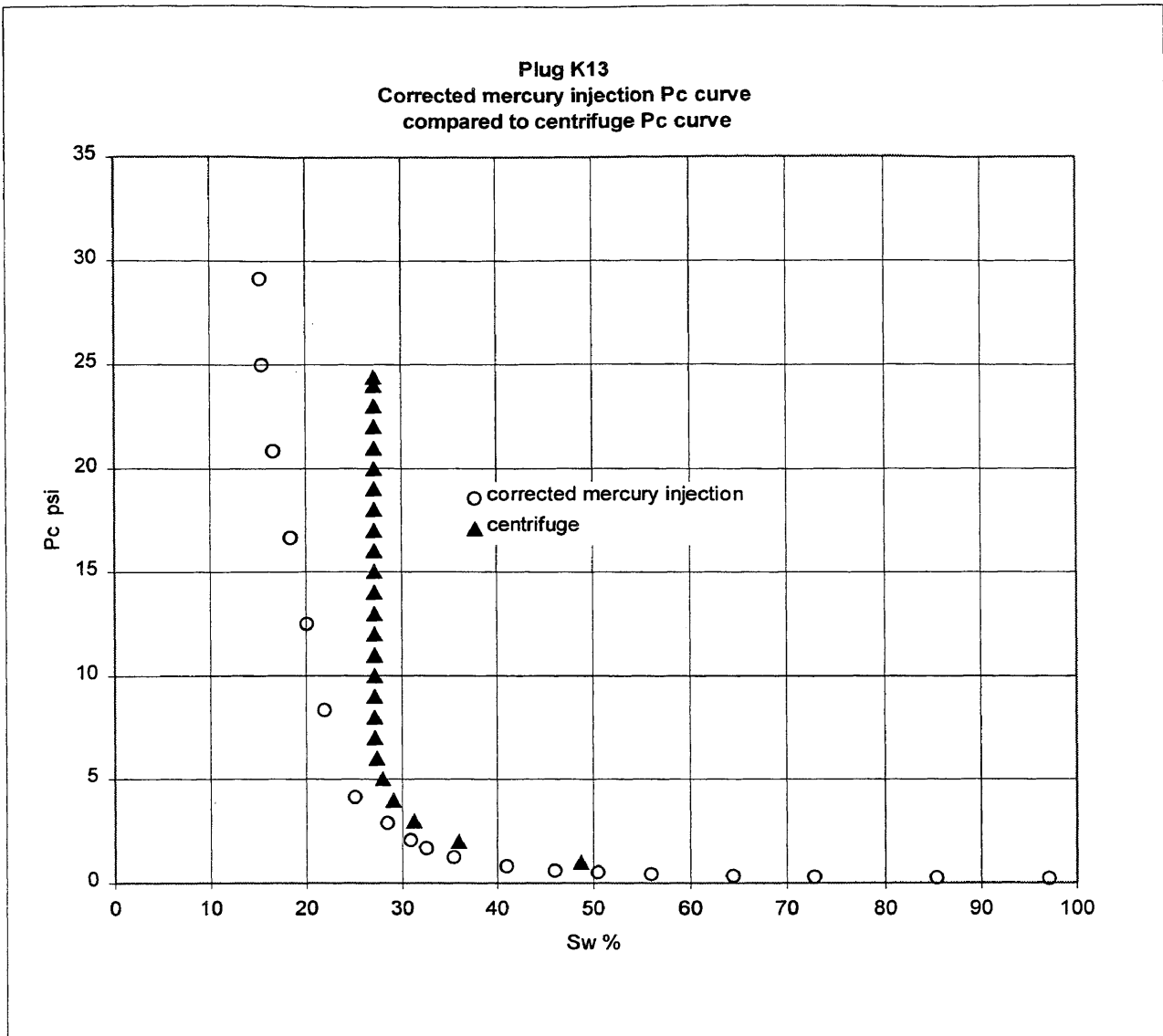


Figure 4.3.8 Sample K13 centrifuge and mercury injection correlation by dividing mercury pressure by 48 and increasing its saturation ( $1-S_{Hg}$ ) by 8%

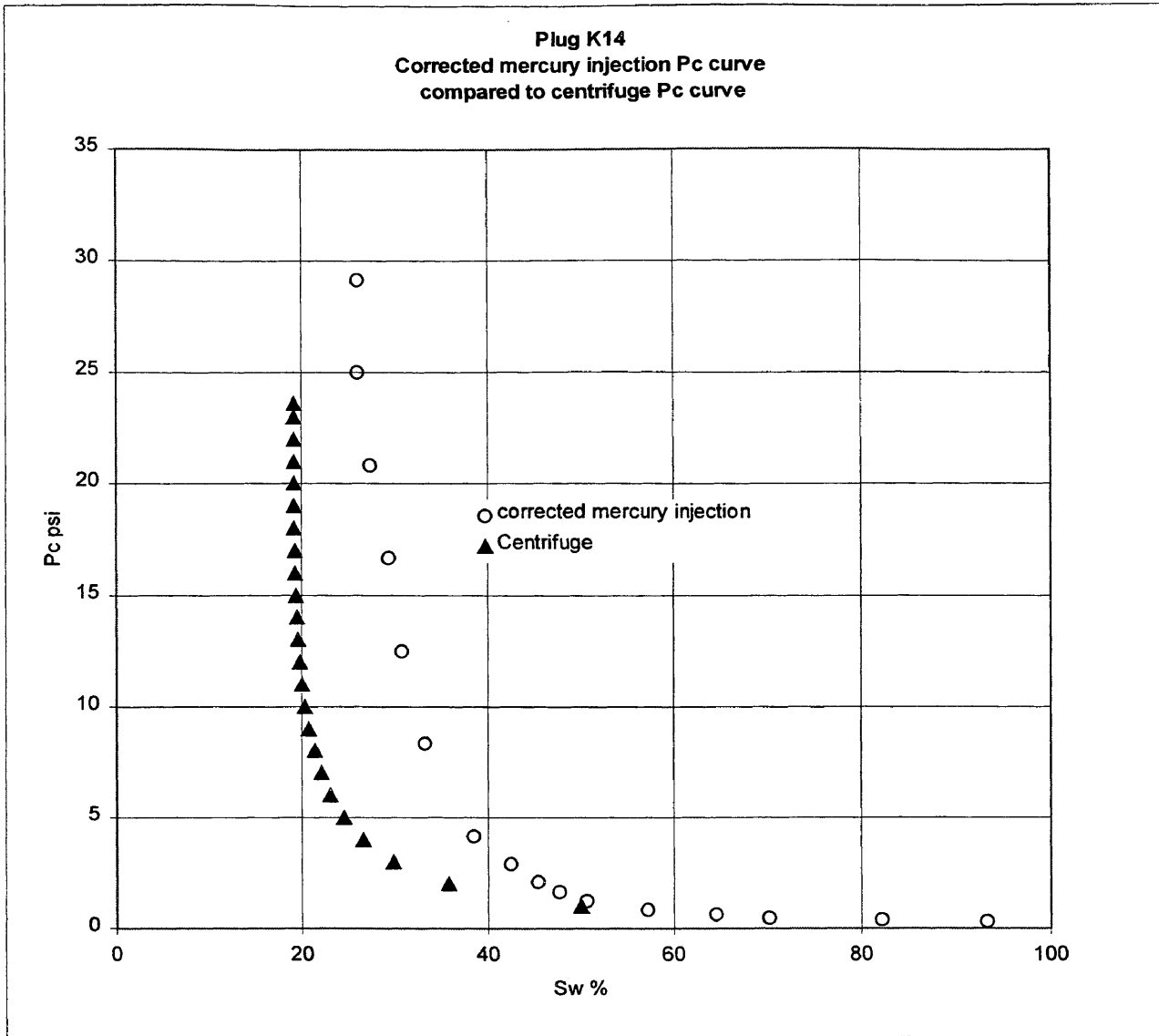


Figure 4.3.9 Sample K14 centrifuge and mercury injection correlation by dividing mercury pressure by 48 and increasing its saturation ( $1-S_{Hg}$ ) by 8%

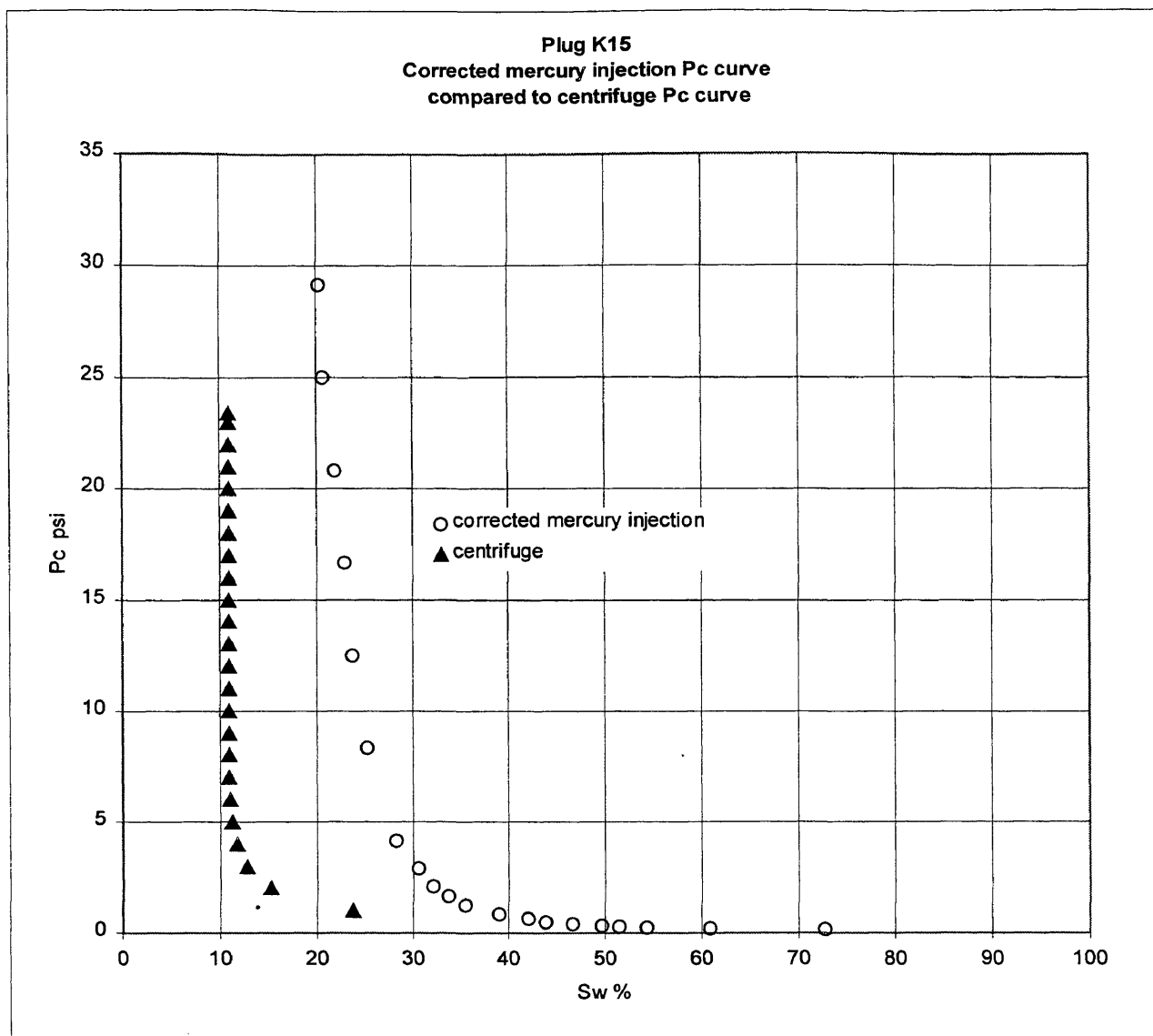


Figure 4.3.10 Sample K15 centrifuge and mercury injection correlation by dividing mercury pressure by 48 and increasing its saturation ( $1-S_{Hg}$ ) by 8%

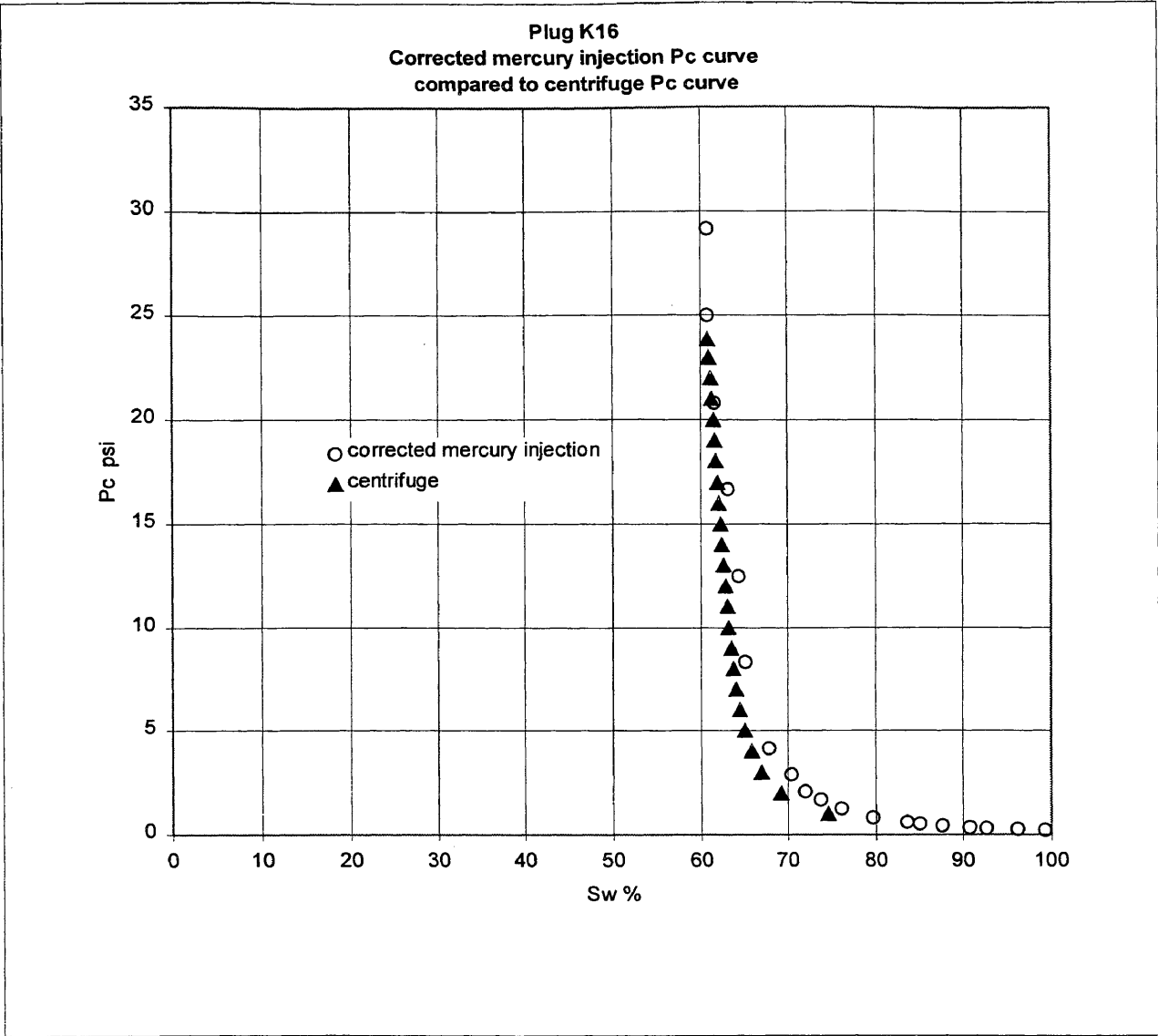


Figure 4.3.11 Sample K16 centrifuge and mercury injection correlation by dividing mercury pressure by 48 and increasing its saturation ( $1-S_{Hg}$ ) by 8%

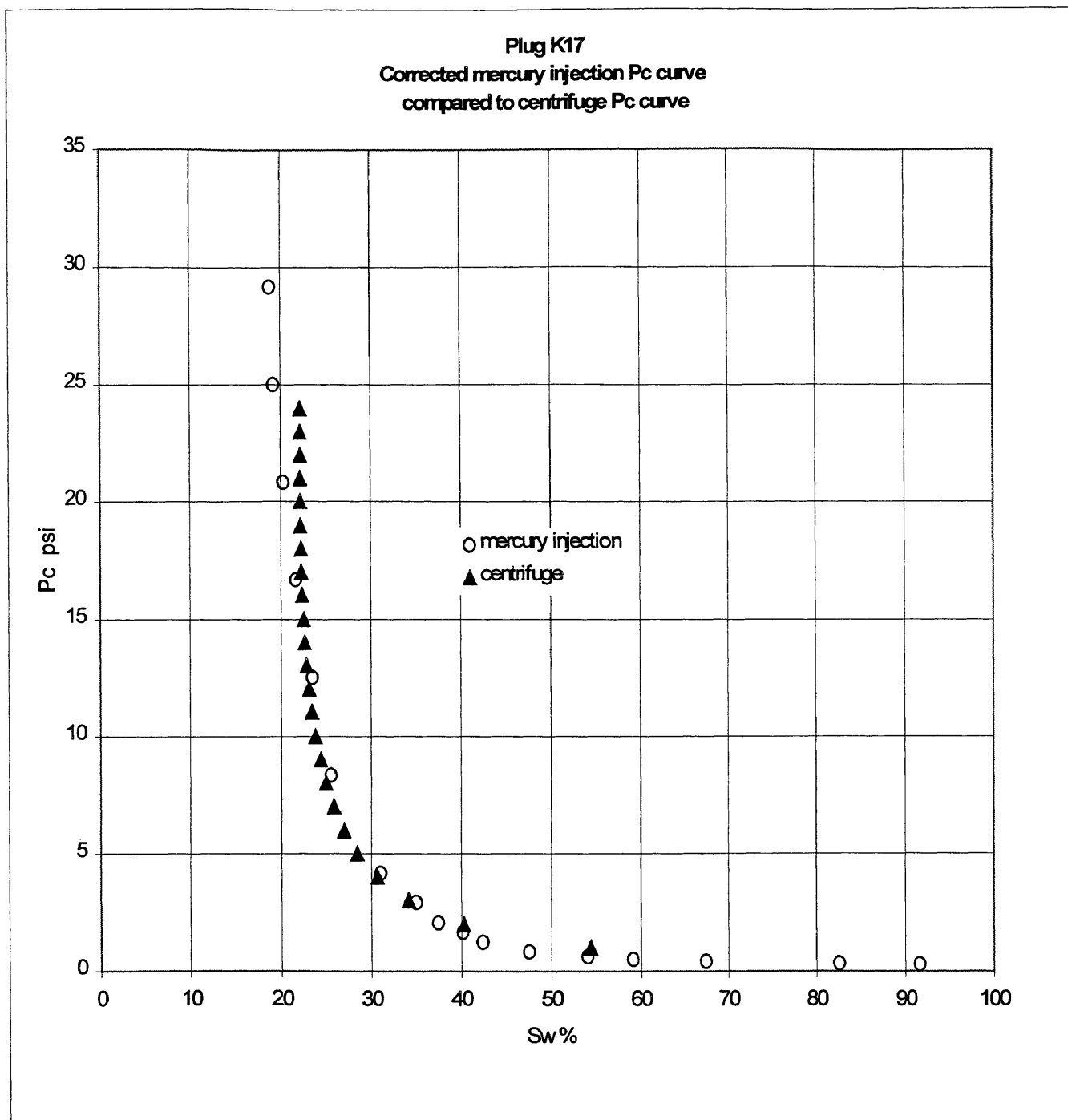


Figure 4.3.12 Sample K17 centrifuge and mercury injection correlation by dividing mercury pressure by 48 and increasing its saturation ( $1-S_{Hg}$ ) by 8%

#### 4.4 Errors in Correlation

From the set of curves in Figures 4.3.1-12, it can be seen that the two curves are not an exact match. In order to find the percentage of error in the empirical correlation, the saturation for both curves were read at four different pressures for each plug. The pressure values were 2.5, 5, 10 and 15 psi. Their corresponding saturation values were plotted (See Figures 4.4.1-2). Each point represent a plug saturation at a certain pressure and the 45 degrees line represent zero percent error. Two sets of graph were plotted one using all plugs and the other only the working nine plugs.

The correlation yielded an average arithmetic error that ranges between 1.4 and 1.9 percent saturation difference for the nine plugs, and 3.6 to 4.8 percent saturation when using all plugs. Accuracy plots can be found in Appendix E.

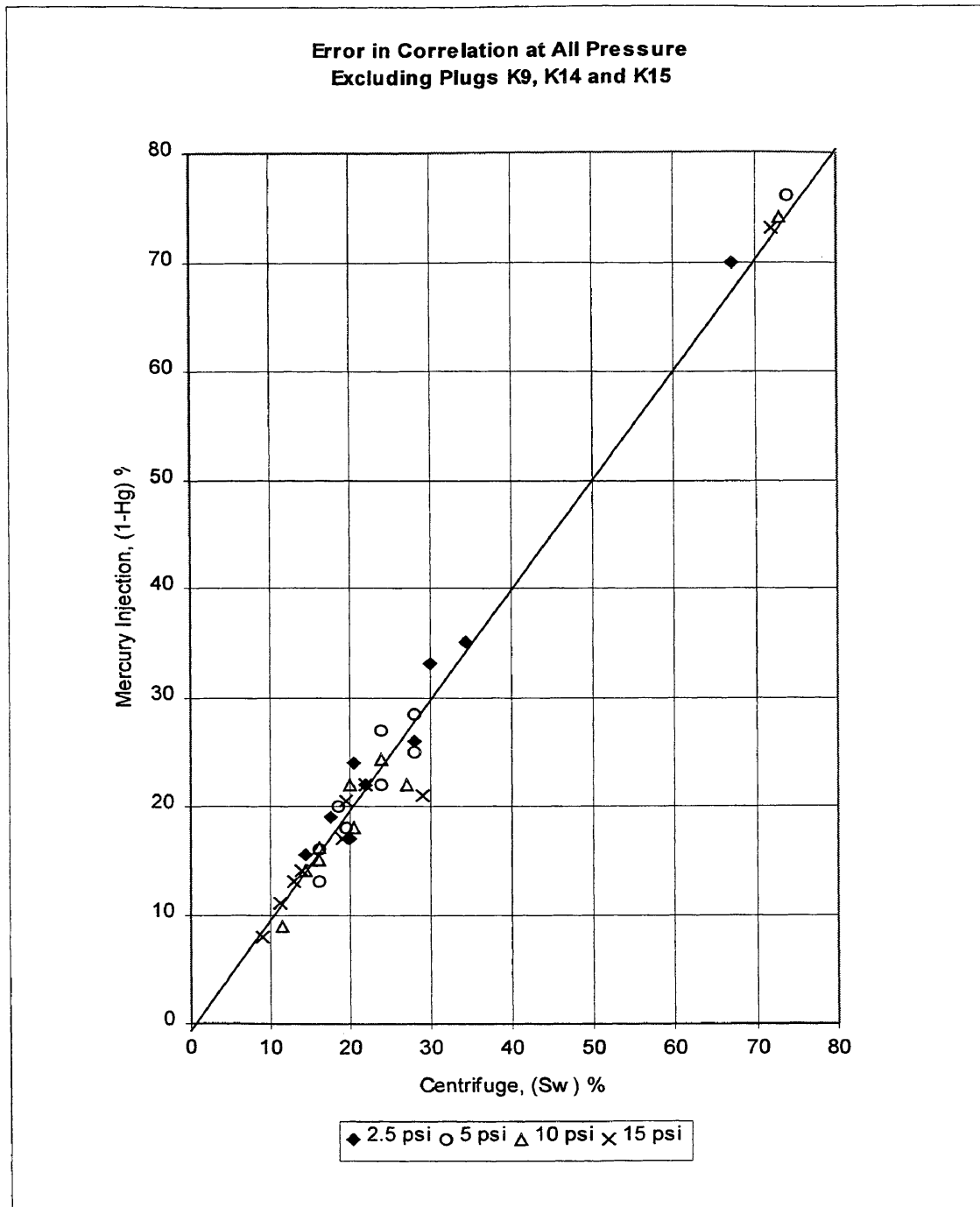


Figure 4.4.1 Correlation Error Plot for all Plugs Excluding Plugs K9, K14 and K15

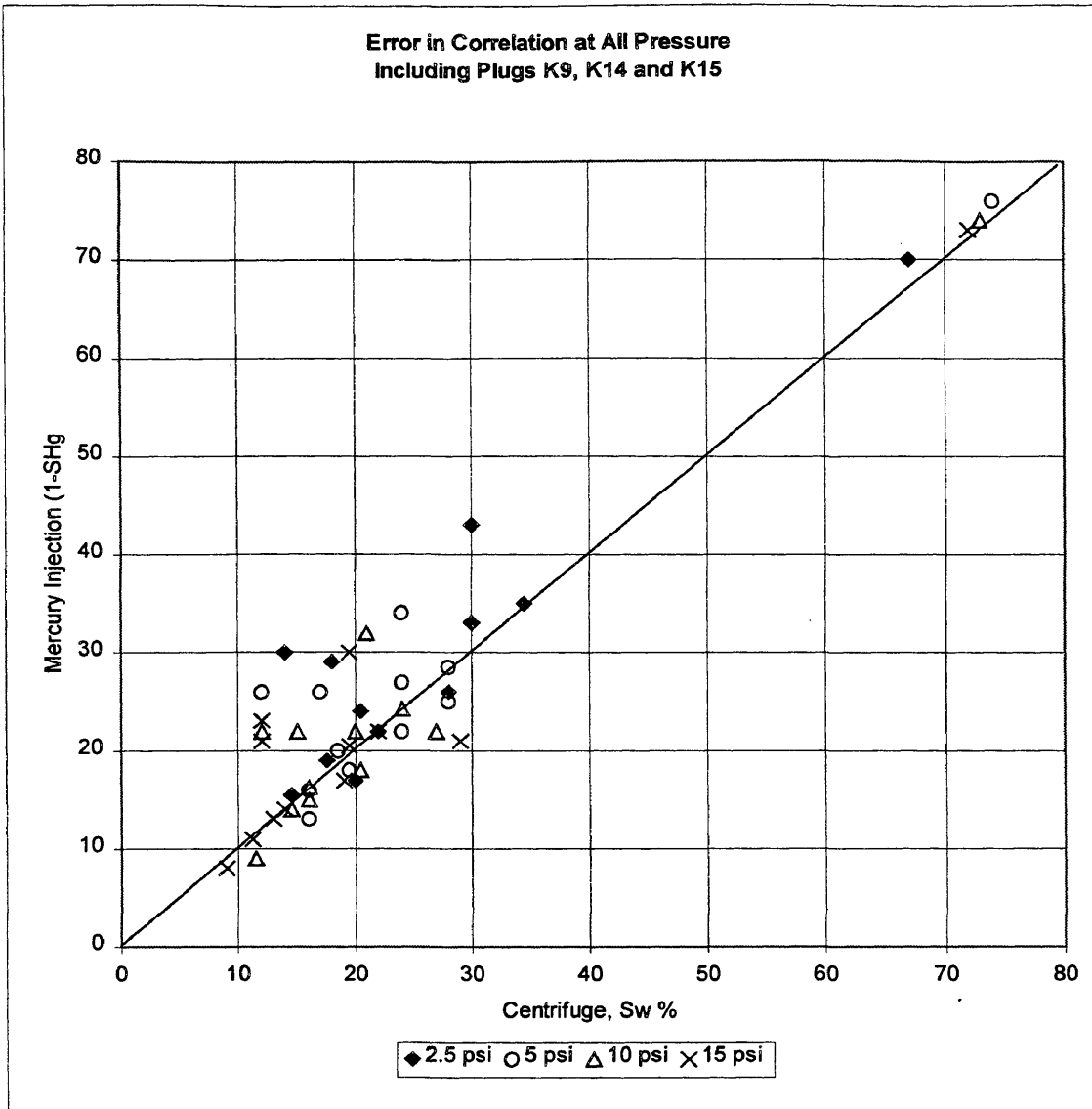


Figure 4.4.2 Correlation Error Plot for all Plugs

#### **4.5 Validation of Conversion Method**

One of the more recent works on conversion factors was Sabatiers (1994). His work contained comparisons between mercury injection and centrifuge using an oil-water fluid system (See Figure 4.5.1). He did not include any data in his paper; instead, he plotted sections of the comparison graphs. Therefore, it was not possible to test the conversion method on his data. Nevertheless, the water saturation divergence was apparent from his graphs. The divergence ranged from 7 to 10 saturation units on the six samples he used. As for the pressure, he used a wettability function to scale it, and he did not include any values.

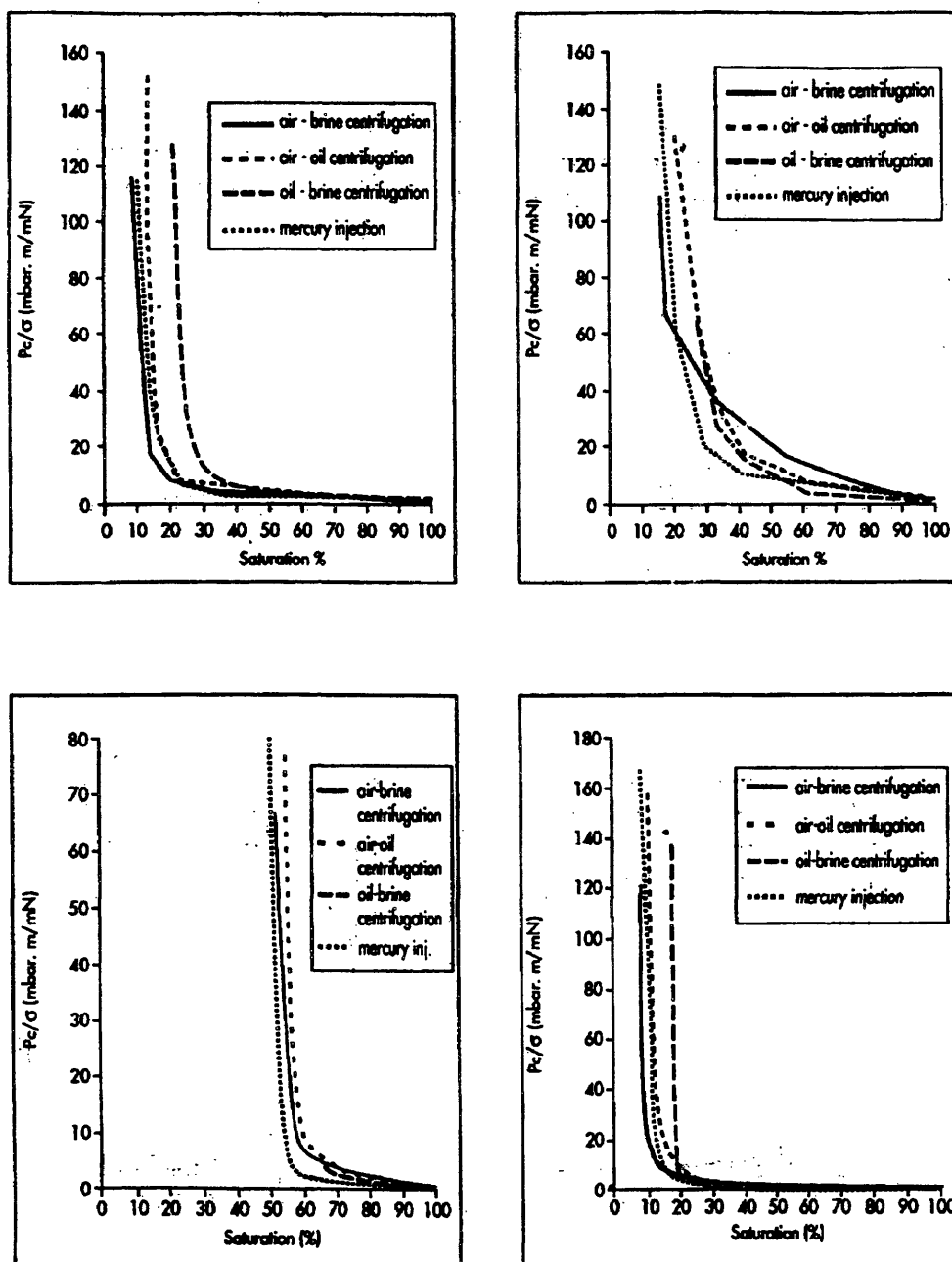


Figure 4.5.1 Samples of Capillary Pressure Comparisons from Sabatiers (1994)

## **CHAPTER 5**

### **CONCLUSIONS AND RECOMMENDATIONS**

In this chapter, conclusions made from the research and recommendations given for future work on related subjects are covered.

#### **5.1 Conclusions**

The conclusions drawn from this thesis are listed below.

- Capillary pressure curves from mercury-gas system and a water-oil system can be adapted for sandstone.
- Reducing the pressure from mercury injection by dividing by 48 and increasing the water saturation in the mercury injection method by 8 units is the conversion method developed for sandstone in this work.
- It was concluded that firing the plugs in temperatures up to 800° C and using a step function in a course of seven hours is optimal for stabilizing the plug

matrix. This procedure is in compliance with API methods and is needed for multiple tests.

- Measurement of capillary pressure curve in different apparatus, require different plug dimensions. We concluded that using part of the plug produces almost identical results compared with using the whole plug.

## 5.2 Recommendations

For future work the following is recommended.

- Increase the number of samples used in the test in order to observe other deviations if they exist.
- Use different plug lithologies and find appropriate conversion methods.
- Use different fluid properties, e.g. density, in order to see the effect on the conversion method.

## NOMENCLATURE

BV	- Bulk volume of the plug (cc).
GV	- Grain volume of the plug in (cc).
K	- Permeability (md).
L	- Laboratory.
P	- Pressure.
P <sub>c</sub>	- Capillary Pressure.
P <sub>oil</sub>	- Oil Pressure.
P <sub>water</sub>	- Water Pressure.
P <sub>Hg-gas</sub>	- Capillary Pressure between Mercury and Gas.
P <sub>water-air</sub>	- Capillary Pressure between Water and Air.
PTS	- Pore Throat Sorting.
PV	- Pore Volume.
r	- Average Pore Throat Radius.
R	- Reservoir
rb	- Distance to Core Bottom.
rt	- Distance to Core Top.
RG	- Reservoir Grade.

$Sw_i$	- Initial Water Saturation.
$Sw_{avg}$	- Average Water Saturation.
$Sw_{adj}$	- Adjusted Water Saturation.
$Sw_{inlet}$	- Inlet Water Saturation.
$Wt_{dry}$	- Dry weight of the plug in (g).

**GREEK SYMBOLS**

- $\sigma$  - Interfacial Tension.
- $\theta$  - Contact Angle.
- $^{\circ}$  - Degrees.
- $\rho$  - Density of Fluid Used.

## REFERENCES CITED

Al-Lawati, S. M. (1995). Oil Recovery by Static Imbibition in Low Tension Fluid Systems. Unpublished Master's of Science Thesis No. T-4753, Colorado School of Mines, Golden, Colorado, USA.

American Petroleum Institute. (1998). Recommended Practices for Core Analysis API Publication Report No. 40. (2nd ed.). Washington, D.C.

Amyx, J. W. Jr., Bass, D. M., Whiting, R. L. (1960). Petroleum Reservoir Engineering. New York: McGraw Hill.

Brown, H. W. (1951). Capillary Pressure Investigation. Trans. AIME: Vol. 192. (pp. 67-74).

Calhoun, J. C. Jr., Lewis, M. Jr., and Newman, R. C. (1949). Experiment on the Capillary Properties of Porous Solids. Trans. AIME. Vol. 186. (pp. 189-96).

Christiansen, Richard. L. (1992). Geometric Concerns For Accurate Measurement of capillary Pressure Relationships with Centrifuge Methods. SPE, Paper No. 19026.

Craig, F. F. (1997). The Reservoir Engineering Aspect of Water Flooding. SPE Monograph Series #3.

Graves, R. M. (1996) Advance Rocks and Fluids Properties. 508 class notes.  
Colorado School of Mines, Golden, Colorado.

Hassler, G. L., and Brunner, E.(1944). Measurement of Capillary Pressure in Small Core Samples. Trans. AIME, Vol. 160. (pp. 114-123).

Jennings, J.B. (1987). Capillary Pressure Techniques: Application to Exploration and Development Geology. AAPG Bulletin, Vol.71, No.10. (pp.1196-1209).

Leverett, M. C. 1941). Capillary Behavior in Porous Solids. Trans. AIME, Vol. 142. (pp. 152-169).

Ma, S., and Morrow, N. R.(1991). Effect of Firing on Petrophysical Properties of Berea Sandstone. SPE, Paper No. 21045, International Symposium on Oilfield Chemistry, Anaheim, California.

McCullough, J. J., Allbaugh, F. W., and Jones, P.H. (1944) Determination of the Interstitial-Water Saturation Content of Oil and Gas Sand by Laboratory Test of Core Samples. Drill. and Prod.Prac., (pp. 180-88). American Petroleum Institute.

Morrow, N. R. (1991) Interfacial Phenomenon in Petroleum Recovery. Marcel-Dakka, Inc., New York.

Omoregle, Z. S. (1988) Factors Affecting the Equivalency of Different Capillary Pressure Measurement Techniques. SPE, Paper No. 15384.

Purcell, W.R.(1949) Capillary Pressure: Their Measurement Using Mercury and The Calculation of Permeability Therefrom. Trans. AIME, Vol. 186. (pp. 39-48).

Sabatier, Lionel. (1994) Comparative Study of Drainage Capillary Pressure Measurement Using Different Techniques and Different Fluid System. International Symposium of The Society of Core Analysts, Stavanger, Norway.

Skuse, Brian. (1992). Computation and Interpretation of Capillary Pressure from Centrifuge. SPE, Paper No. 18297.

Swanson, Ben. F, A Simple Correlation Between Air Permeabilities and Stressed Brine Permeabilities with Mercury Capillary Pressures. SPE, Paper No. 8234, 53rd Annual Technical Conference and Exhibition of SPE ,Texas.

Thomeer, J. H. M. (1960). Introduction of a Pore Geometrical Factory Define By Capillary Pressure Curve. Journal of Petroleum Technology, Vol. 12. (pp. 73-77).

# APPENDICES

## **Appendix – A**

### **Calculation Procedure for Centrifuge Method**

## Calculation Procedure for Centrifuge Method

CPDA is a computer program that uses the Rajan method to calculate adjusted saturation. The Rajan method is a theoretically correct analytical solution of the equation originally presented by Hassler and Brunner (1944). Curve fits required are found by performing polynomial regression on the natural log of the data. Results are in Appendix B.

### Equation for Capillary Pressure.

$$P_c = 7.94^{-8} (\rho_1 - \rho_2) \text{RPM}^2 (rb^2 - rt^2)$$

$\rho_1$  = density one (g/cc) lab temp.

$\rho_2$  = density two (g/cc) lab temp.

rb = distance to core bottom (cm).

rt = distance to core top (cm).

### Equation for Adjusted Saturation.

$$S_{adj}(P_{cl}) = S_{avg}(P_{cl}) + \left[ \frac{2R}{1+R} \cdot P_{cl} \cdot \frac{dS_{avg}(P_{cl})}{dP_{cl}} \right]$$

$$+ \frac{R}{(1-R^2)} \int_0^{P_{cl}} \left\{ \frac{1 - \left[ 1 - \frac{P_c}{P_{cl}} (1-R^2) \right]^{1/2}}{\left[ 1 - \frac{P_c}{P_{cl}} (1-R^2) \right]^{1/2}} \right\}^2 \left[ \frac{dS_{avg}(P_c)}{dP_c} \right] dP_c$$

$S_{adj}$  = adjusted saturation (%).

$S_{avg}$  = average saturation (%).

$P_c$  = capillary pressure (psi).

### Equation to Convert to Reservoir Conditions.

$$P_{cR} = \frac{P_{cL} (\sigma \cos \theta)_R}{(\sigma \cos \theta)_L}$$

$P_c$  = capillary pressure (psi).

$\sigma$  = interfacial tension (dynes/cm).

$\theta$  = contact angle (degrees).

$L$  = laboratory.

R = reservoir.

**Equation for Height above Zero Capillary Pressure.**

$$H = \frac{Pc_R}{(\rho_1 - \rho_2)(0.4335265)}$$

H = height (ft).

$Pc_R$  = reservoir capillary pressure (psi).

$\rho_1$  = density 1, reservoir temp.(g/cc).

$\rho_2$  = density 2, reservoir temp.(g/cc).

**Equation for Pore Entry Radii.**

$$R_i = \frac{2(\sigma \cos \theta)_L (0.145)}{Pc_L}$$

$R_i$  = pore entry radii (microns).

$\sigma$  = interfacial tension (dynes/cm).

$\theta$  = contact angle (degrees).

$Pc_L$  = laboratory capillary pressure (psi).

L = laboratory.

## **Appendix – B**

### **Centrifuge Raw Data**

Sample No: K1  
Centrifuge raw data

Table B-1

<b>Pc psi psi lab</b>	<b>Sw avg % PV</b>	<b>Sw inlet % PV Adjusted</b>	<b>Pc psi Reservoir</b>	<b>Height Ft</b>	<b>Pore throat radius microns</b>
1	68.198	45.700	1	17.881	8.69867
2	52.411	33.542	2	35.762	4.34934
3	44.729	28.632	3	53.643	2.89956
4	40.046	25.944	4	71.524	2.17467
5	36.843	24.247	5	89.406	1.73973
6	34.495	23.083	6	107.287	1.44978
7	32.690	22.242	7	125.168	1.24267
8	31.255	21.610	8	143.049	1.08733
9	30.084	21.124	9	160.930	0.96652
10	29.110	20.743	10	178.811	0.86987
11	28.286	20.440	11	196.692	0.79079
12	27.581	20.198	12	214.573	0.72489
13	26.970	20.003	13	232.455	0.66913
14	26.436	19.845	14	250.336	0.62133
15	25.966	19.718	15	268.217	0.57991
16	25.549	19.617	16	286.098	0.54367
17	25.178	19.537	17	303.979	0.51169
18	24.845	19.474	18	321.860	0.48326
19	24.545	19.426	19	339.741	0.45782
20	24.275	19.392	20	357.622	0.43493
21	24.029	19.369	21	375.503	0.41422
22	23.806	19.355	22	393.385	0.39539
23	23.603	19.350	23	411.266	0.37820
24	23.417	19.350	24	429.147	0.36244
24.306	23.364	19.350	24.306	434.618	0.35788

Sample No. K3  
Centrifuge raw data

Table B-2

<b>Pc psi Psi Lab</b>	<b>Sw avg % PV</b>	<b>Sw inlet % PV adjusted</b>	<b>Pc Psi Reservoir</b>	<b>Height Ft</b>	<b>Pore throat radius microns</b>
1	74.728	52.485	1	17.881	8.69867
2	57.995	36.695	2	35.762	4.34934
3	49.105	30.015	3	53.643	2.89956
4	43.495	26.399	4	71.524	2.17467
5	39.602	24.186	5	89.406	1.73973
6	36.734	22.734	6	107.287	1.44978
7	34.531	21.739	7	125.168	1.24267
8	32.787	21.041	8	143.049	1.08733
9	31.375	20.547	9	160.930	0.96652
10	30.212	20.198	10	178.811	0.86987
11	29.240	19.958	11	196.692	0.79079
12	28.418	19.800	12	214.573	0.72489
13	27.717	19.707	13	232.455	0.66913
14	27.116	19.665	14	250.336	0.62133
15	26.596	19.665	15	268.217	0.57991
16	26.145	19.665	16	286.098	0.54367
17	25.752	19.665	17	303.979	0.51169
18	25.410	19.665	18	321.860	0.48326
19	25.110	19.665	19	339.741	0.45782
20	24.848	19.665	20	357.622	0.43493
21	24.619	19.665	21	375.503	0.41422
22	24.419	19.665	22	393.385	0.39539
22.794	24.278	19.665	22.794	407.586	0.38162

Sample No. K4  
Centrifuge raw data

Table B-3

<b>Pc psi psi lab</b>	<b>Sw avg % PV</b>	<b>Sw inlet % PV Adjusted</b>	<b>Pc psi reservoir</b>	<b>Height ft</b>	<b>Pore throat Radius Microns</b>
1	46.900	33.136	1	17.881	8.69867
2	34.015	28.380	2	35.762	4.34934
3	28.895	26.507	3	53.643	2.89956
4	25.990	25.242	4	71.524	2.17467
5	24.030	24.206	5	89.406	1.73973
6	22.564	23.285	6	107.287	1.44978
7	21.391	22.438	7	125.168	1.24267
8	20.408	21.644	8	143.049	1.08733
9	19.556	20.893	9	160.930	0.96652
10	18.800	20.179	10	178.811	0.86987
11	18.117	19.499	11	196.692	0.79079
12	17.490	18.85	12	214.573	0.72489
13	16.910	18.232	13	232.455	0.66913
14	16.369	17.641	14	250.336	0.62133
15	15.860	17.077	15	268.217	0.57991
16	15.380	16.538	16	286.098	0.54367
17	14.924	16.023	17	303.979	0.51169
18	14.490	15.532	18	321.86	0.48326
19	14.077	15.062	19	339.741	0.45782
20	13.681	14.615	20	357.622	0.43493
21	13.301	14.187	21	375.503	0.41422
22	12.937	13.779	22	393.385	0.39539
23	12.587	13.390	23	411.266	0.37820
24	12.250	13.019	24	429.147	0.36244
24.010	12.247	13.015	24.010	429.336	0.36228

Sample No. K5  
Centrifuge raw data

Table B-4

<b>Pc psi psi lab</b>	<b>Sw avg % PV</b>	<b>Sw inlet % PV Adjusted</b>	<b>Pc psi reservoir</b>	<b>Height Ft</b>	<b>Pore throat radius microns</b>
1	37.702	19.208	1	17.881	8.69867
2	27.204	16.653	2	35.762	4.34934
3	23.406	16.009	3	53.643	2.89956
4	21.432	15.690	4	71.524	2.17467
5	20.208	15.455	5	89.406	1.73973
6	19.360	15.240	6	107.287	1.44978
7	18.726	15.022	7	125.168	1.24267
8	18.223	14.794	8	143.049	1.08733
9	17.806	14.555	9	160.930	0.96652
10	17.447	14.304	10	178.811	0.86987
11	17.129	14.042	11	196.692	0.79079
12	16.841	13.772	12	214.573	0.72489
13	16.575	13.495	13	232.455	0.66913
14	16.32593	13.211	14	250.336	0.62133
15	16.089	12.924	15	268.217	0.57991
16	15.863	12.633	16	286.098	0.54367
17	15.646	12.339	17	303.979	0.51169
18	15.435	12.045	18	321.860	0.48326
19	15.230	11.750	19	339.741	0.45782
20	15.030	11.456	20	357.622	0.43493
21	14.834	11.162	21	375.503	0.41422
22	14.642	10.870	22	393.385	0.39539
23	14.453	10.581	23	411.266	0.37820
24	14.267	10.294	24	429.147	0.36244
25	14.084	10.010	25	447.028	0.34795
25.197	14.048	9.9544	25.197	450.558	0.34522

Sample No. K6  
Centrifuge raw data

Table B-5

<b>Pc psi</b>	<b>Sw avg</b>	<b>Sw inlet</b>	<b>Pc</b>	<b>Height</b>	<b>Pore throat radius</b>
<b>psi lab</b>	<b>% PV</b>	<b>% PV Adjusted</b>	<b>psi reservoir</b>	<b>Ft</b>	<b>microns</b>
1	46.018	29.419	1	17.881	8.69867
2	32.939	23.975	2	35.762	4.34934
3	27.639	21.925	3	53.643	2.89956
4	24.634	20.667	4	71.524	2.17467
5	22.631	19.723	5	89.406	1.73973
6	21.160	18.943	6	107.287	1.44978
7	20.008	18.262	7	125.168	1.24267
8	19.065	17.648	8	143.049	1.08733
9	18.267	17.084	9	160.930	0.96652
10	17.574	16.559	10	178.811	0.86987
11	16.961	16.066	11	196.692	0.79079
12	16.410	15.600	12	214.573	0.72489
13	15.908	15.157	13	232.455	0.66913
14	15.446	14.736	14	250.336	0.62133
15	15.018	14.334	15	268.217	0.57991
16	14.619	13.950	16	286.098	0.54367
17	14.244	13.581	17	303.979	0.51169
18	13.891	13.228	18	321.860	0.48326
19	13.556	12.889	19	339.741	0.45782
20	13.237	12.563	20	357.622	0.43493
21	12.934	12.250	21	375.503	0.41422
22	12.644	11.949	22	393.385	0.39539
23	12.366	11.659	23	411.266	0.37820
24	12.099	11.380	24	429.147	0.36244
24.883	11.872	11.142	24.883	444.950	0.34957

Sample No. K9  
Centrifuge raw data

Table B-6

<b>Pc psi psi lab</b>	<b>Sw avg % PV</b>	<b>Sw inlet % PV adjusted</b>	<b>Pc psi reservoir</b>	<b>Height Ft</b>	<b>Pore throat radius microns</b>
1	42.098	22.400	1	17.881	8.69867
2	30.534	18.373	2	35.762	4.34934
3	26.04	17.051	3	53.643	2.89956
4	23.593	16.322	4	71.524	2.17467
5	22.014	15.804	5	89.406	1.73973
6	20.891	15.384	6	107.287	1.44978
7	20.036	15.016	7	125.168	1.24267
8	19.353	14.677	8	143.049	1.08733
9	18.78	14.357	9	160.930	0.96652
10	18.300	14.050	10	178.811	0.86987
11	17.875	13.752	11	196.692	0.79079
12	17.492	13.461	12	214.573	0.72489
13	17.154	13.175	13	232.455	0.66913
14	16.839	12.895	14	250.336	0.62133
15	16.547	12.619	15	268.217	0.57991
16	16.274	12.34	16	286.098	0.54367
17	16.017	12.080	17	303.979	0.51169
18	15.773	11.817	18	321.860	0.48326
19	15.541	11.557	19	339.741	0.45782
20	15.318	11.302	20	357.622	0.43493
21	15.104	11.050	21	375.503	0.41422
22	14.898	10.803	22	393.385	0.39539
23	14.699	10.559	23	411.266	0.3782
23.324	14.635	10.481	23.324	417.075	0.37294

Sample No. K10  
Centrifuge raw data

Table B-7

<b>Pc psi psi lab</b>	<b>Sw avg % PV</b>	<b>Sw inlet % PV Adjusted</b>	<b>Pc psi reservoir</b>	<b>Height Ft</b>	<b>Pore throat Radius Microns</b>
1	53.177	30.658	1	17.881	8.69867
2	37.290	23.057	2	35.762	4.34934
3	30.706	20.407	3	53.643	2.89956
4	26.986	18.949	4	71.524	2.17467
5	24.542	17.968	5	89.406	1.73973
6	22.784	17.229	6	107.287	1.44978
7	21.442	16.634	7	125.168	1.24267
8	20.371	16.130	8	143.049	1.08733
9	19.489	15.691	9	160.930	0.96652
10	18.744	15.291	10	178.811	0.86987
11	18.102	14.942	11	196.692	0.79079
12	17.539	14.613	12	214.573	0.72489
13	17.039	14.307	13	232.455	0.66913
14	16.590	14.020	14	250.336	0.62133
15	16.182	13.749	15	268.217	0.57991
16	15.809	13.492	16	286.098	0.54367
17	15.465	13.247	17	303.979	0.51169
18	15.146	13.012	18	321.860	0.48326
19	14.849	12.787	19	339.741	0.45782
20	14.570	12.571	20	357.622	0.43493
21	14.308	12.362	21	375.503	0.41422
22	14.060	12.160	22	393.385	0.39539
23	13.825	11.965	23	411.266	0.37820
24	13.602	11.776	24	429.147	0.36244
24.710	13.450	11.64	24.710	441.850	0.35202

Sample No. K13  
Centrifuge raw data

Table B-8

<b>Pc psi psi lab</b>	<b>Sw avg % PV</b>	<b>Sw inlet % PV Adjusted</b>	<b>Pc Psi Reservoir</b>	<b>Height ft</b>	<b>Pore throat Radius Microns</b>
1	75.408	54.388	1	17.881	8.69867
2	59.762	40.298	2	35.762	4.34934
3	51.580	34.177	3	53.643	2.89956
4	46.402	30.718	4	71.524	2.17467
5	42.778	28.497	5	89.406	1.73973
6	40.078	26.961	6	107.287	1.44978
7	37.978	25.844	7	125.168	1.24267
8	36.293	25.005	8	143.049	1.08733
9	34.910	24.360	9	160.930	0.96652
10	33.754	23.856	10	178.811	0.86987
11	32.772	23.457	11	196.692	0.79079
12	31.929	23.140	12	214.573	0.72489
13	31.197	22.887	13	232.455	0.66913
14	30.557	22.686	14	250.336	0.62133
15	29.993	22.527	15	268.217	0.57991
16	29.493	22.403	16	286.098	0.54367
17	29.047	22.308	17	303.979	0.51169
18	28.648	22.238	18	321.860	0.48326
19	28.289	22.188	19	339.741	0.45782
20	27.966	22.157	20	357.622	0.43493
21	27.674	22.141	21	375.503	0.41422
22	27.409	22.140	22	393.385	0.39539
23	27.168	22.140	23	411.266	0.37820
24	26.949	22.140	24	429.147	0.36244
24.805	26.787	22.140	24.805	443.543	0.35068

Sample No. K14  
Centrifuge raw data

Table B-9

<b>Pc psi Psi Lab</b>	<b>Sw avg % PV</b>	<b>Sw inlet % PV Adjusted</b>	<b>Pc psi reservoir</b>	<b>Height ft</b>	<b>Pore throat Radius Microns</b>
1	72.408	50.153	1	17.881	8.69867
2	56.117	35.894	2	35.762	4.34934
3	47.734	29.888	3	53.643	2.89956
4	42.491	26.577	4	71.524	2.17467
5	38.858	24.497	5	89.406	1.73973
6	36.173	23.087	6	107.287	1.44978
7	34.102	22.082	7	125.168	1.24267
8	32.452	21.344	8	143.049	1.08733
9	31.106	20.788	9	160.930	0.96652
10	29.987	20.365	10	178.811	0.86987
11	29.043	20.041	11	196.692	0.79079
12	28.237	19.792	12	214.573	0.72489
13	27.542	19.602	13	232.455	0.66913
14	26.937	19.460	14	250.336	0.62133
15	26.407	19.356	15	268.217	0.57991
16	25.940	19.284	16	286.098	0.54367
17	25.527	19.239	17	303.979	0.51169
18	25.160	19.216	18	321.860	0.48326
19	24.831	19.212	19	339.741	0.45782
20	24.538	19.212	20	357.622	0.43493
21	24.274	19.212	21	375.503	0.41422
22	24.037	19.212	22	393.385	0.39539
23	23.824	19.212	23	411.266	0.37820
23.592	23.707	19.212	23.592	421.855	0.36871

Sample No. K15  
Centrifuge raw data

Table B-10

<b>Pc psi Psi Lab</b>	<b>Sw avg % PV</b>	<b>Sw inlet % PV Adjusted</b>	<b>Pc psi reservoir</b>	<b>Height ft</b>	<b>Pore throat Radius Microns</b>
1	49.807	23.727	1	17.881	8.69867
2	33.311	15.182	2	35.762	4.34934
3	26.454	12.699	3	53.643	2.89956
4	22.693	11.669	4	71.524	2.17467
5	20.328	11.192	5	89.406	1.73973
6	18.716	10.982	6	107.287	1.44978
7	17.559	10.920	7	125.168	1.24267
8	16.698	10.920	8	143.049	1.08733
9	16.042	10.920	9	160.930	0.96652
10	15.533	10.920	10	178.811	0.86987
11	15.135	10.920	11	196.692	0.79079
12	14.821	10.920	12	214.573	0.72489
13	14.573	10.920	13	232.455	0.66913
14	14.378	10.920	14	250.336	0.62133
15	14.227	10.920	15	268.217	0.57991
16	14.112	10.920	16	286.098	0.54367
17	14.027	10.920	17	303.979	0.51169
18	13.968	10.920	18	321.860	0.48326
19	13.931	10.920	19	339.741	0.45782
20	13.912	10.920	20	357.622	0.43493
21	13.911	10.920	21	375.503	0.41422
22	13.924	10.920	22	393.385	0.39539
23	13.951	10.920	23	411.266	0.37820
23.389	13.964	10.920	23.389	418.238	0.37190

Sample No. K16  
Centrifuge raw data

Table B-11

<b>Pc psi psi lab</b>	<b>Sw avg % PV</b>	<b>Sw inlet % PV Adjusted</b>	<b>Pc psi reservoir</b>	<b>Height Ft</b>	<b>Pore throat radius microns</b>
1	84.896	74.555	1	17.881	8.69867
2	77.719	69.161	2	35.762	4.34934
3	74.254	66.988	3	53.643	2.89956
4	72.149	65.797	4	71.524	2.17467
5	70.710	65.034	5	89.406	1.73973
6	69.652	64.493	6	107.287	1.44978
7	68.835	64.081	7	125.168	1.24267
8	68.180	63.749	8	143.049	1.08733
9	67.639	63.469	9	160.930	0.96652
10	67.182	63.224	10	178.811	0.86987
11	66.787	63.003	11	196.692	0.79079
12	66.442	62.800	12	214.573	0.72489
13	66.135	62.610	13	232.455	0.66913
14	65.859	62.429	14	250.336	0.62133
15	65.609	62.255	15	268.217	0.57991
16	65.378	62.086	16	286.098	0.54367
17	65.166	61.921	17	303.979	0.51169
18	64.967	61.759	18	321.860	0.48326
19	64.781	61.599	19	339.741	0.45782
20	64.606	61.441	20	357.622	0.43493
21	64.439	61.284	21	375.503	0.41422
22	64.281	61.129	22	393.385	0.39539
23	64.129	60.974	23	411.266	0.37820
23.850	64.005	60.843	23.850	426.466	0.36472

Sample No. K17  
Centrifuge raw data

Table B-12

<b>Pc psi psi lab</b>	<b>Sw avg % PV</b>	<b>Sw inlet % PV Adjusted</b>	<b>Pc psi reservoir</b>	<b>Height ft</b>	<b>Pore throat radius microns</b>
1	75.408	54.388	1	17.881	8.69867
2	59.76	40.298	2	35.762	4.34934
3	51.580	34.177	3	53.643	2.89956
4	46.402	30.718	4	71.524	2.17467
5	42.778	28.497	5	89.406	1.73973
6	40.078	26.961	6	107.287	1.44978
7	37.978	25.844	7	125.168	1.24267
8	36.293	25.005	8	143.049	1.08733
9	34.910	24.360	9	160.930	0.96652
10	33.754	23.856	10	178.811	0.86987
11	32.772	23.457	11	196.692	0.79079
12	31.929	23.140	12	214.573	0.72489
13	31.197	22.887	13	232.455	0.66913
14	30.557	22.686	14	250.336	0.62133
15	29.993	22.527	15	268.217	0.57991
16	29.493	22.403	16	286.098	0.54367
17	29.047	22.308	17	303.979	0.51169
18	28.648	22.238	18	321.86	0.48326
19	28.289	22.188	19	339.741	0.45782
20	27.966	22.157	20	357.622	0.43493
21	27.674	22.141	21	375.503	0.41422
22	27.409	22.140	22	393.385	0.39539
23	27.168	22.140	23	411.266	0.37820
24	26.949	22.140	24	429.147	0.36244
24.805	26.787	22.140	24.805	443.543	0.35068

## **Appendix – C**

### **Capillary Pressure Curves from Centrifuge and Mercury Injection Methods**

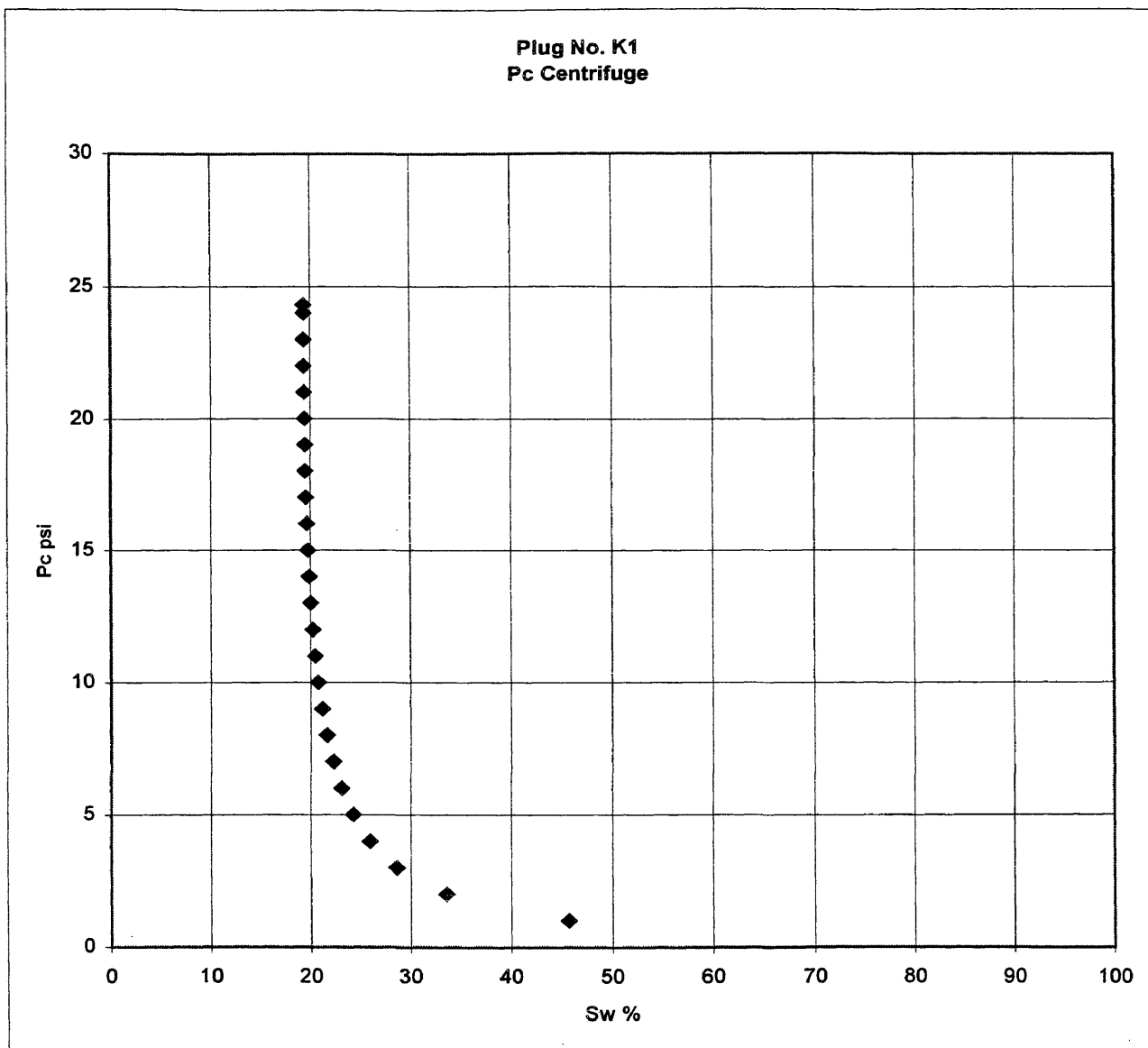


Figure C-1 Centrifugal capillary pressure curve

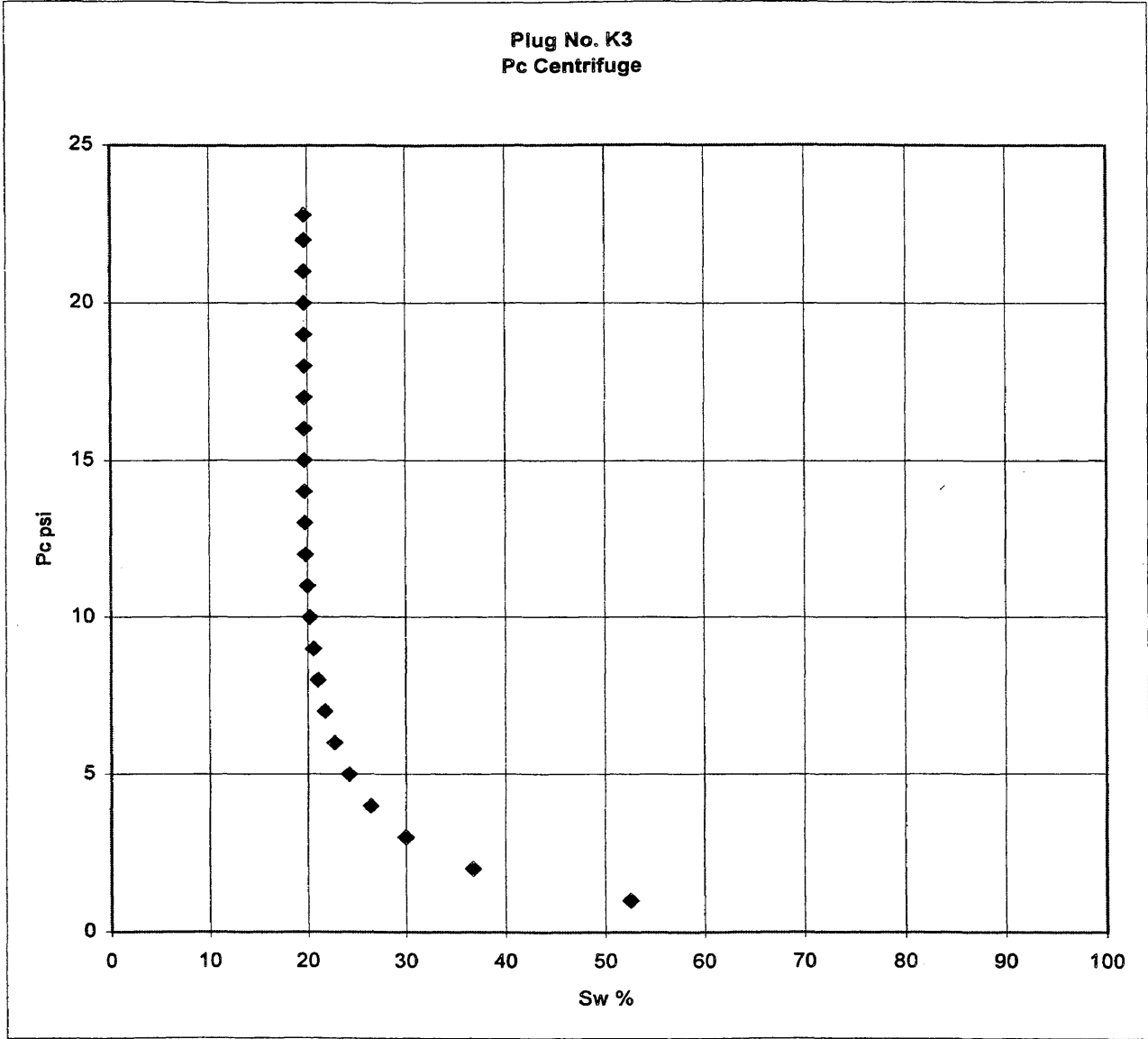


Figure C-2 Centrifugal capillary pressure curve

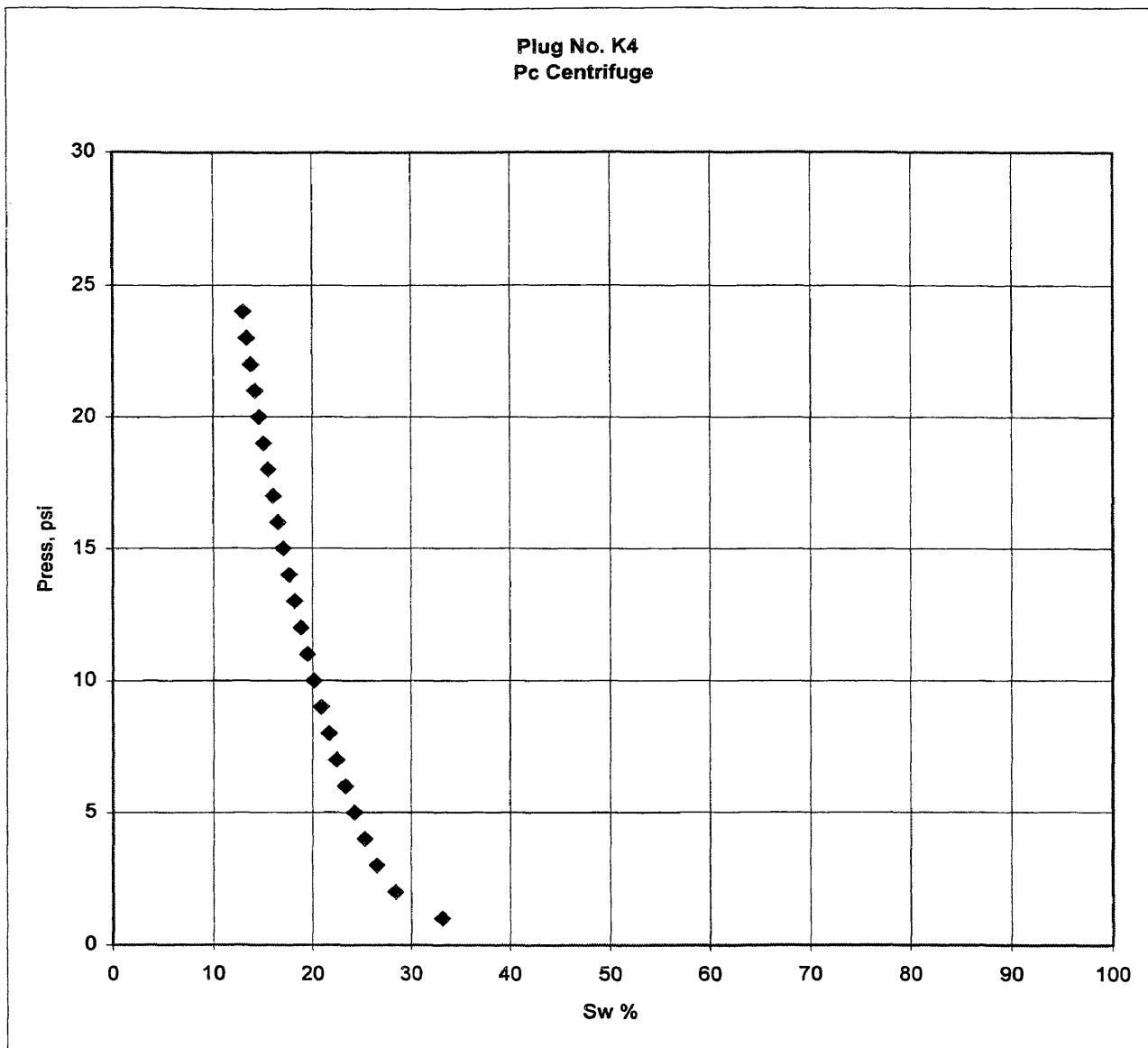


Figure C-3 Centrifugal capillary pressure curve

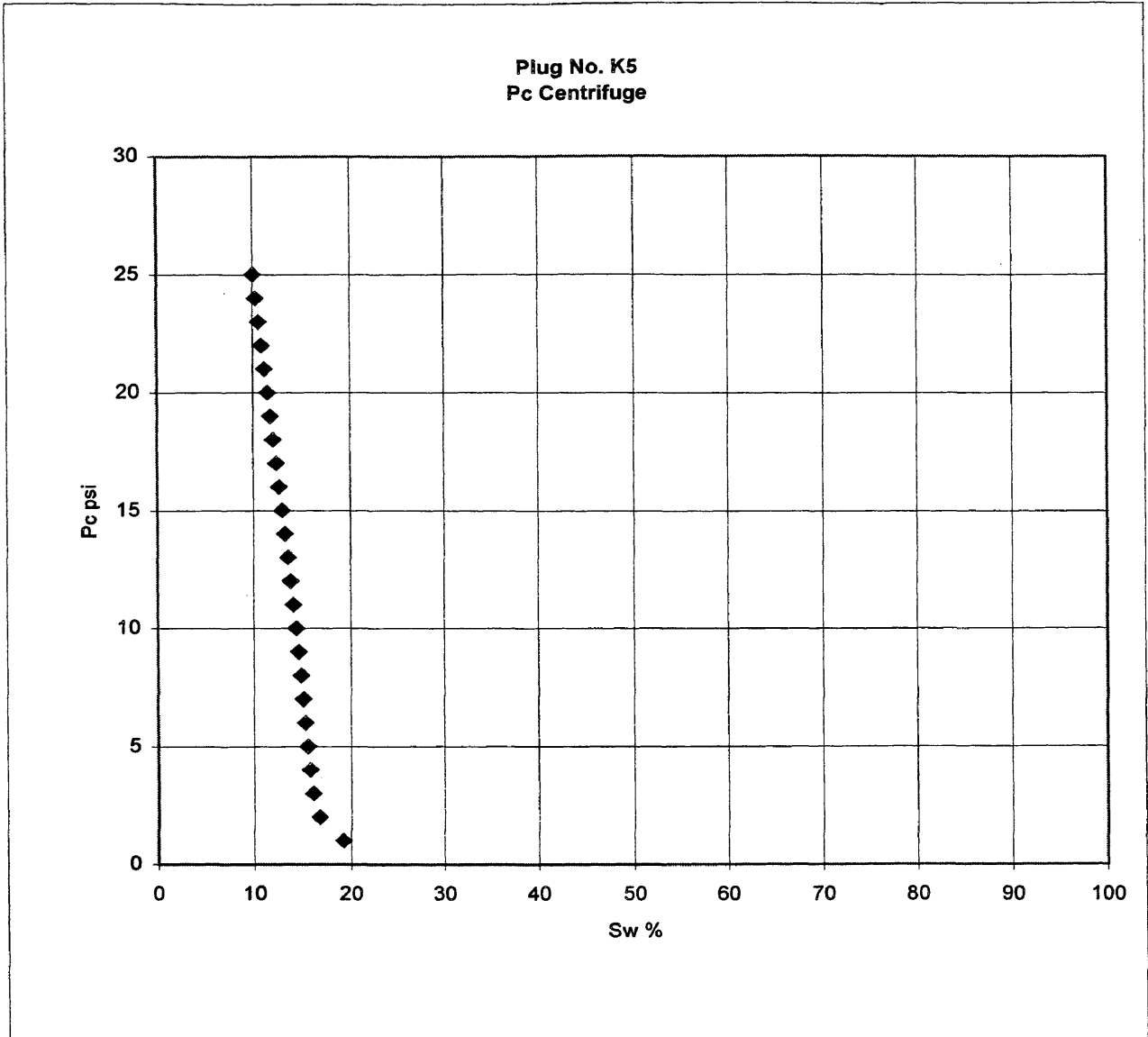


Figure C-4 Centrifugal capillary pressure curve

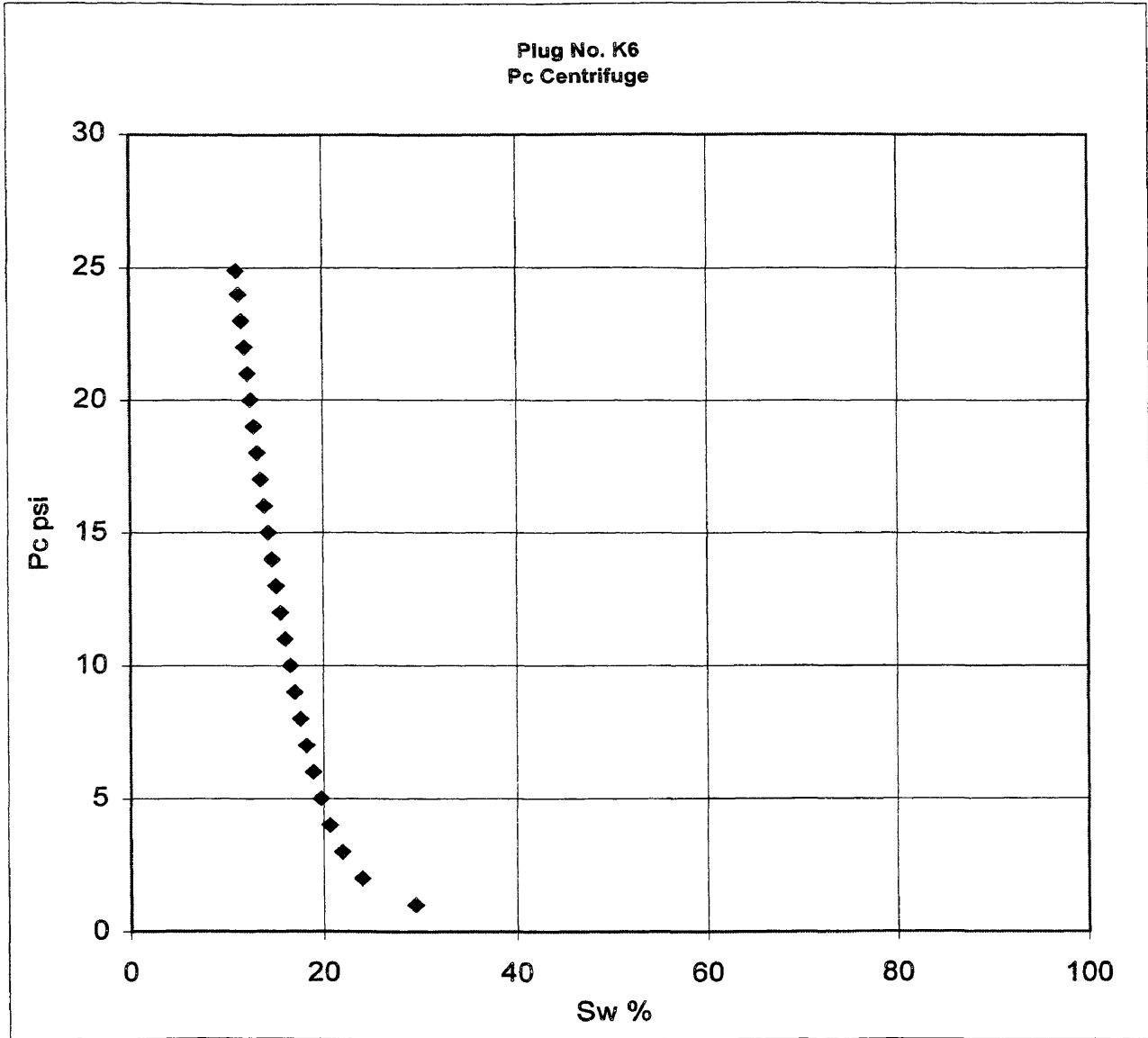


Figure C-5 Centrifugal capillary pressure curve

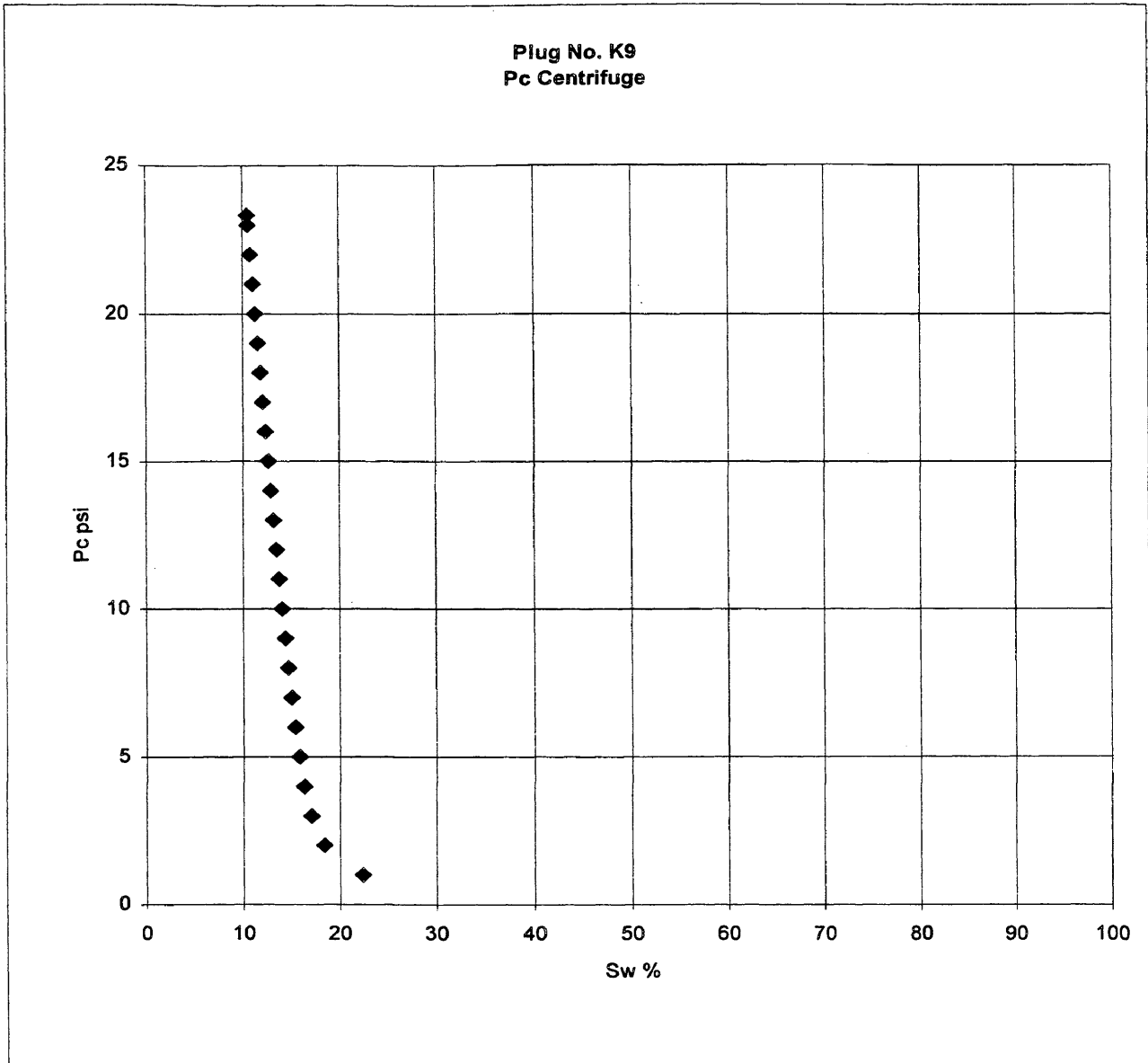


Figure C-6 Centrifugal capillary pressure curve

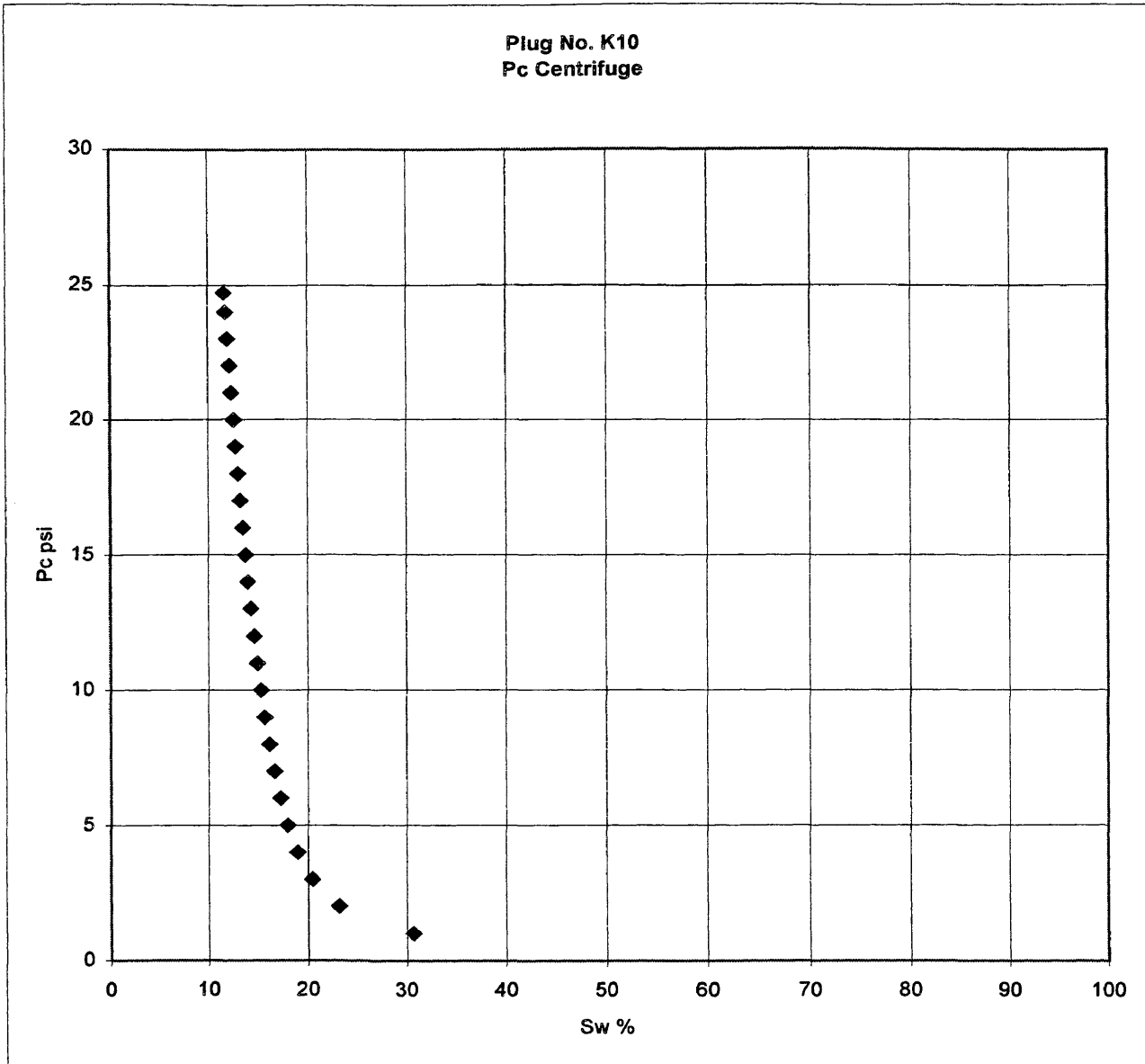


Figure C-7 Centrifugal capillary pressure curve

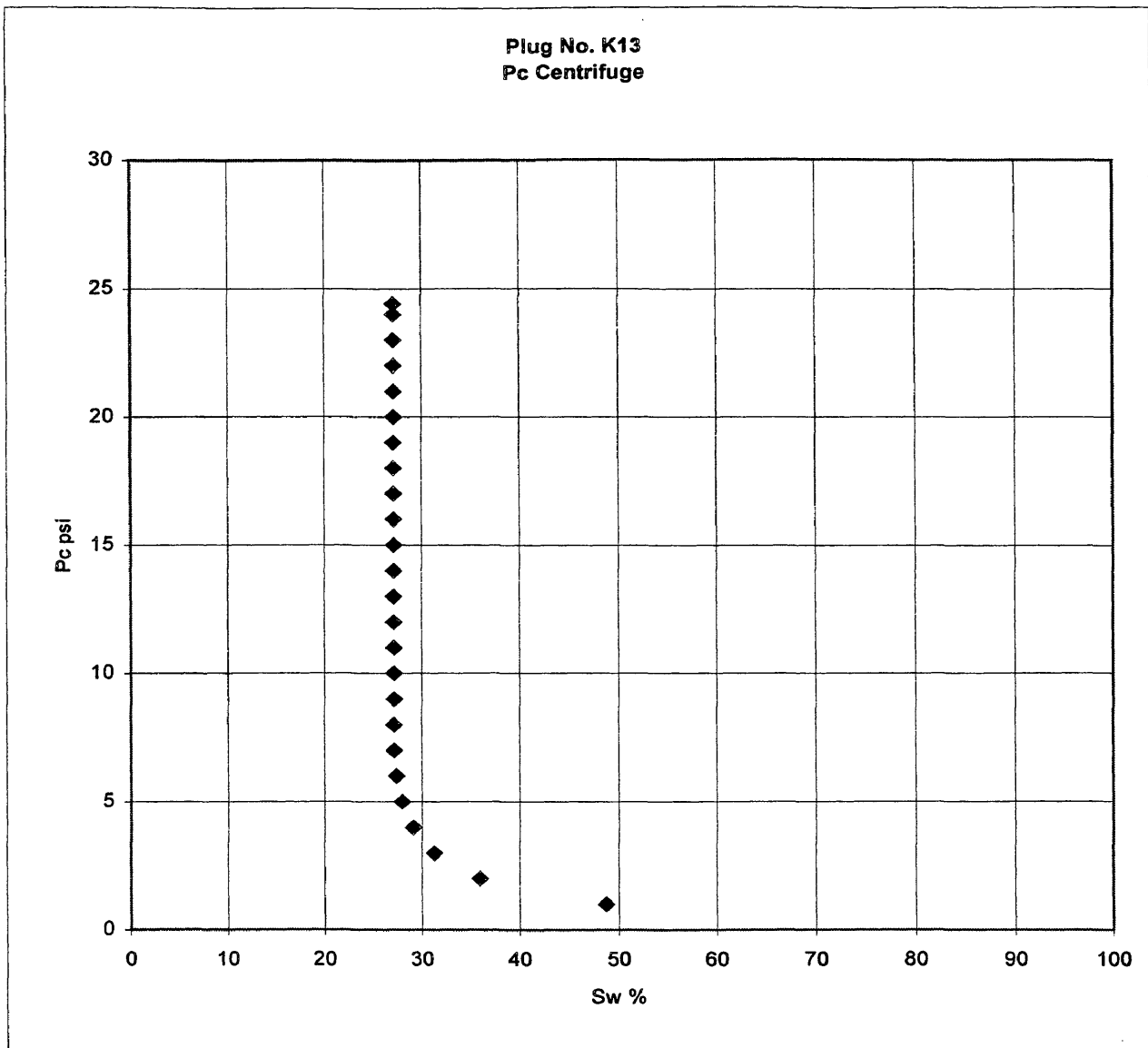


Figure C-8 Centrifugal capillary pressure curve

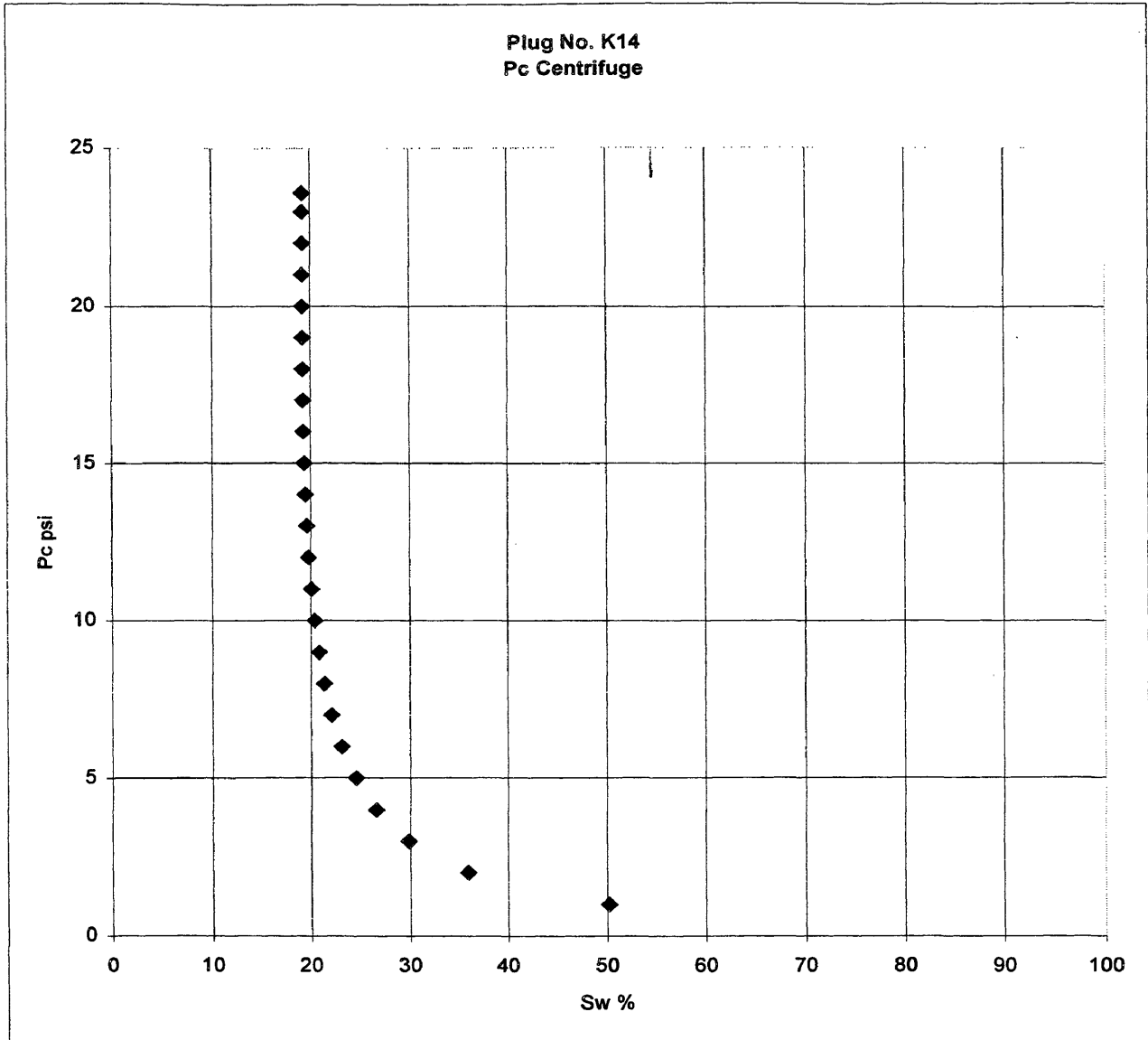


Figure C-9 Centrifugal capillary pressure curve

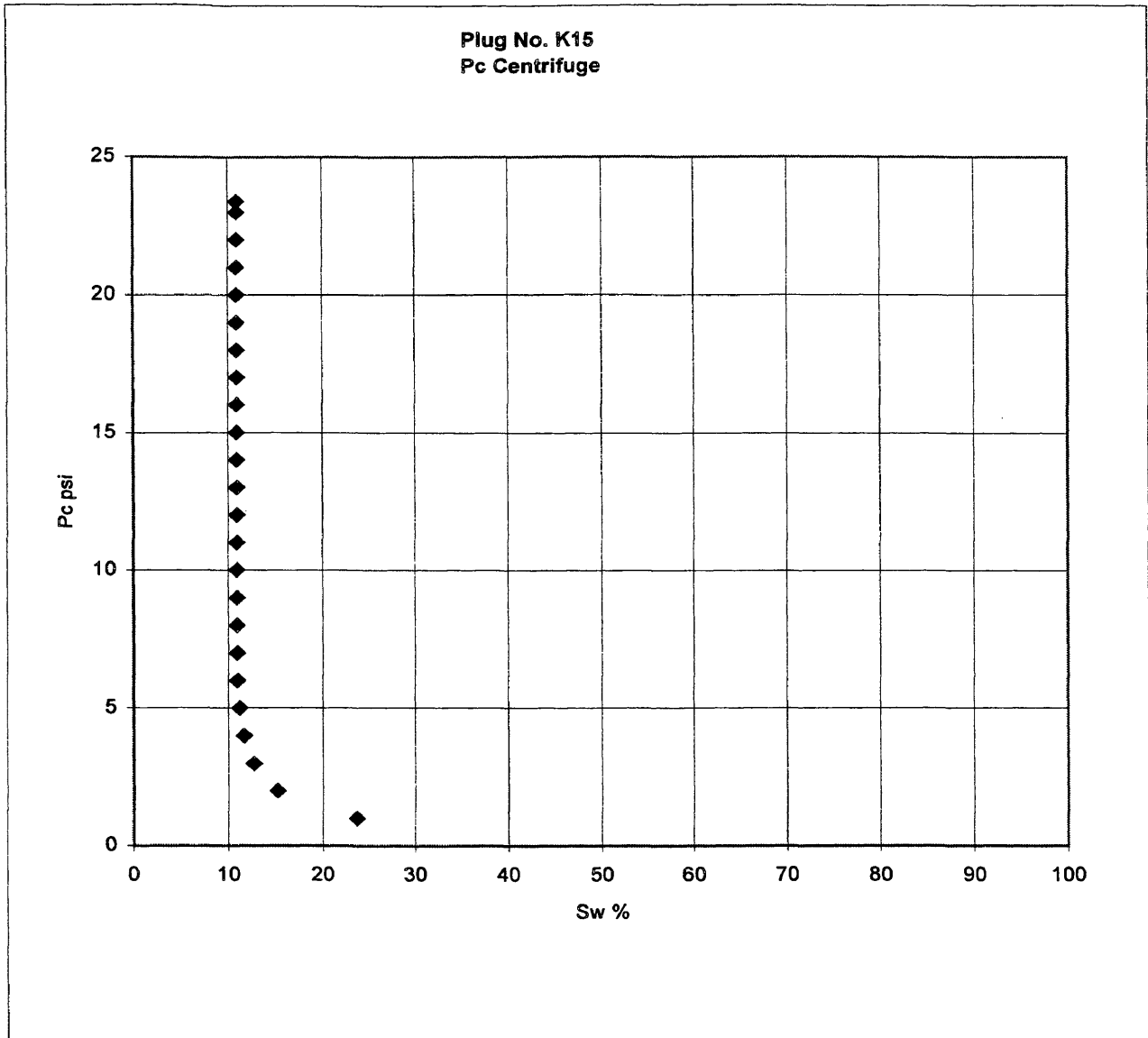


Figure C-10 Centrifugal capillary pressure curve

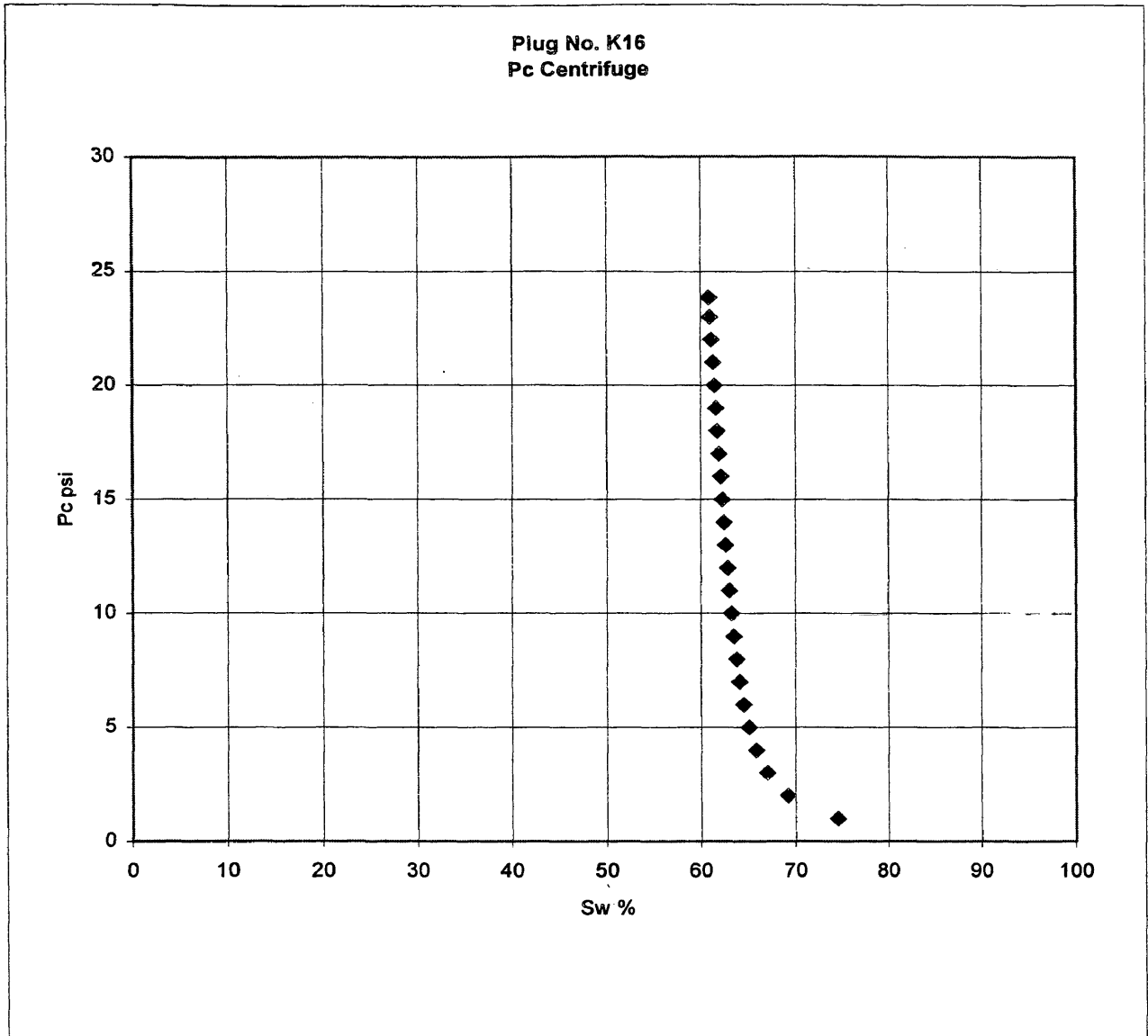


Figure C-11 Centrifugal capillary pressure curve

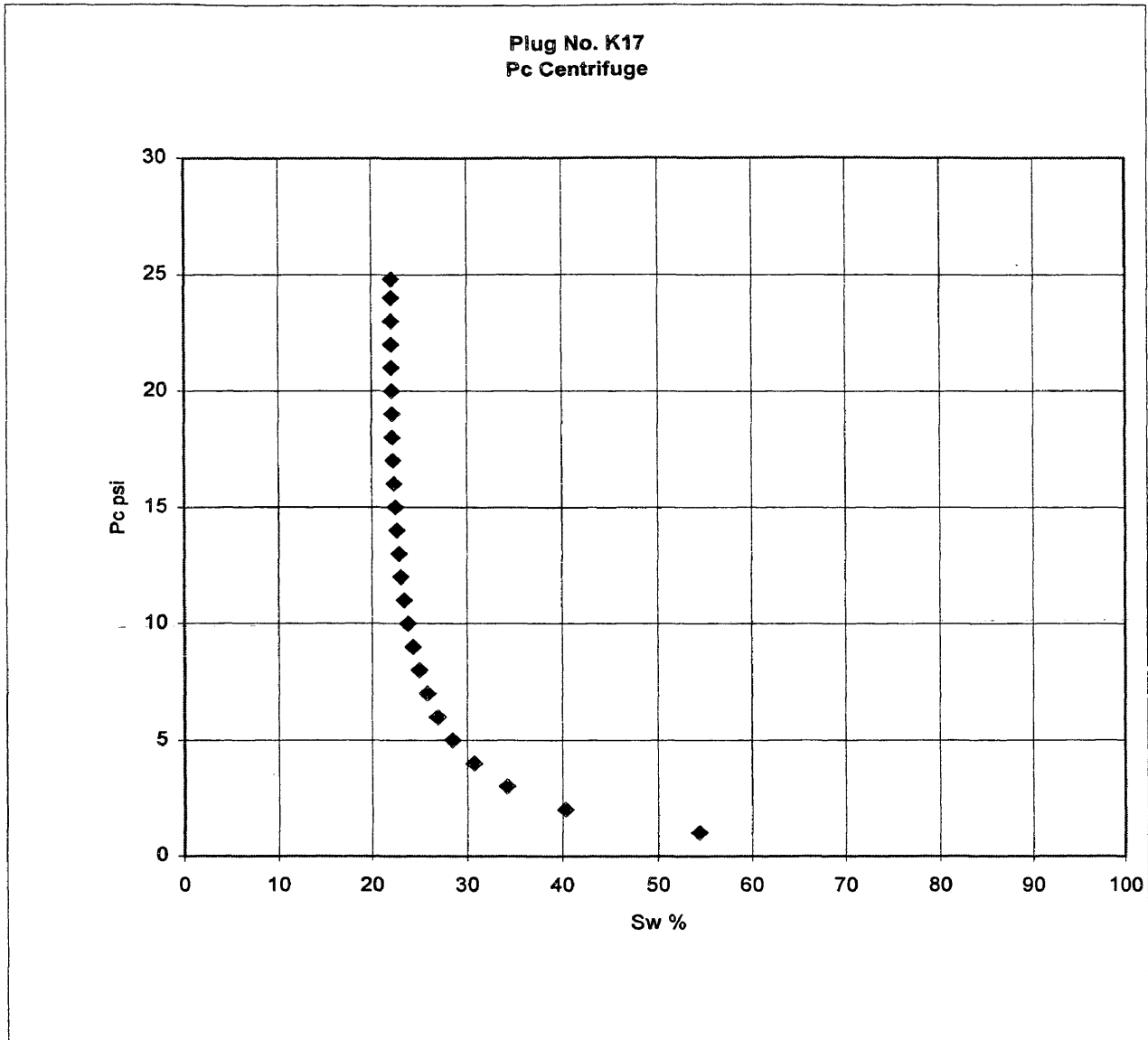


Figure C-12 Centrifugal capillary pressure curve

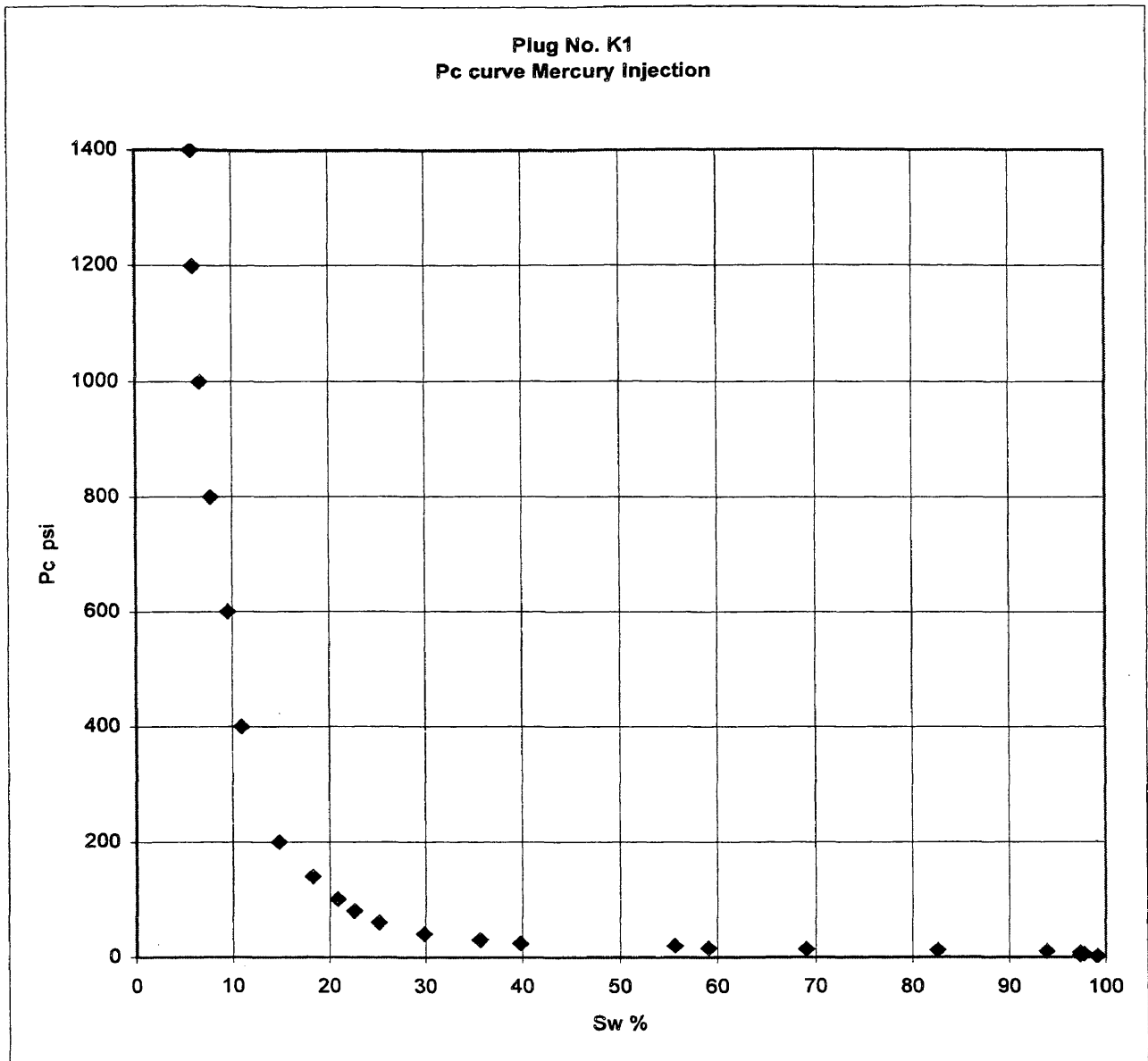


Figure C-13 Capillary pressure curve using mercury injection method

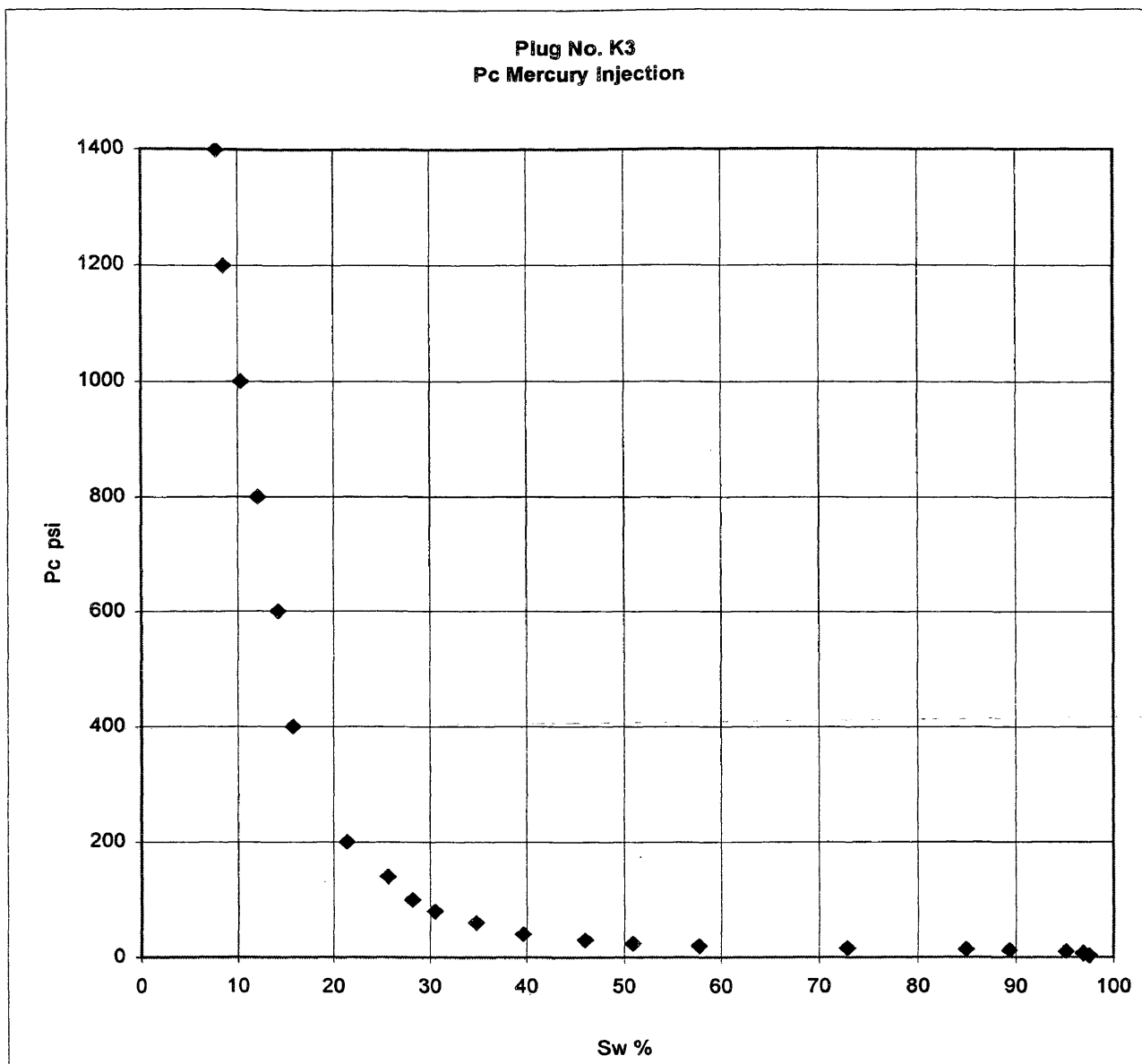


Figure C-14 Capillary pressure curve using mercury injection method

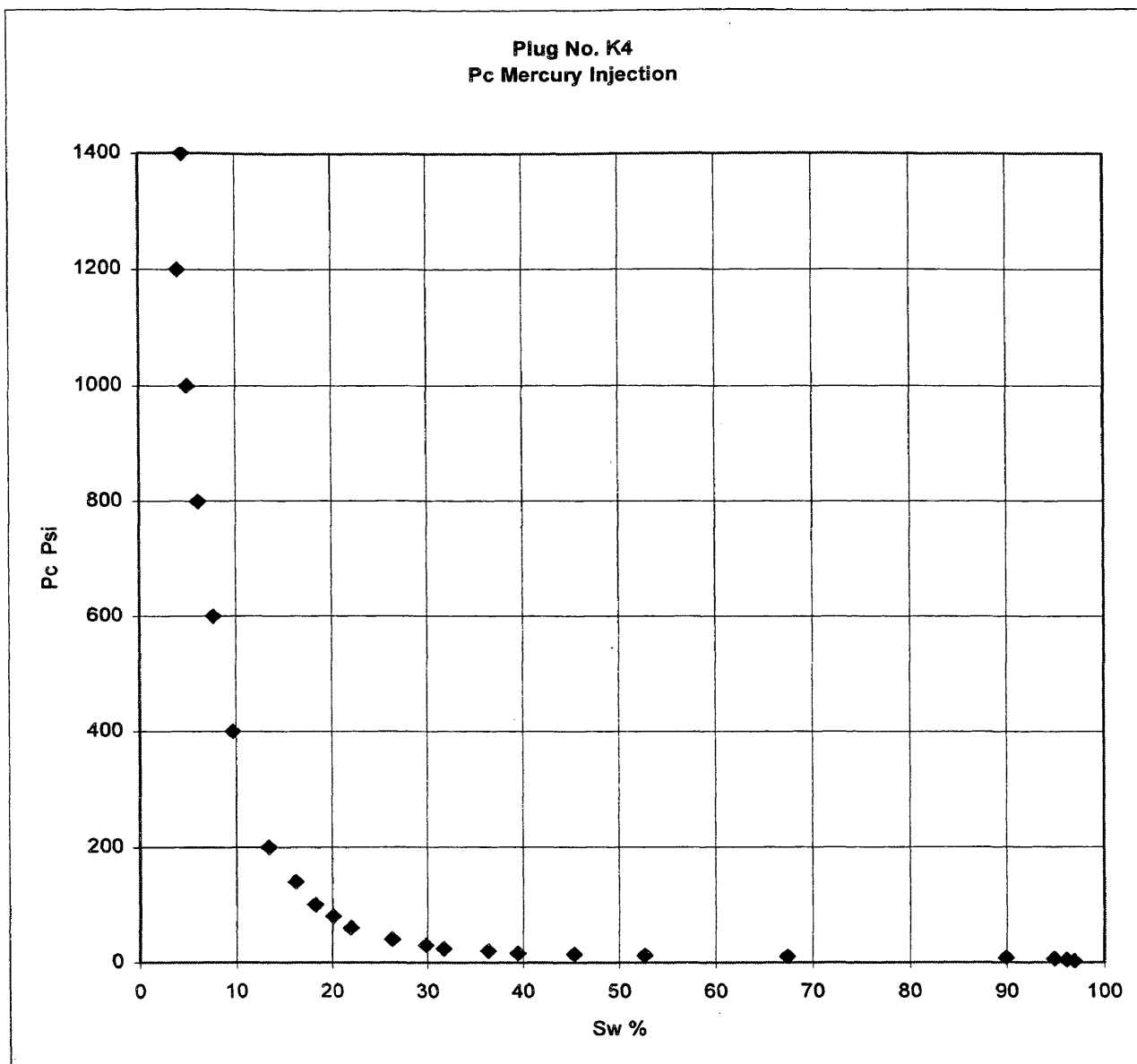


Figure C-15 Capillary pressure curve using mercury injection method

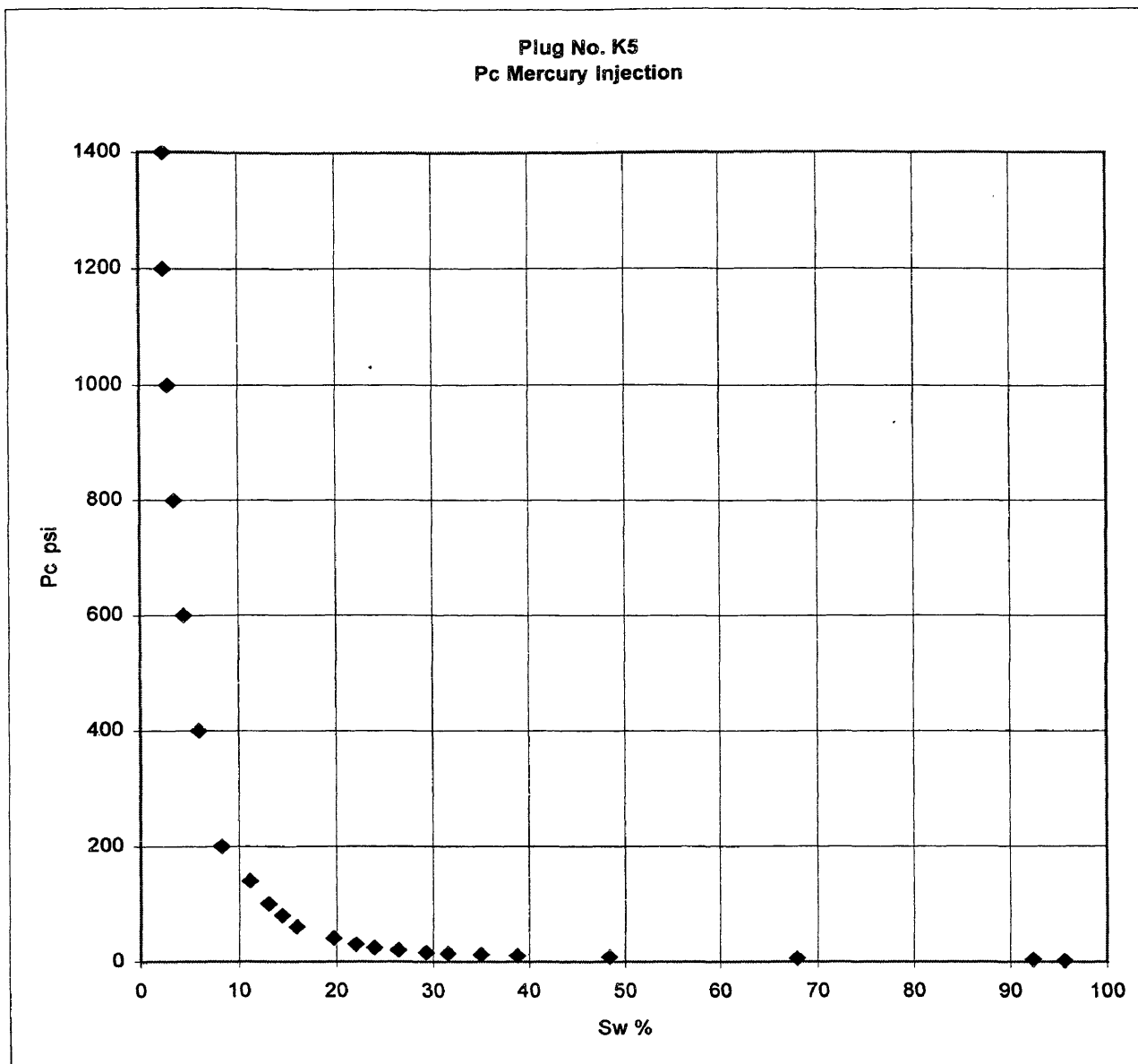


Figure C-16 Capillary pressure curve using mercury injection method

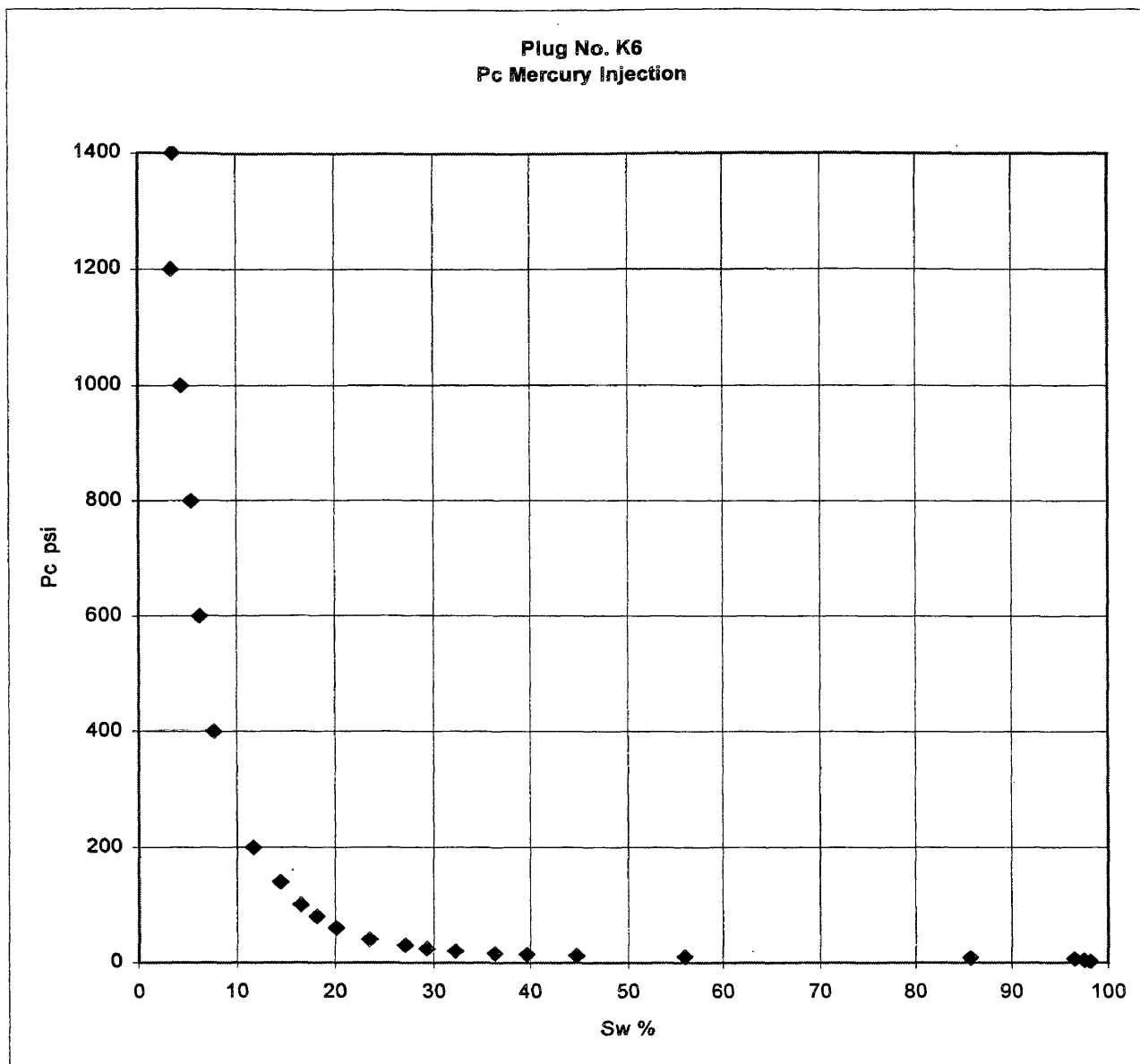


Figure C-17 Capillary pressure curve using mercury injection method

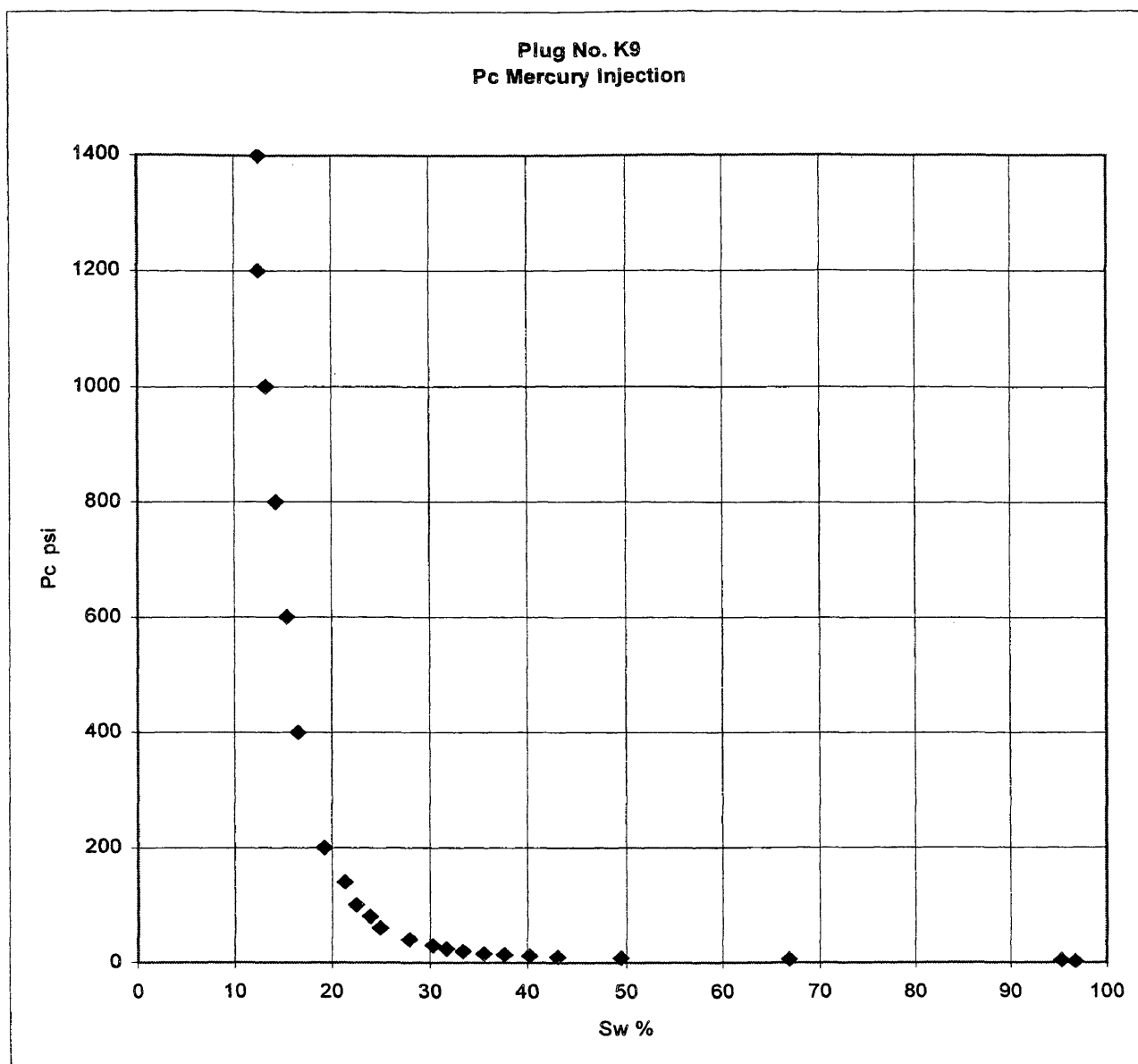


Figure C-18 Capillary pressure curve using mercury injection method

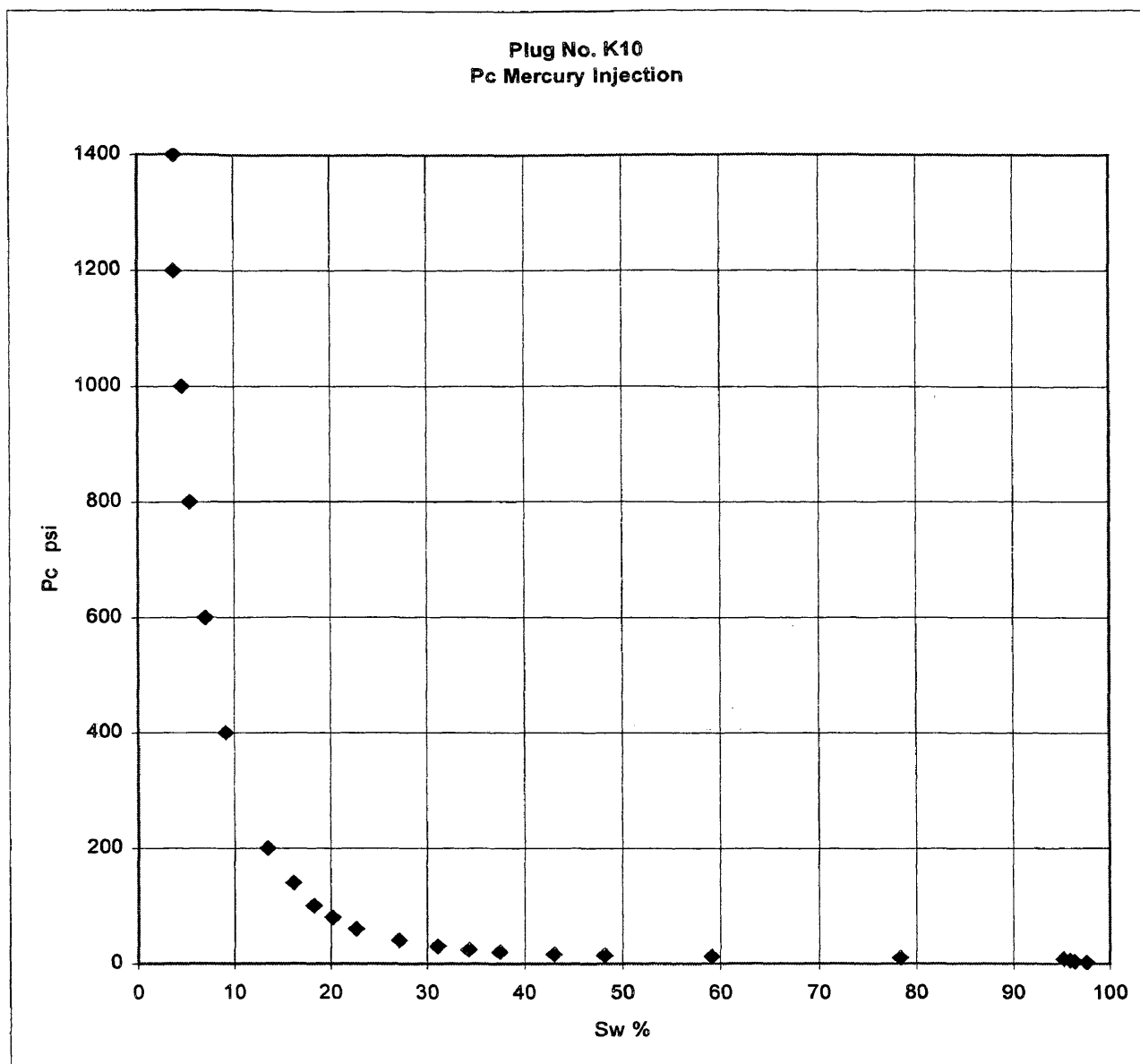


Figure C-19 Capillary pressure curve using mercury injection method

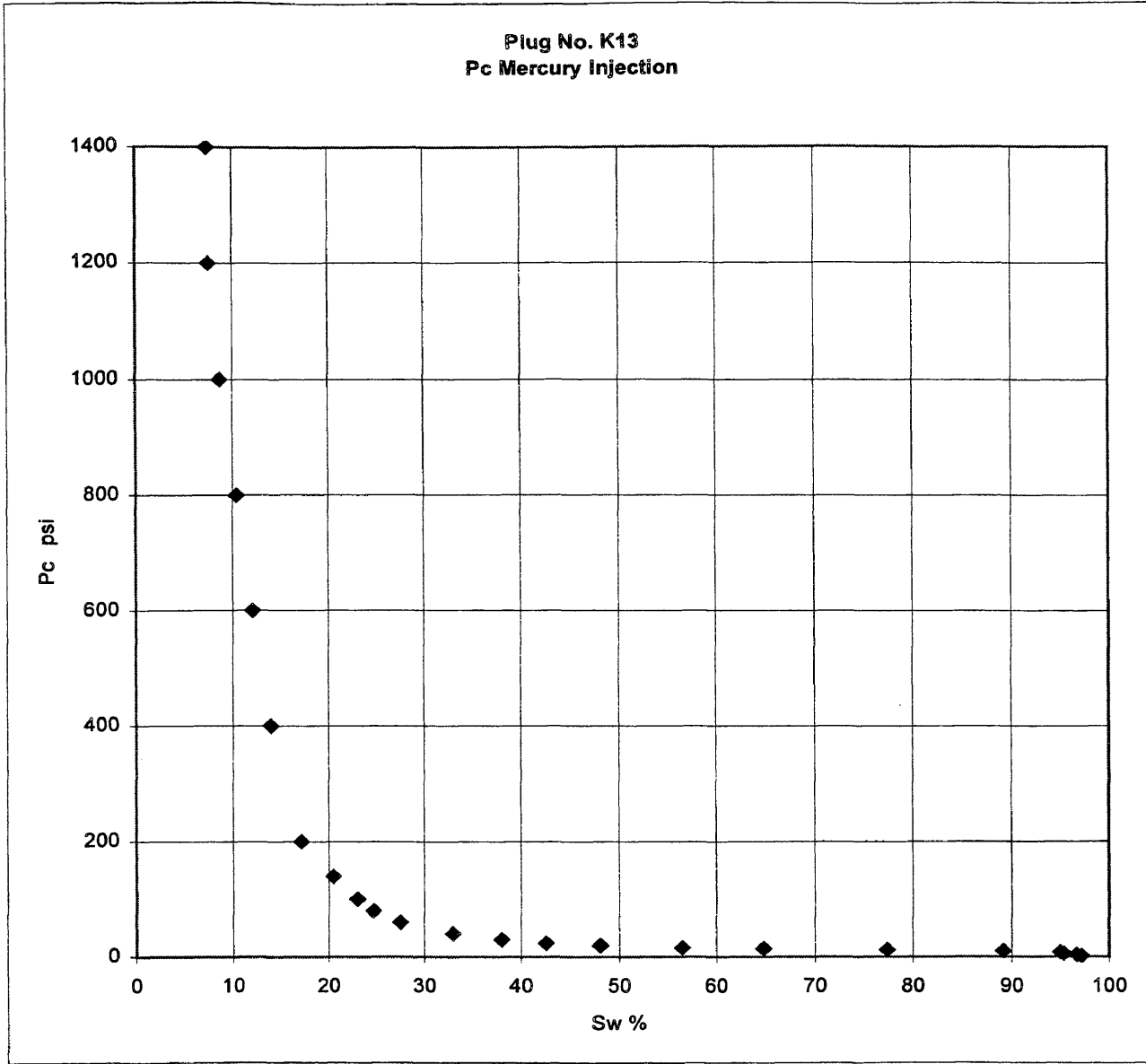


Figure C-20 Capillary pressure curve using mercury injection method

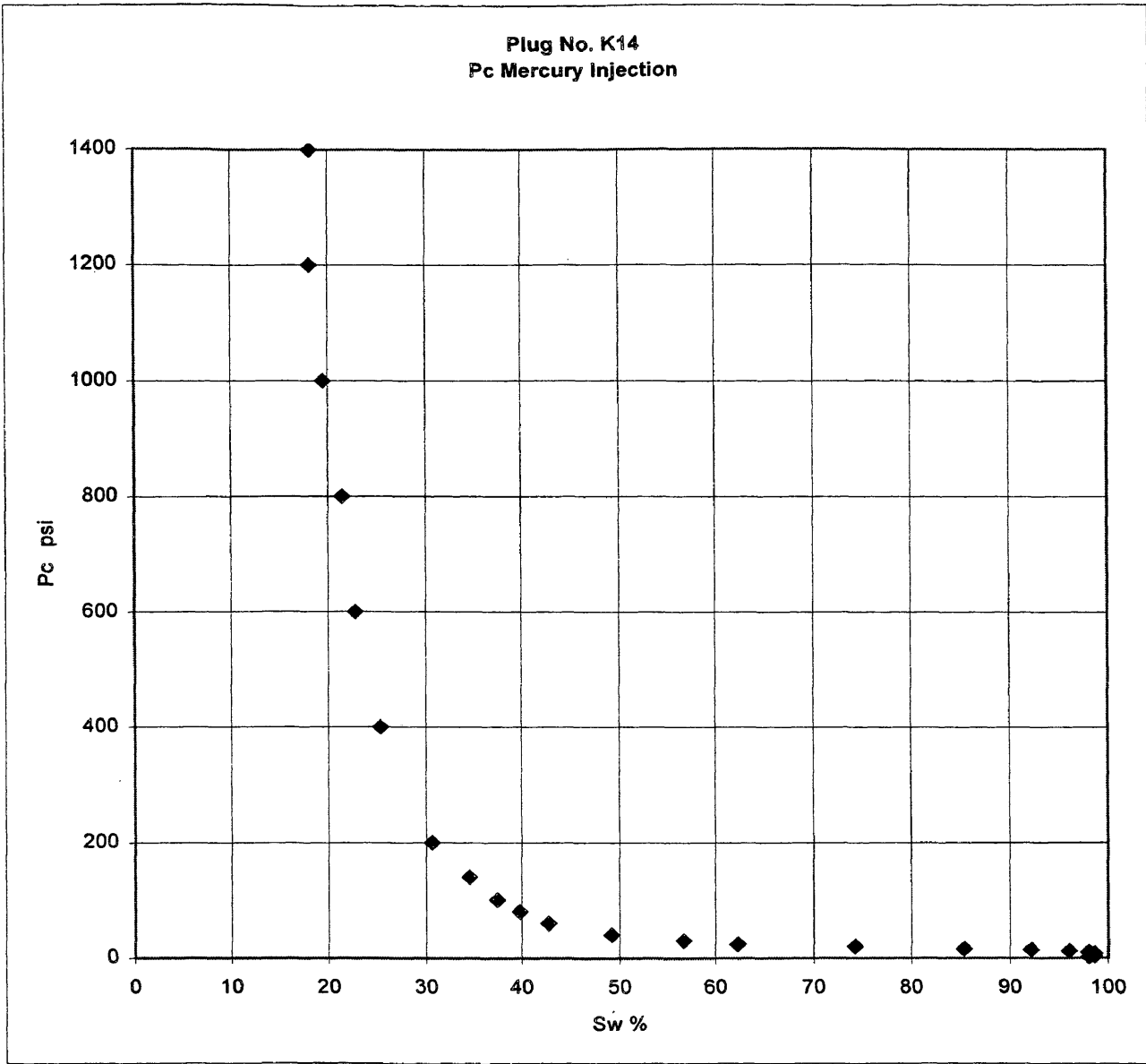


Figure C-21 Capillary pressure curve using mercury injection method

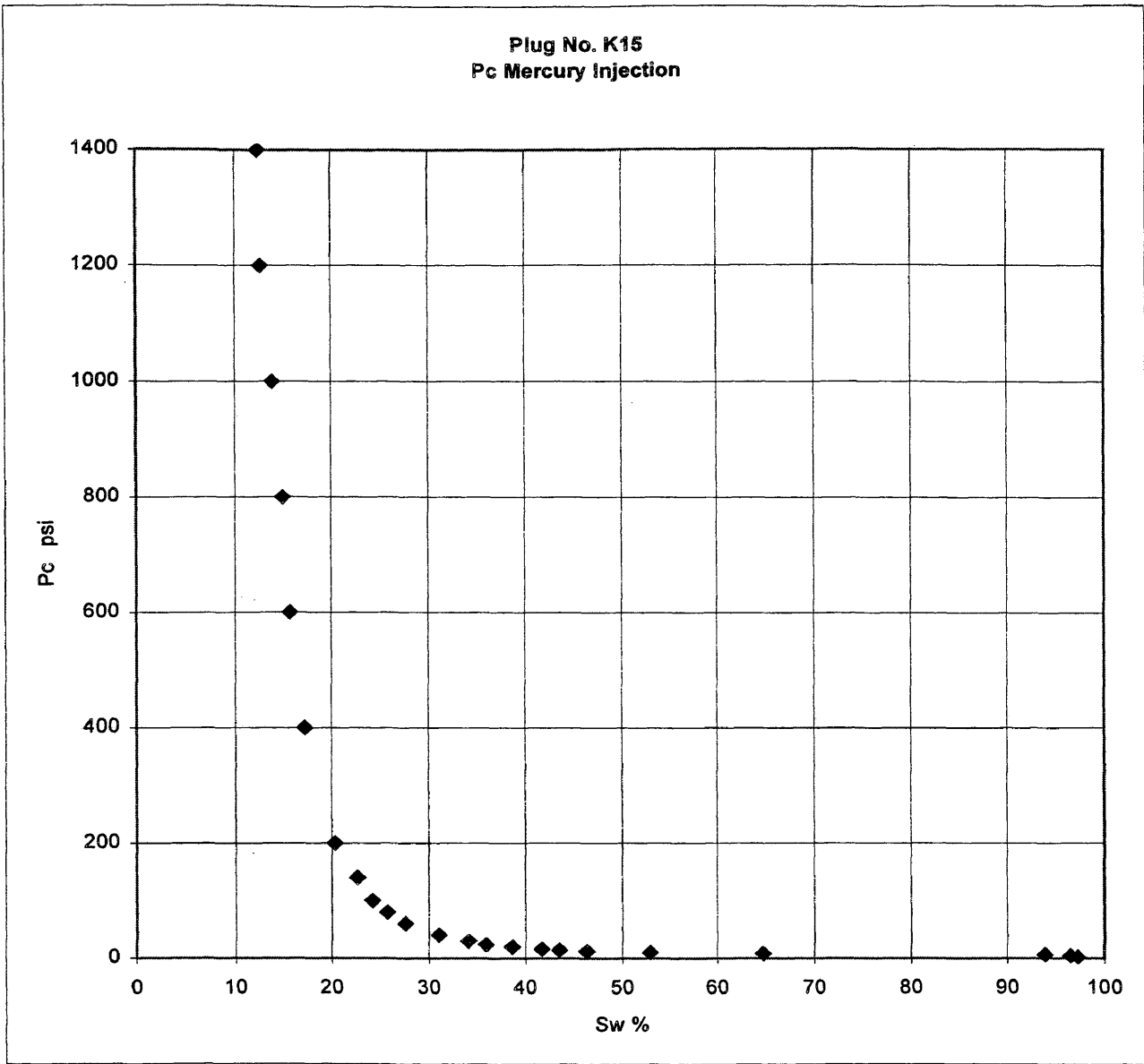


Figure C-22 Capillary pressure curve using mercury injection method

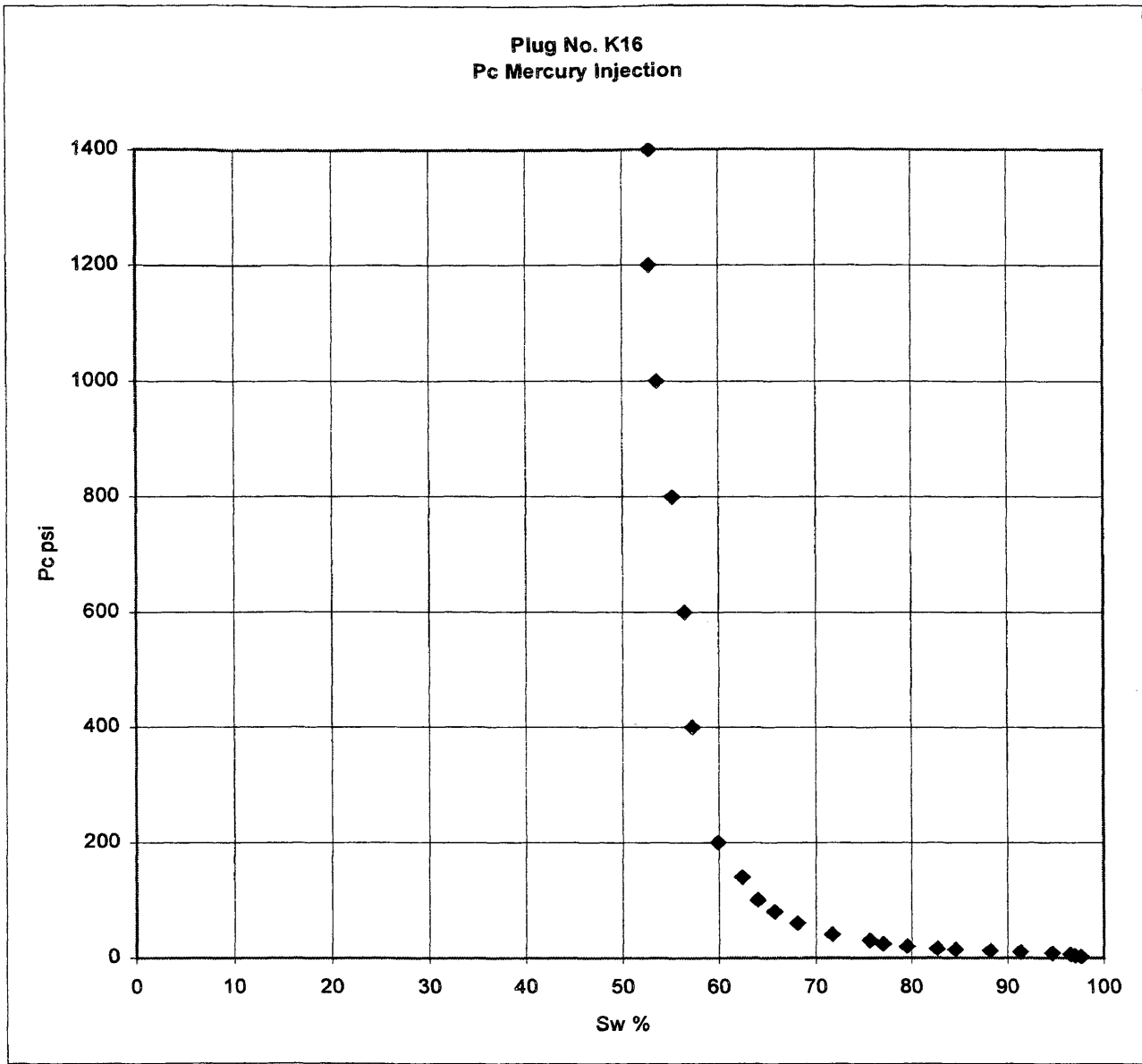


Figure C-23 Capillary pressure curve using mercury injection method

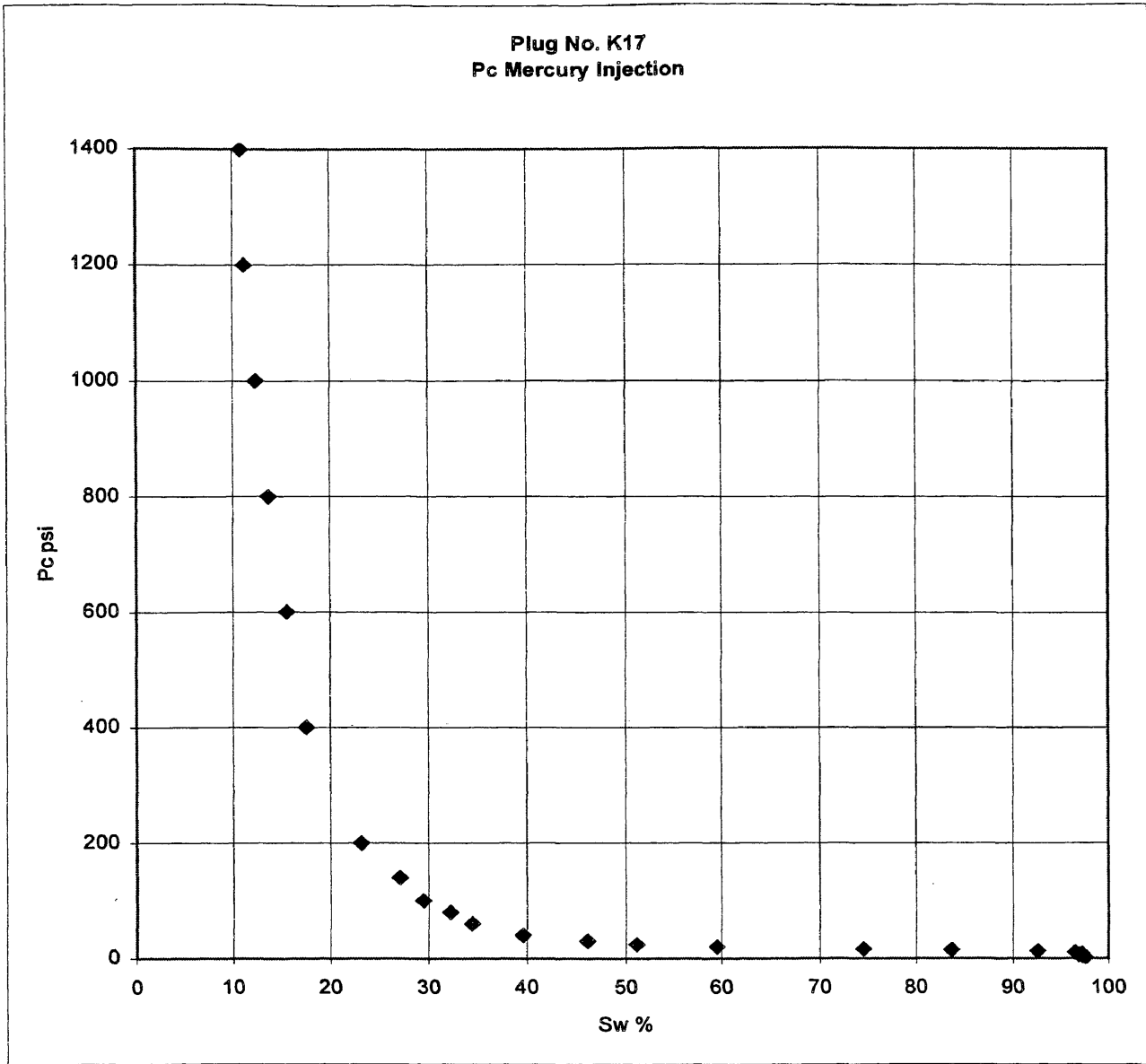


Figure C-24 Capillary pressure curve using mercury injection method

# **Appendix – D**

## **Correlation Attempts**

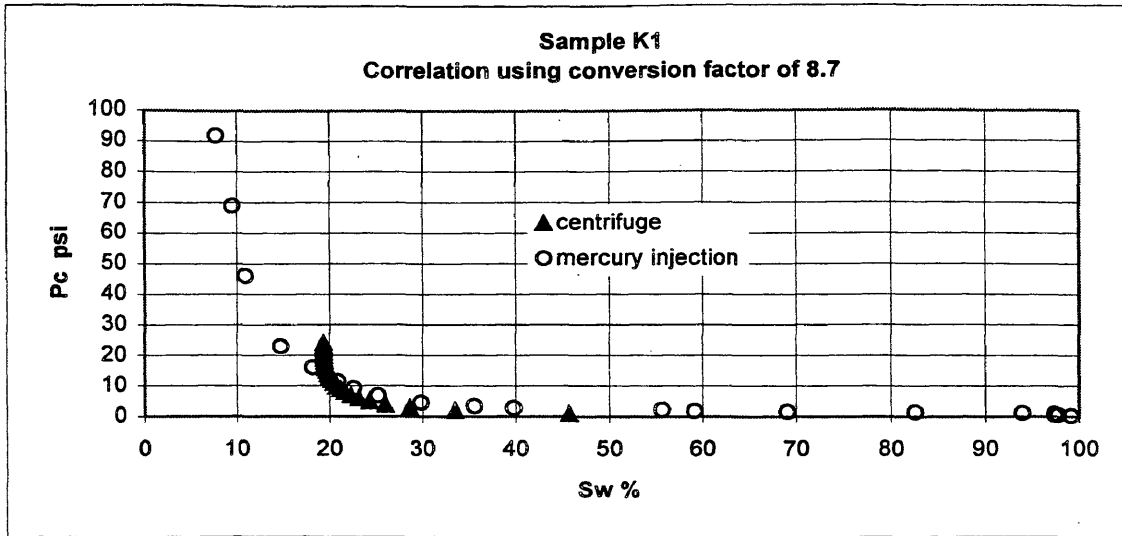


Figure D-1. Sample K1 testing conversion factor 8.7.

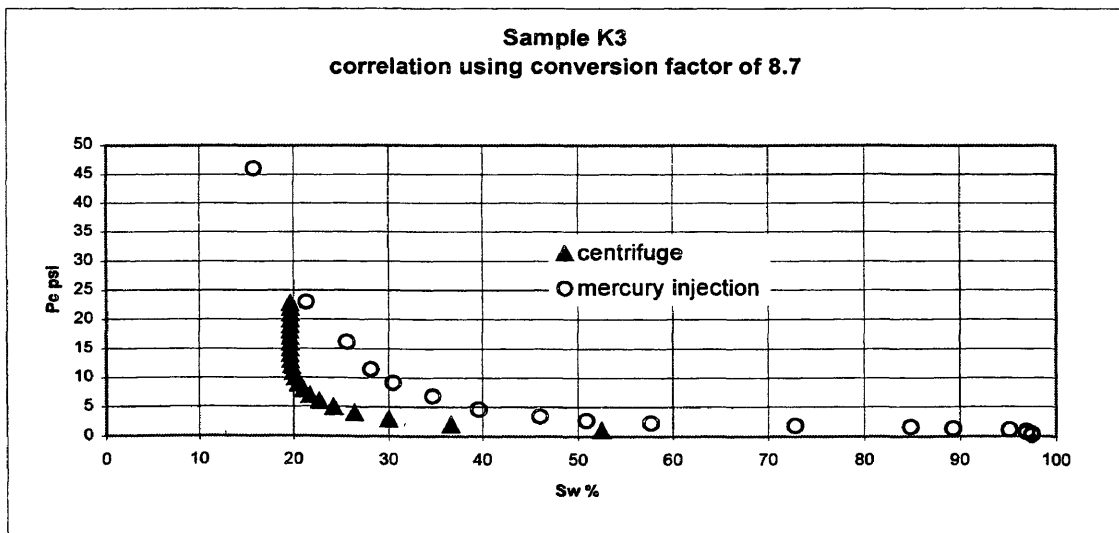


Figure D-2. Sample K3 testing conversion factor 8.7.

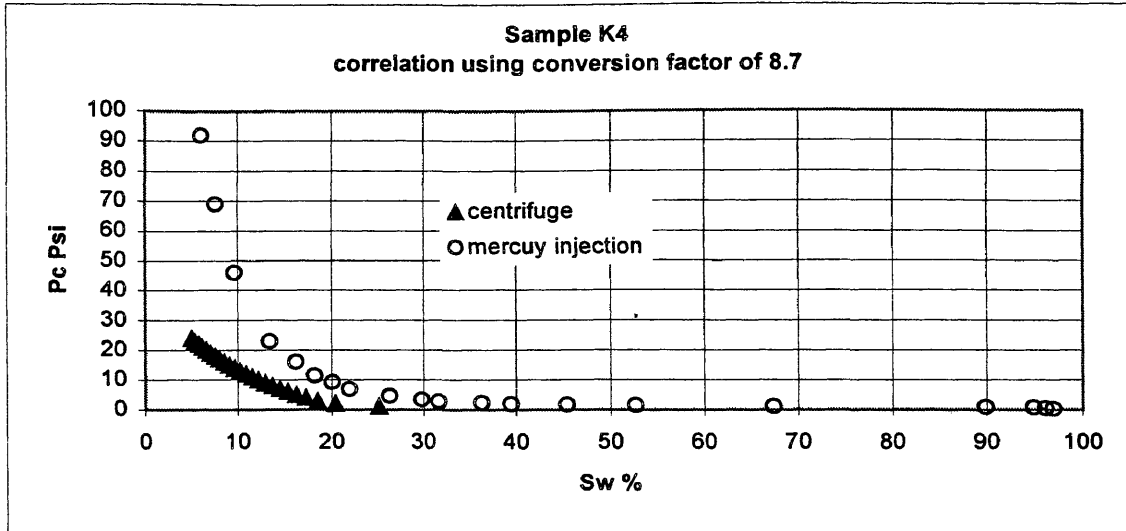


Figure D-3. Sample K4 testing conversion factor 8.7.

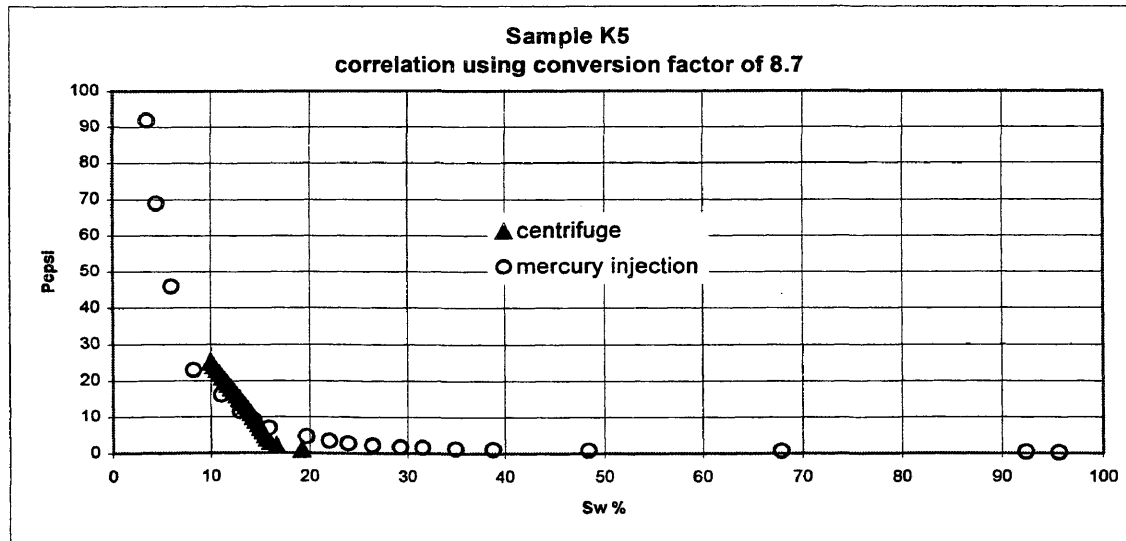


Figure D-4. Sample K5 testing conversion factor 8.7.

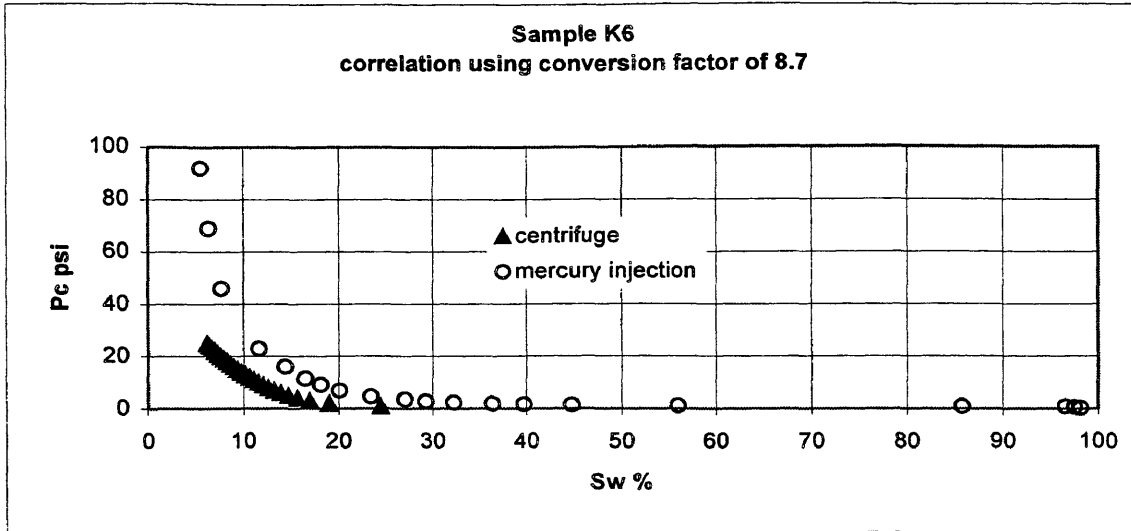


Figure D-5. Sample K6 testing conversion factor 8.7.

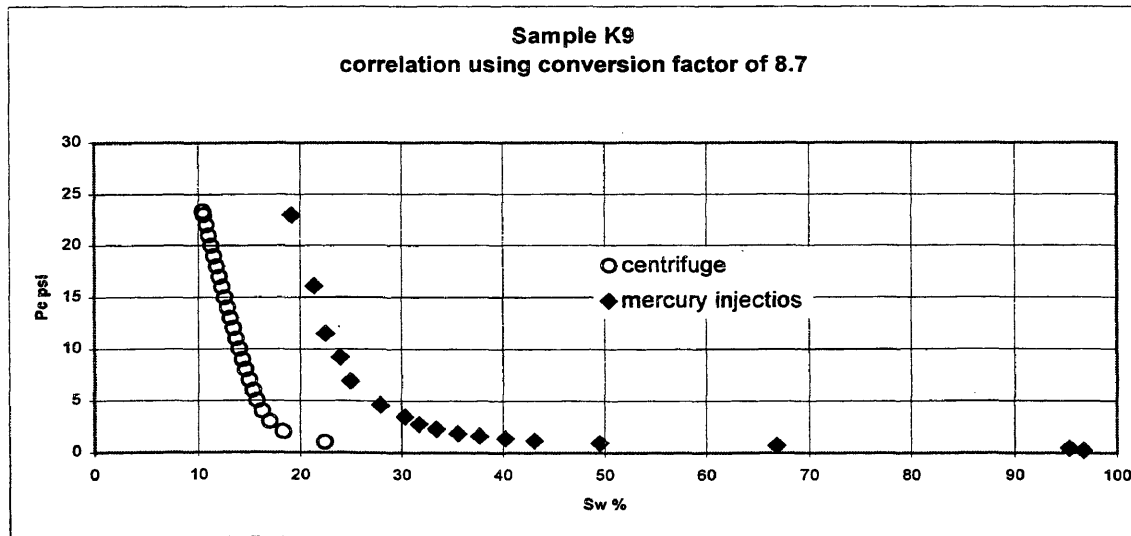


Figure D-6. Sample K9 testing conversion factor 8.7.

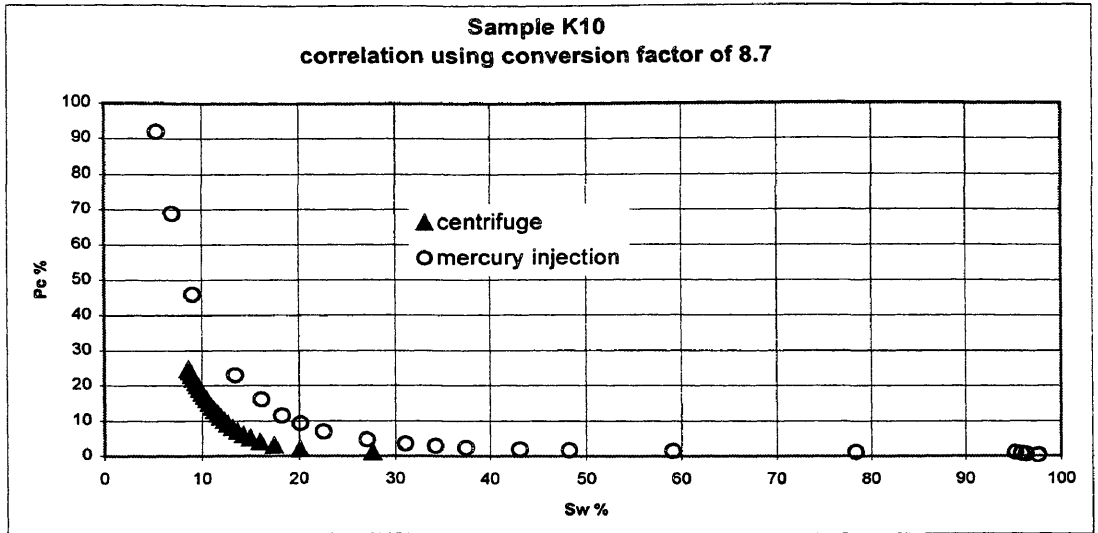


Figure D-7. Sample K10 testing conversion factor 8.7.

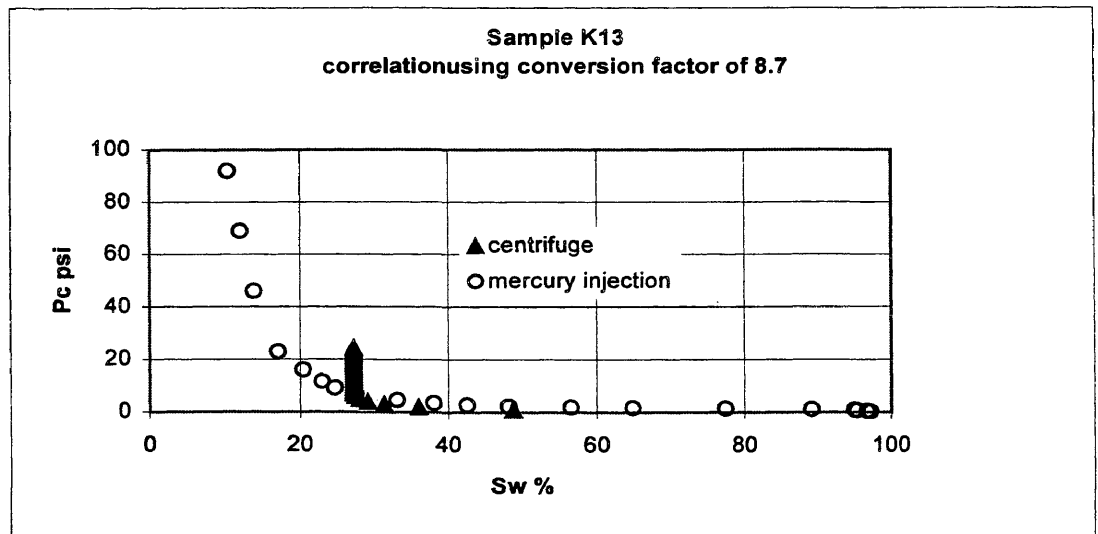


Figure D-8. Sample K13 testing conversion factor 8.7.

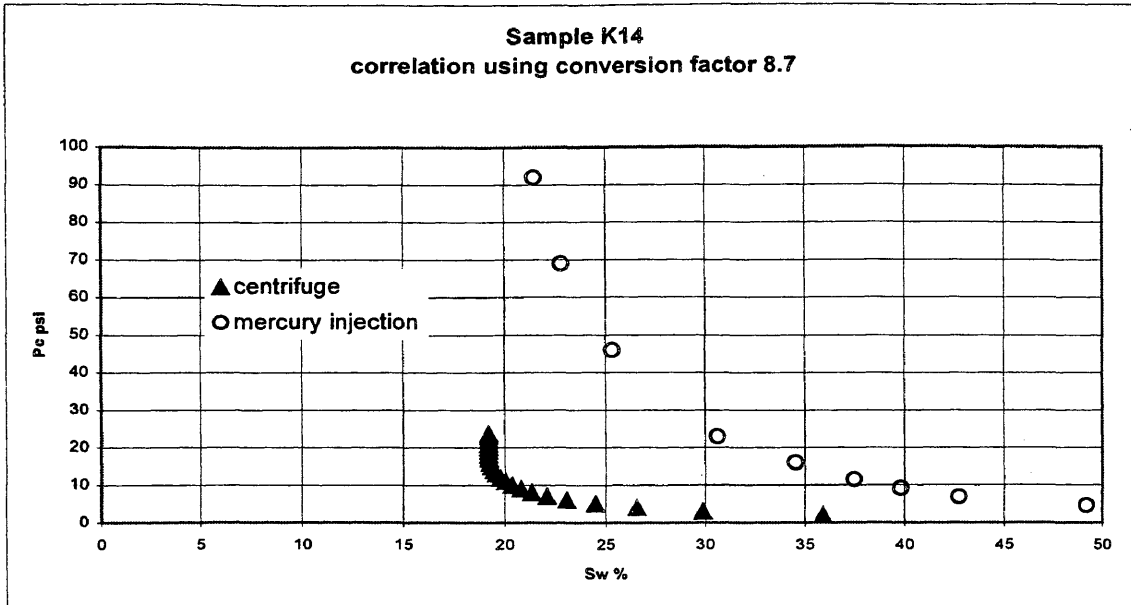


Figure D-9. Sample K14 testing conversion factor 8.7.

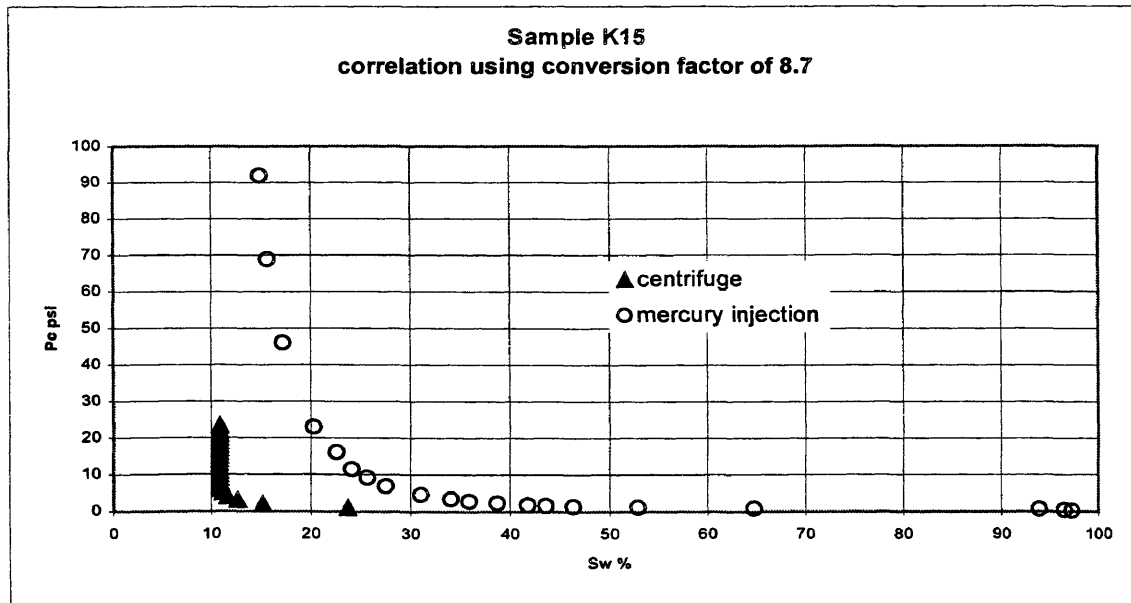


Figure D-10. Sample K15 testing conversion factor 8.7.

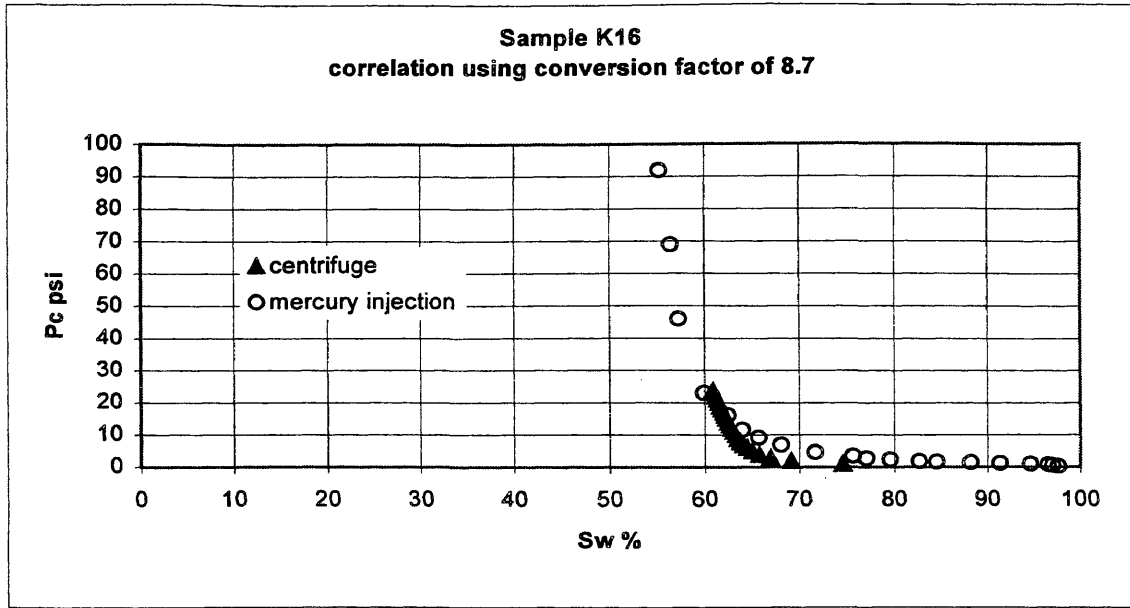


Figure D-11. Sample K16 testing conversion factor 8.7.

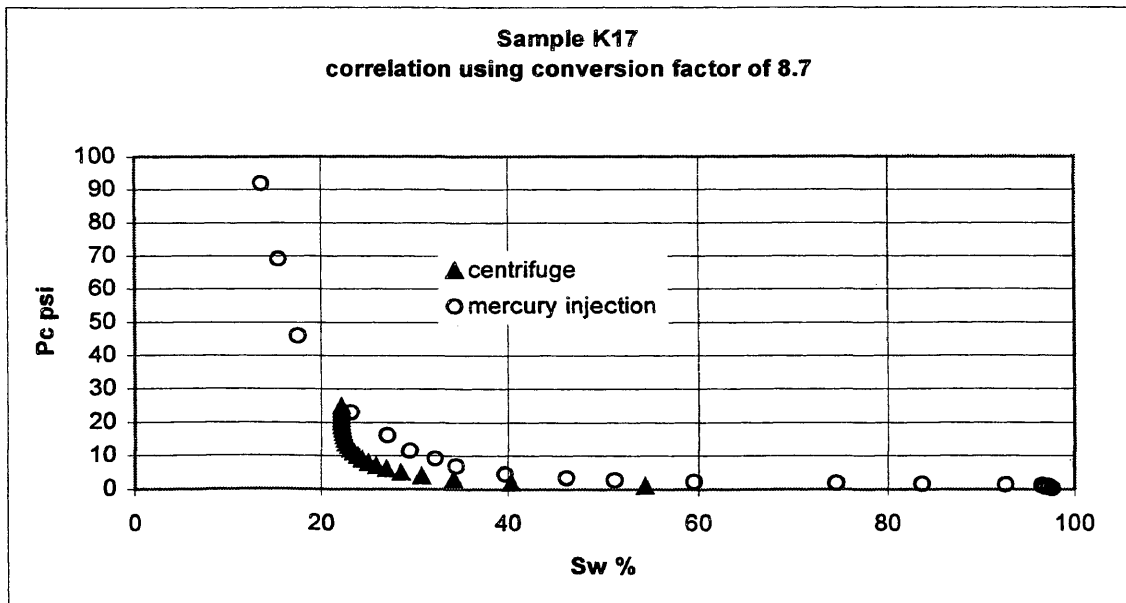


Figure D-12. Sample K17 testing conversion factor 8.7.

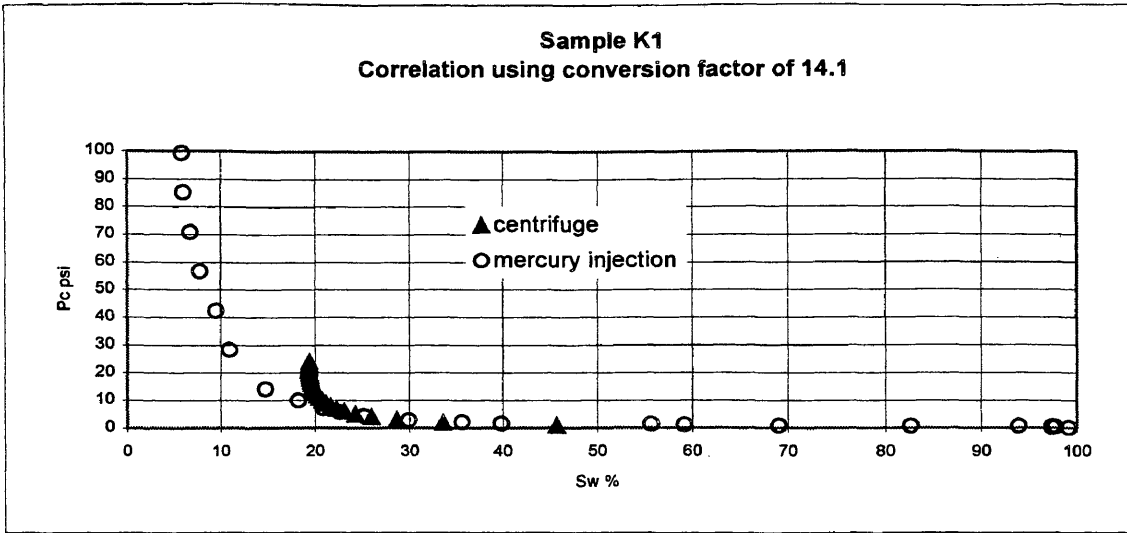


Figure D-13. Sample K1 testing conversion factor 14.1.

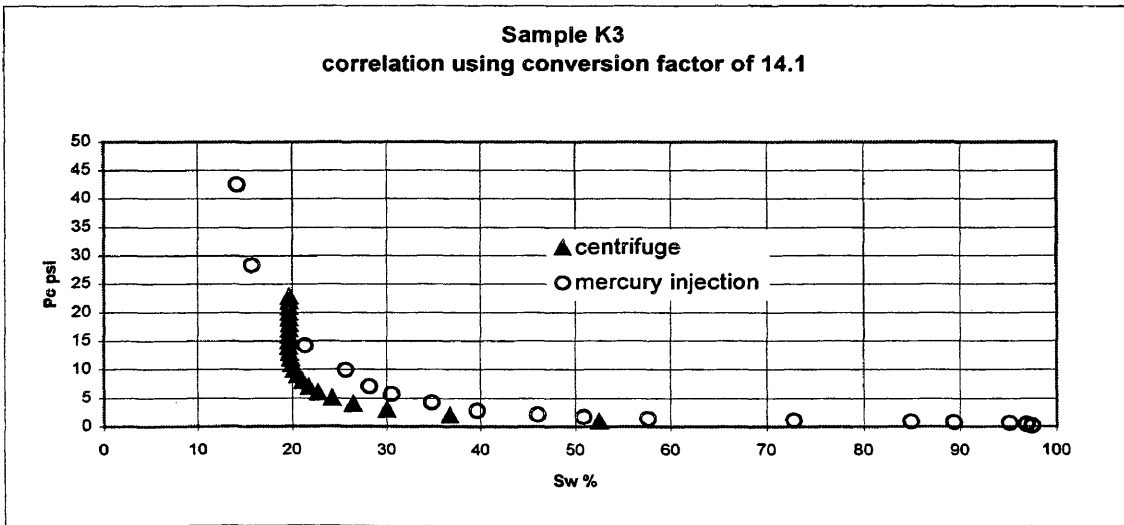


Figure D-14. Sample K3 testing conversion factor 14.1.

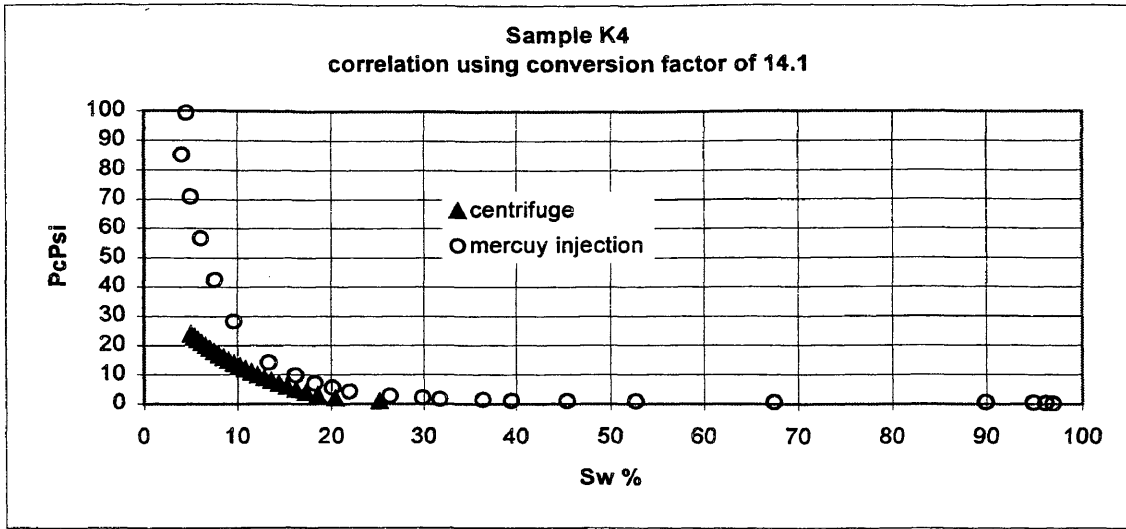


Figure D-15. Sample K4 testing conversion factor 14.1.

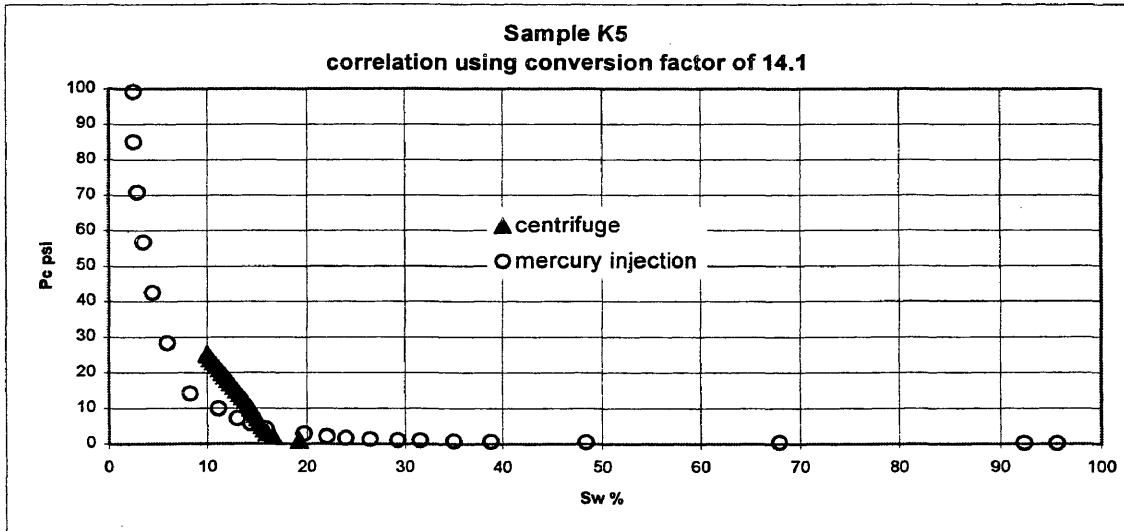


Figure D-16. Sample K5 testing conversion factor 14.1.

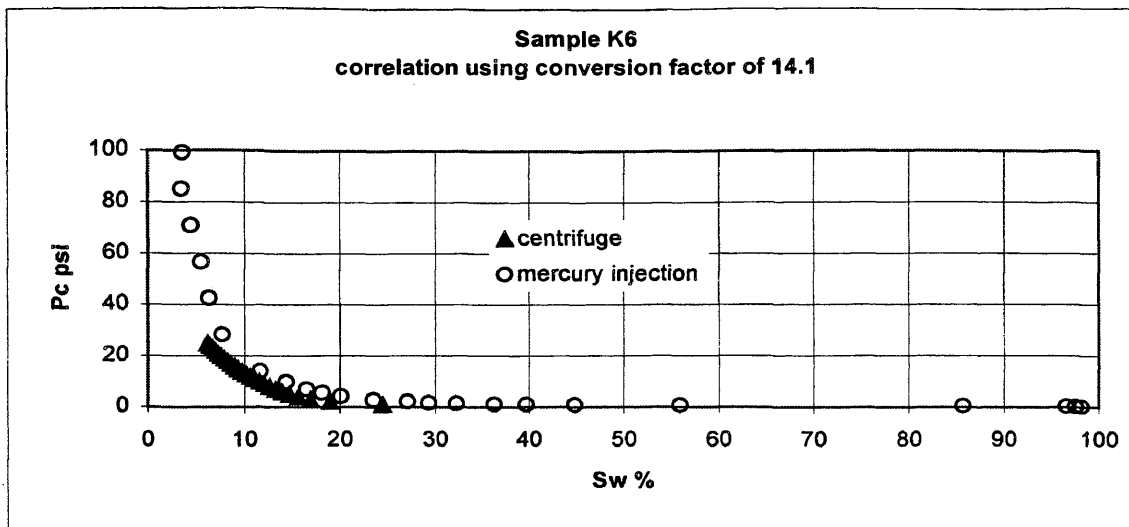


Figure D-17. Sample K6 testing conversion factor 14.1.

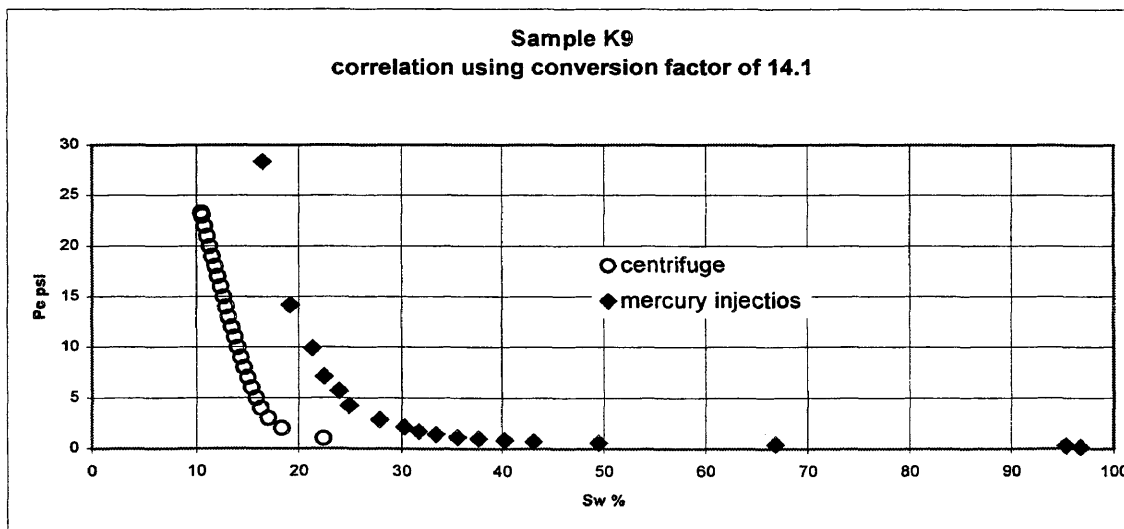


Figure D-18. Sample K9 testing conversion factor 14.1.

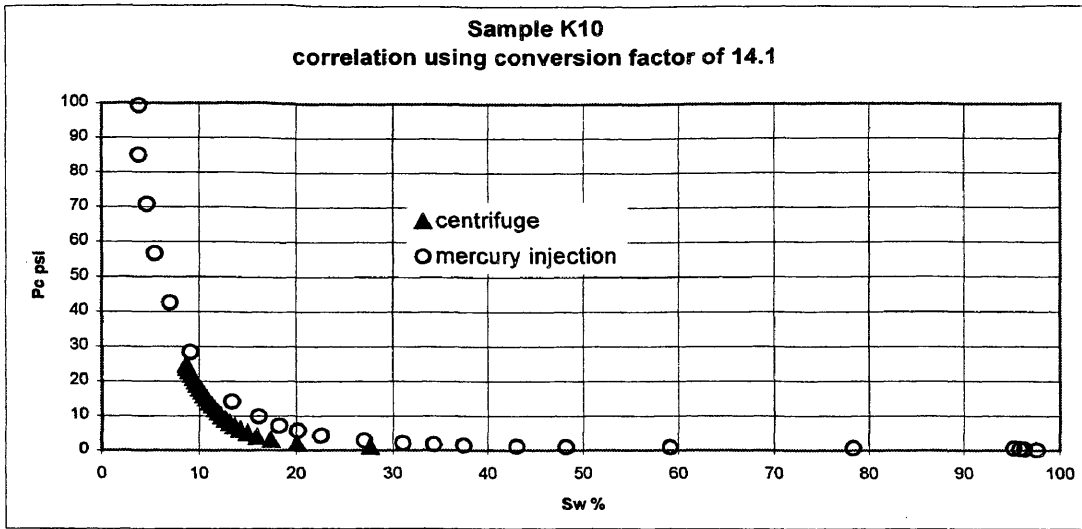


Figure D-19. Sample K10 testing conversion factor 14.1.

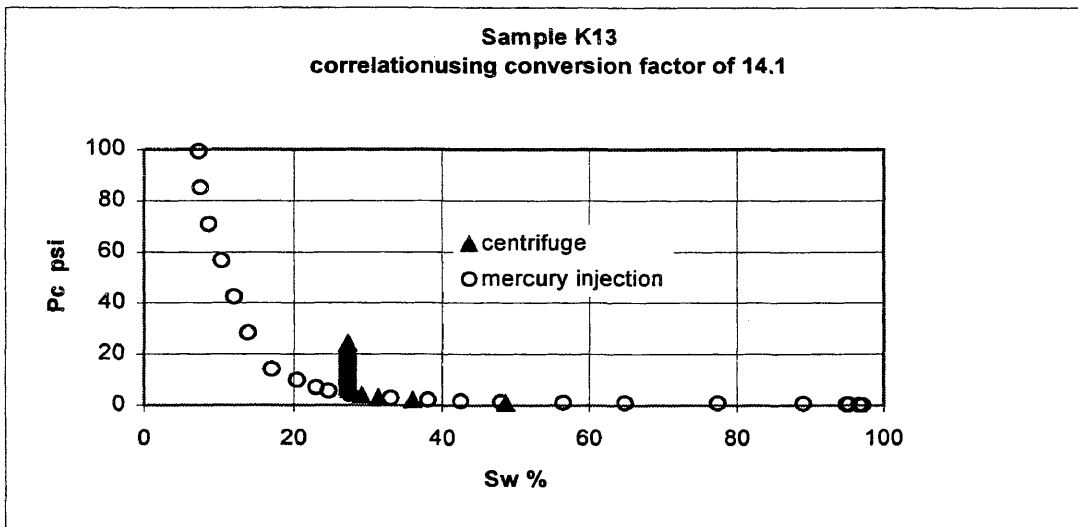


Figure D-20. Sample K13 testing conversion factor 14.1.

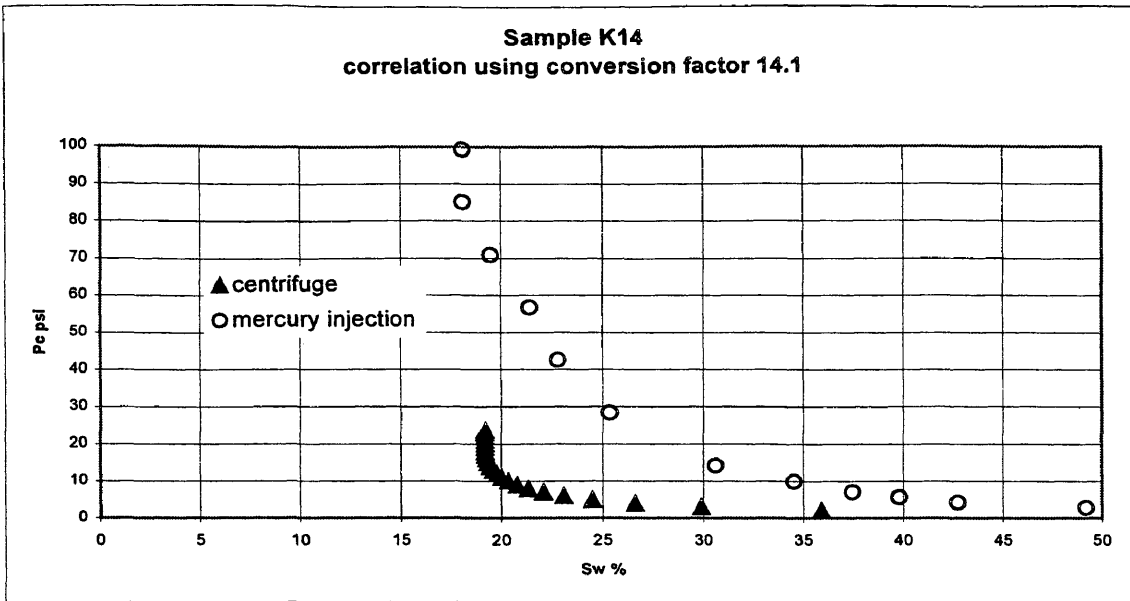


Figure D-21. Sample K14 testing conversion factor 14.1.

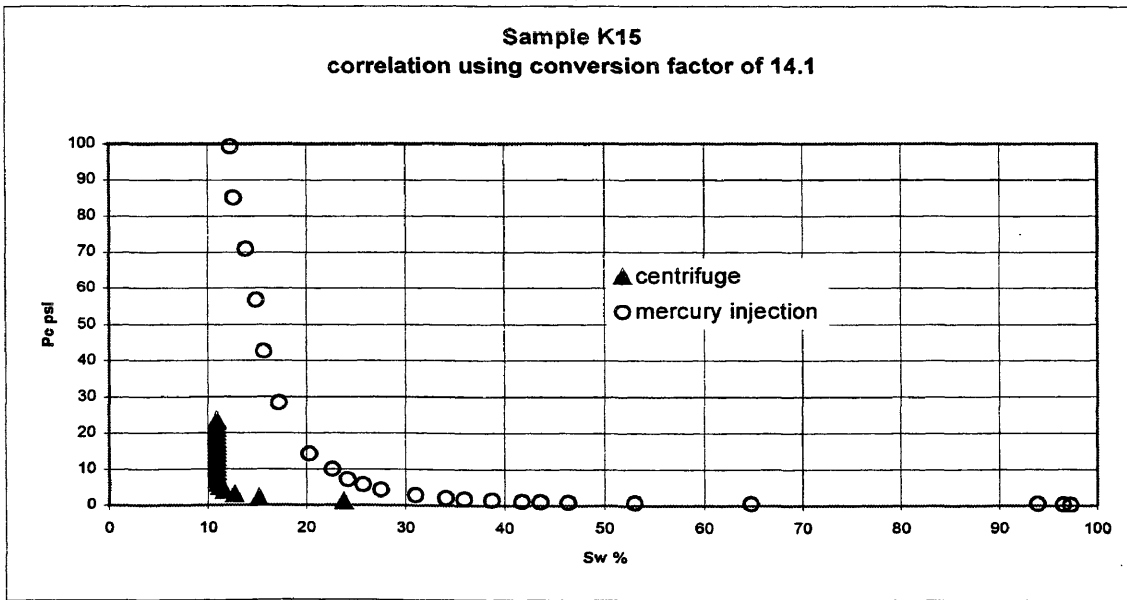


Figure D-22. Sample K15 testing conversion factor 14.1.

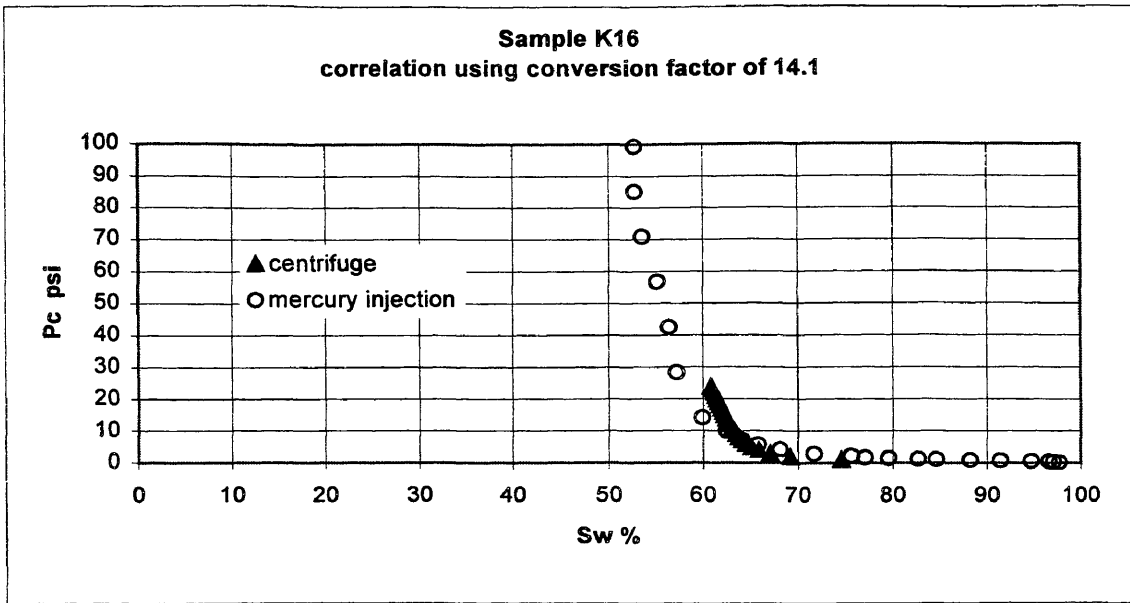


Figure D-23. Sample K16 testing conversion factor 14.1.

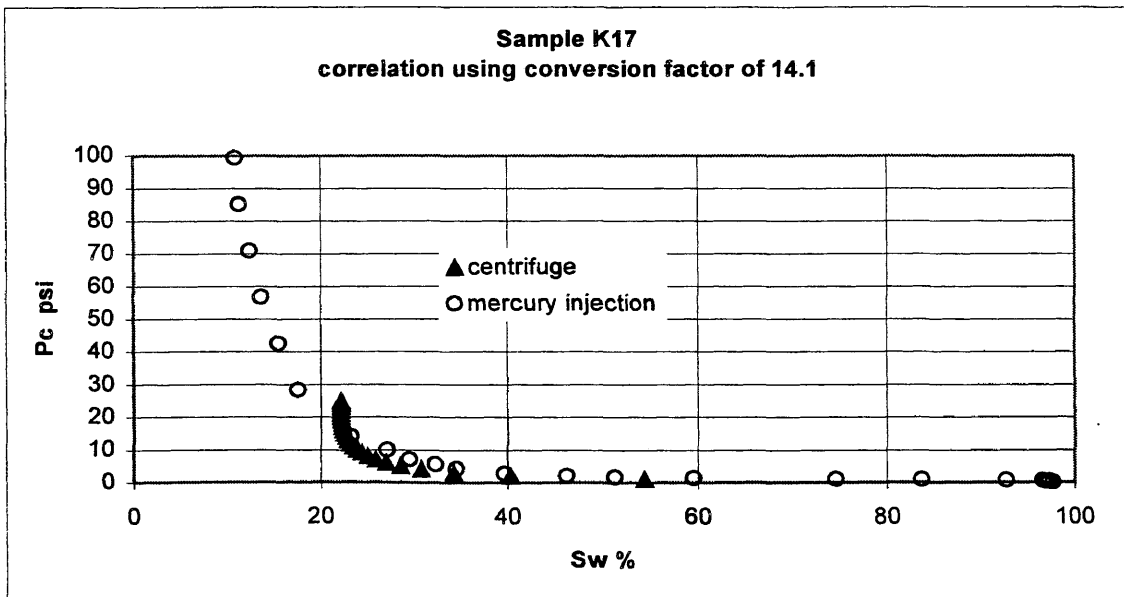


Figure D-24. Sample K17 testing conversion factor 14.1.

# **Appendix – E**

## **Accuracy Plots**

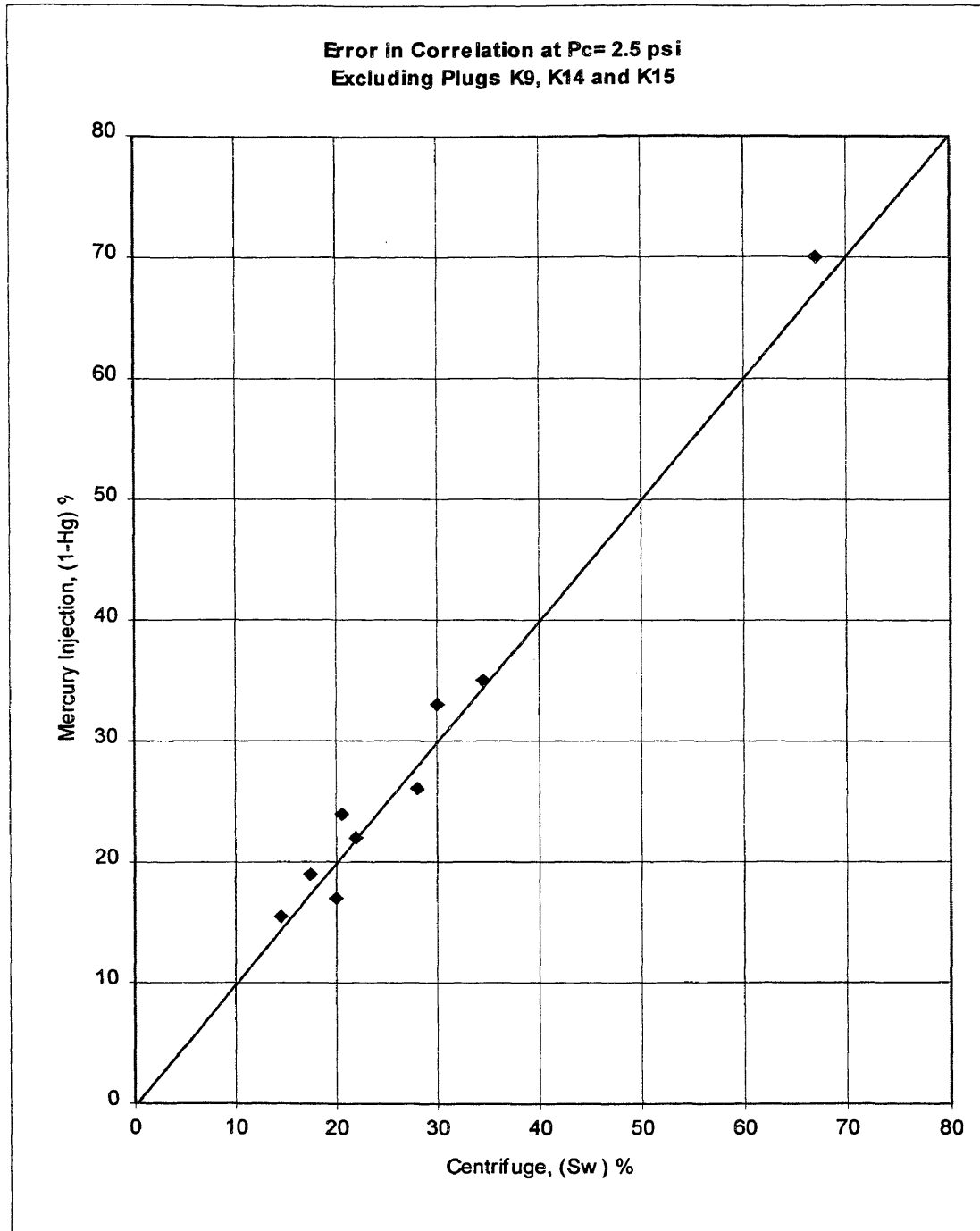


Figure E-1 Accuracy Plot at 2.5 psi

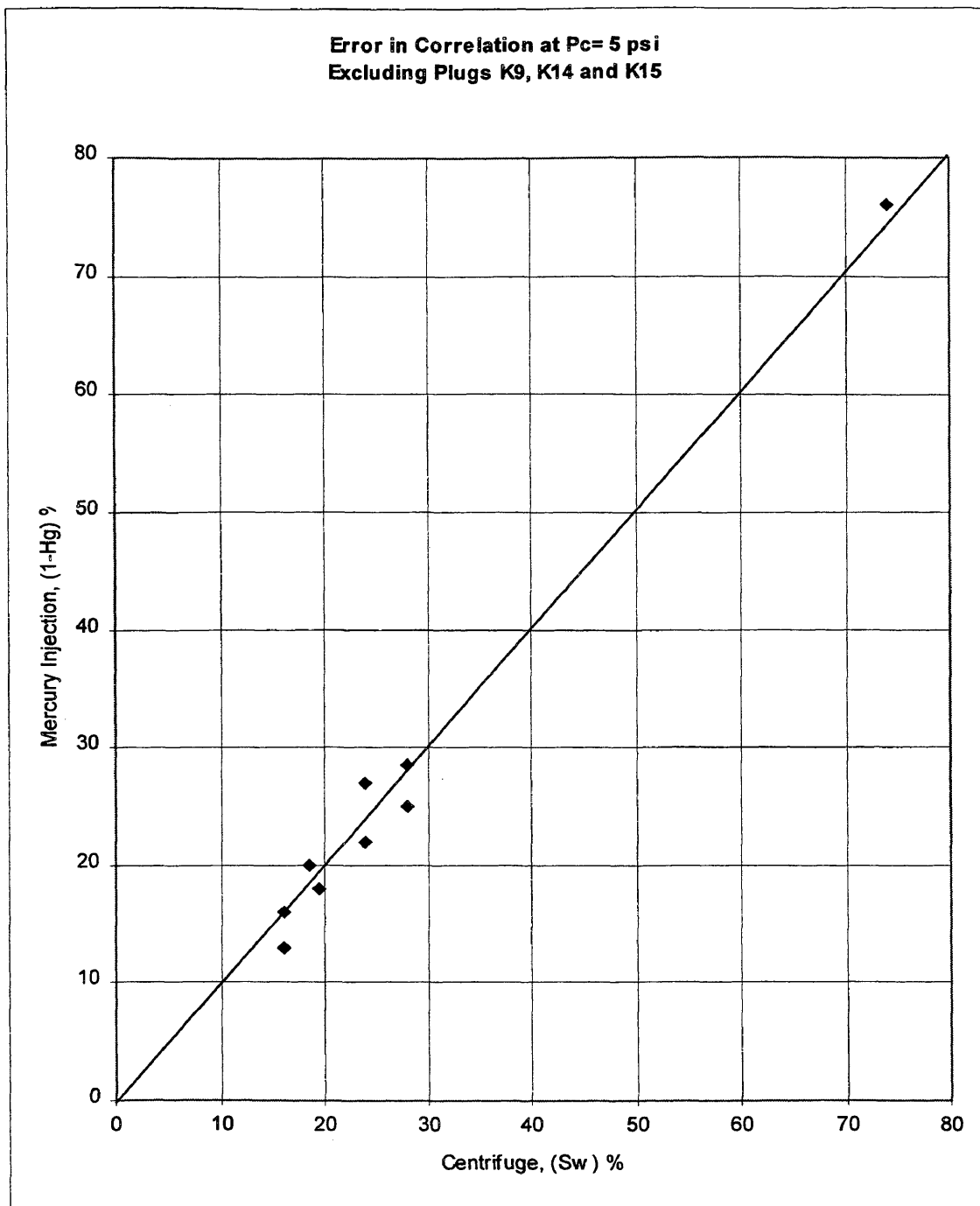


Figure E-2 Accuracy Plot at 5 psi

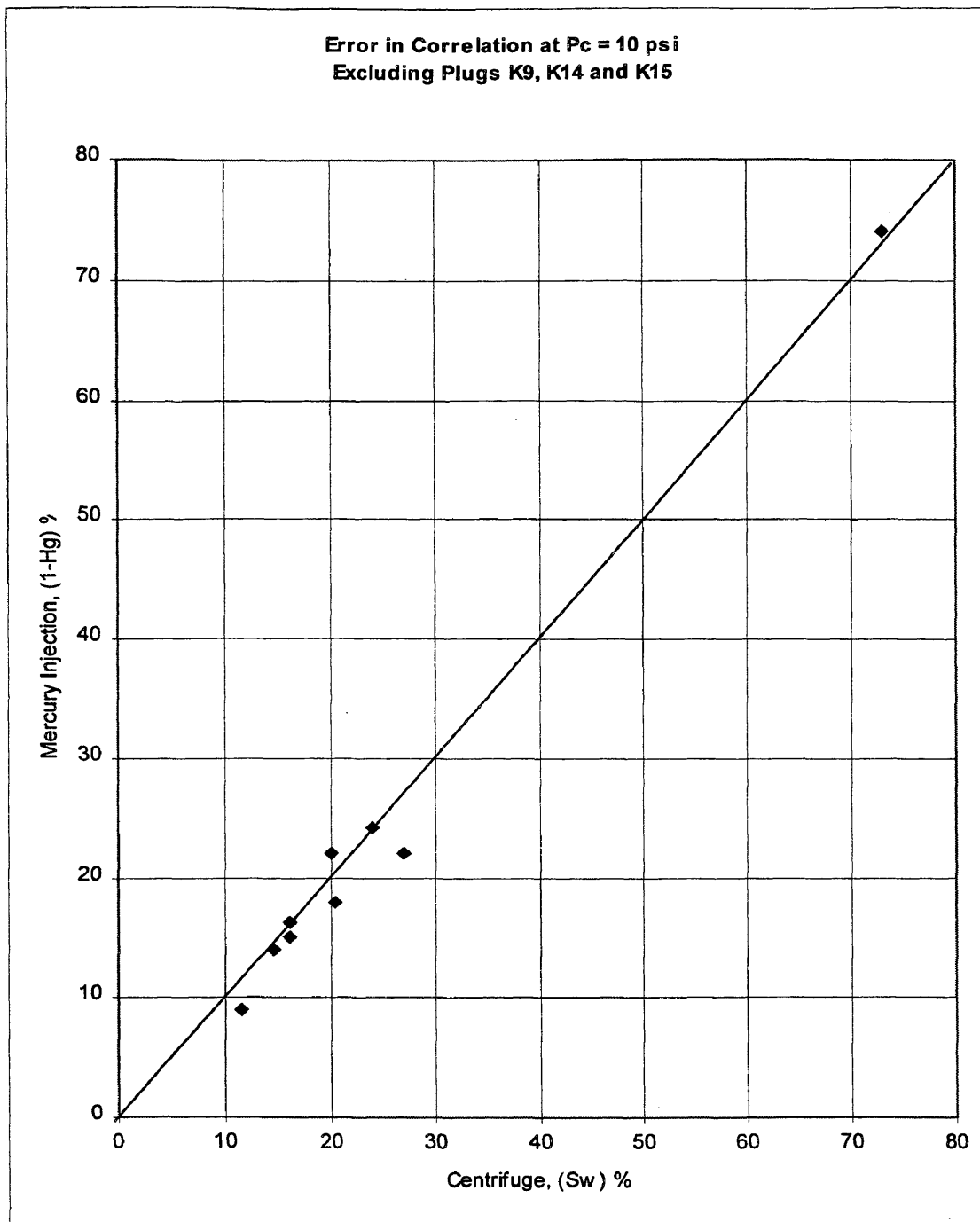


Figure E-3 Accuracy Plot at 10 psi

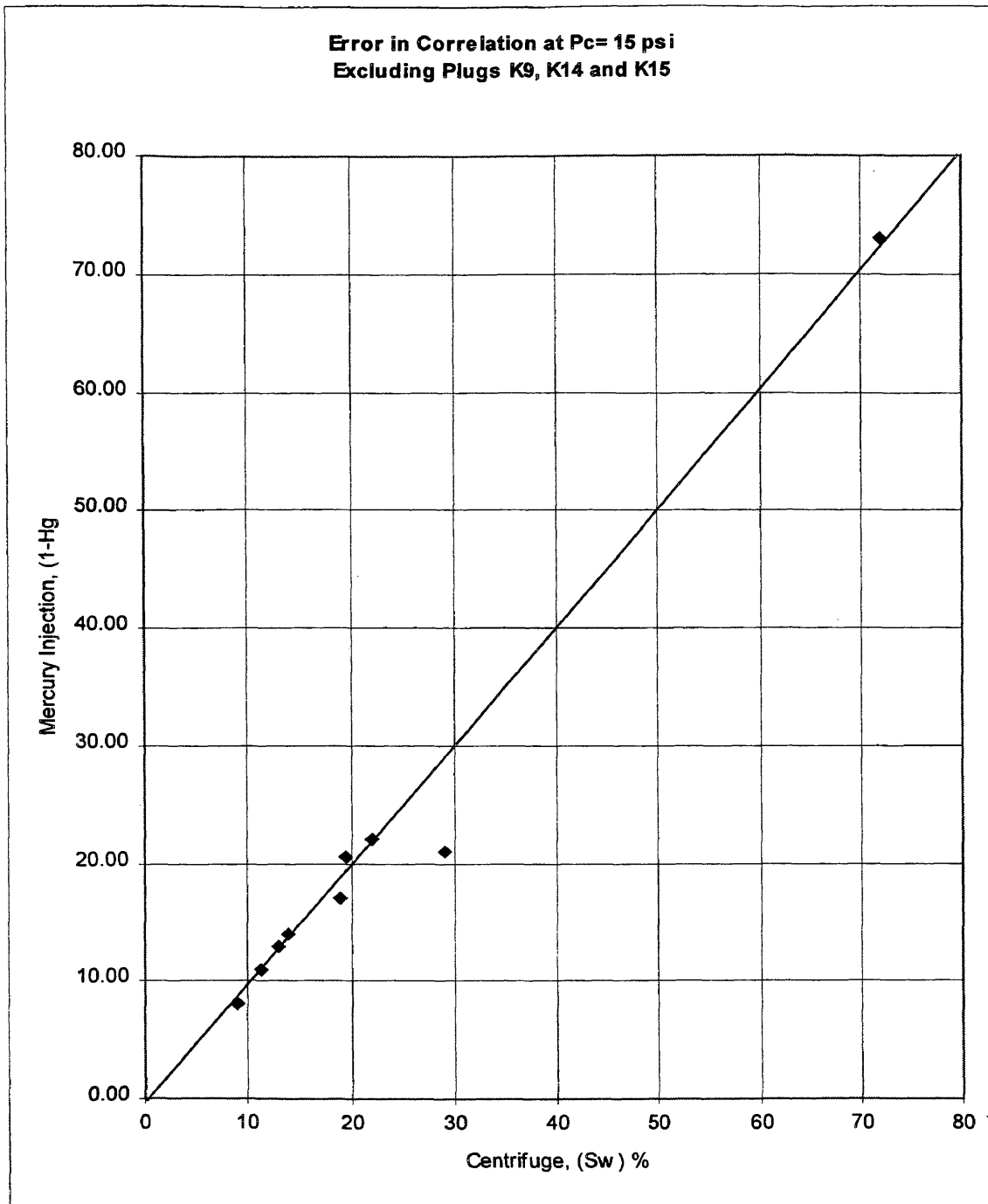


Figure E-4 Accuracy Plot at 15 psi

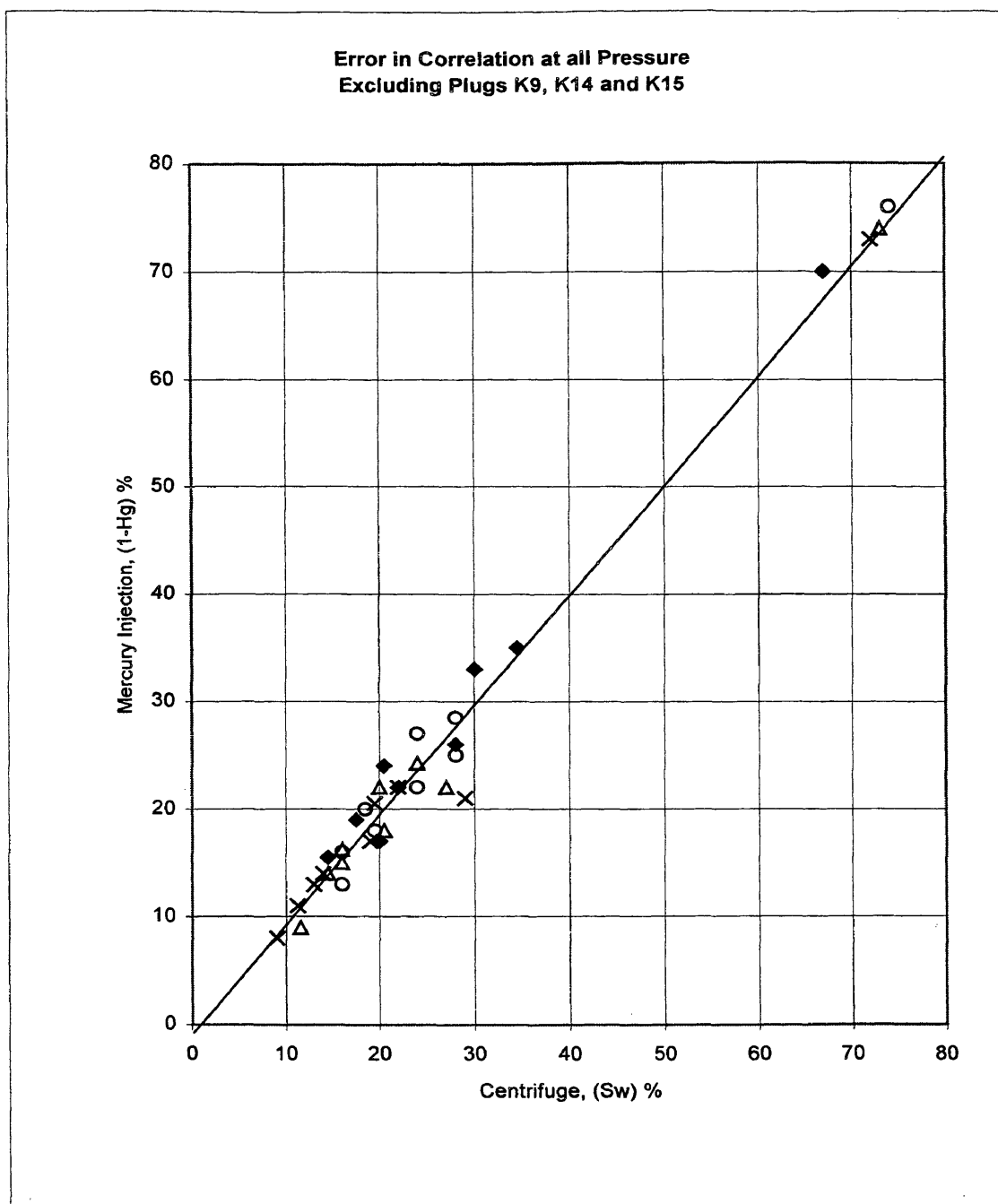


Figure E-5 Accuracy Plot at All Pressure

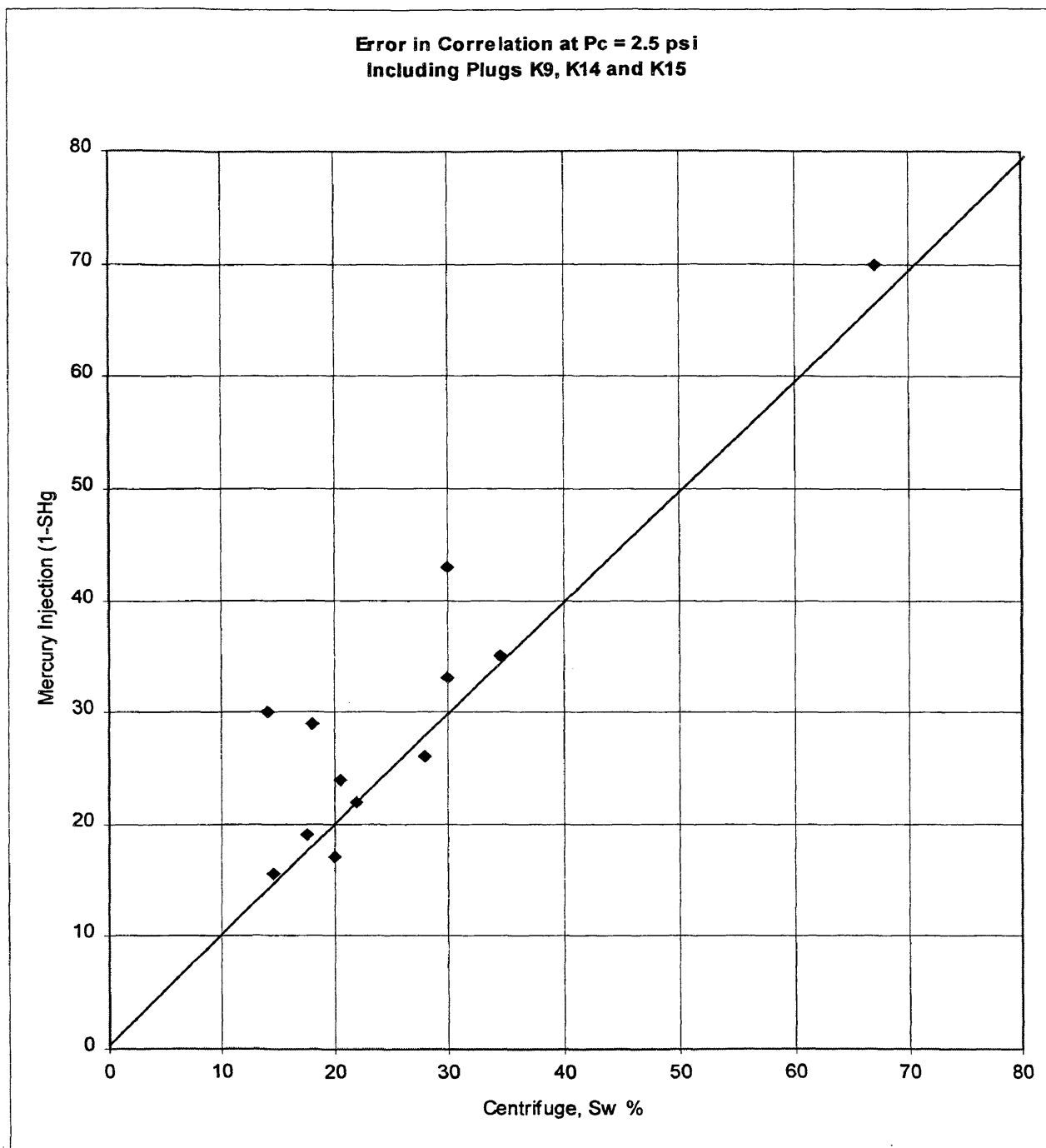


Figure E-6 Accuracy Plot at 2.5 psi

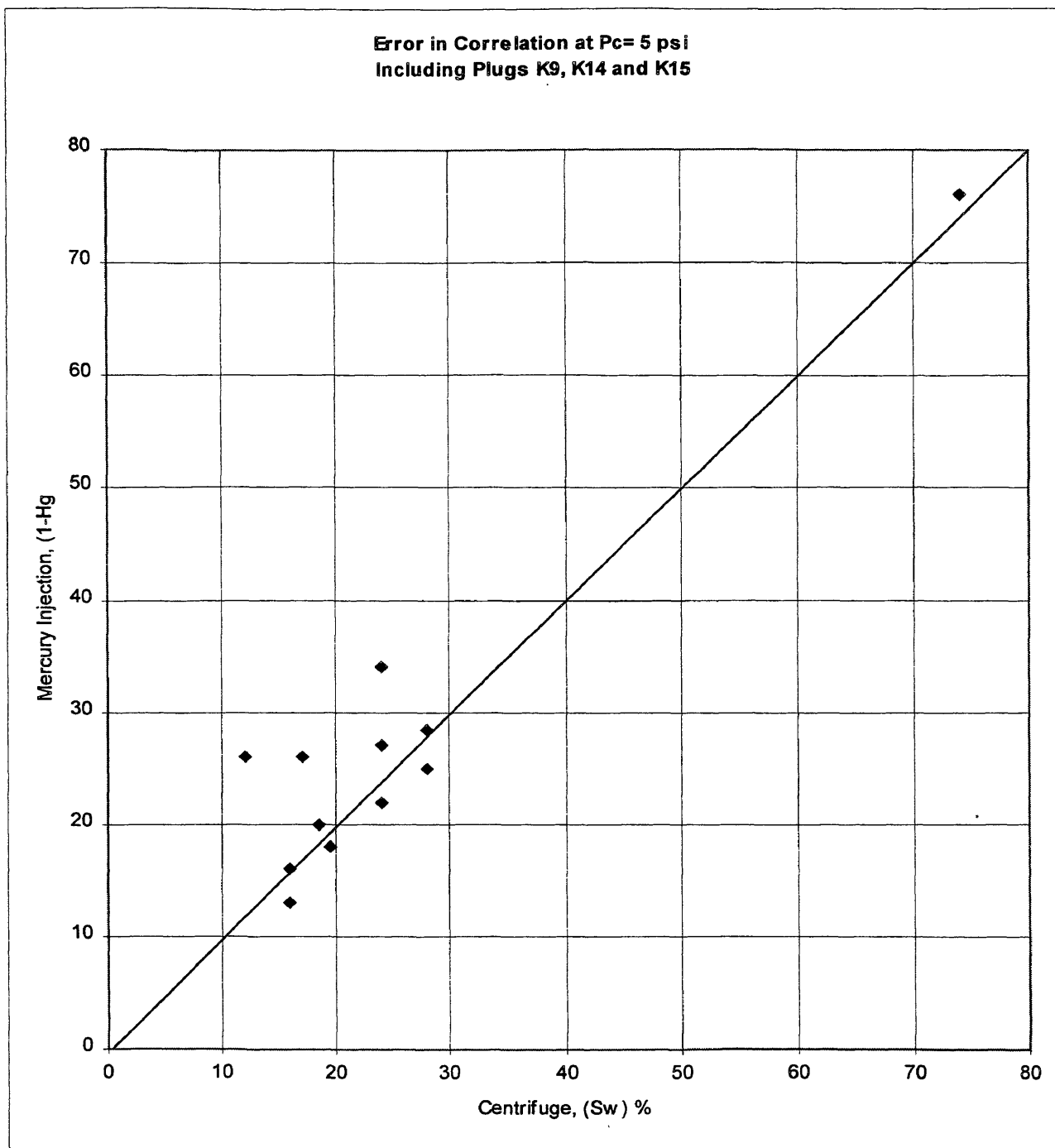


Figure E-7 Accuracy Plot at 5 psi

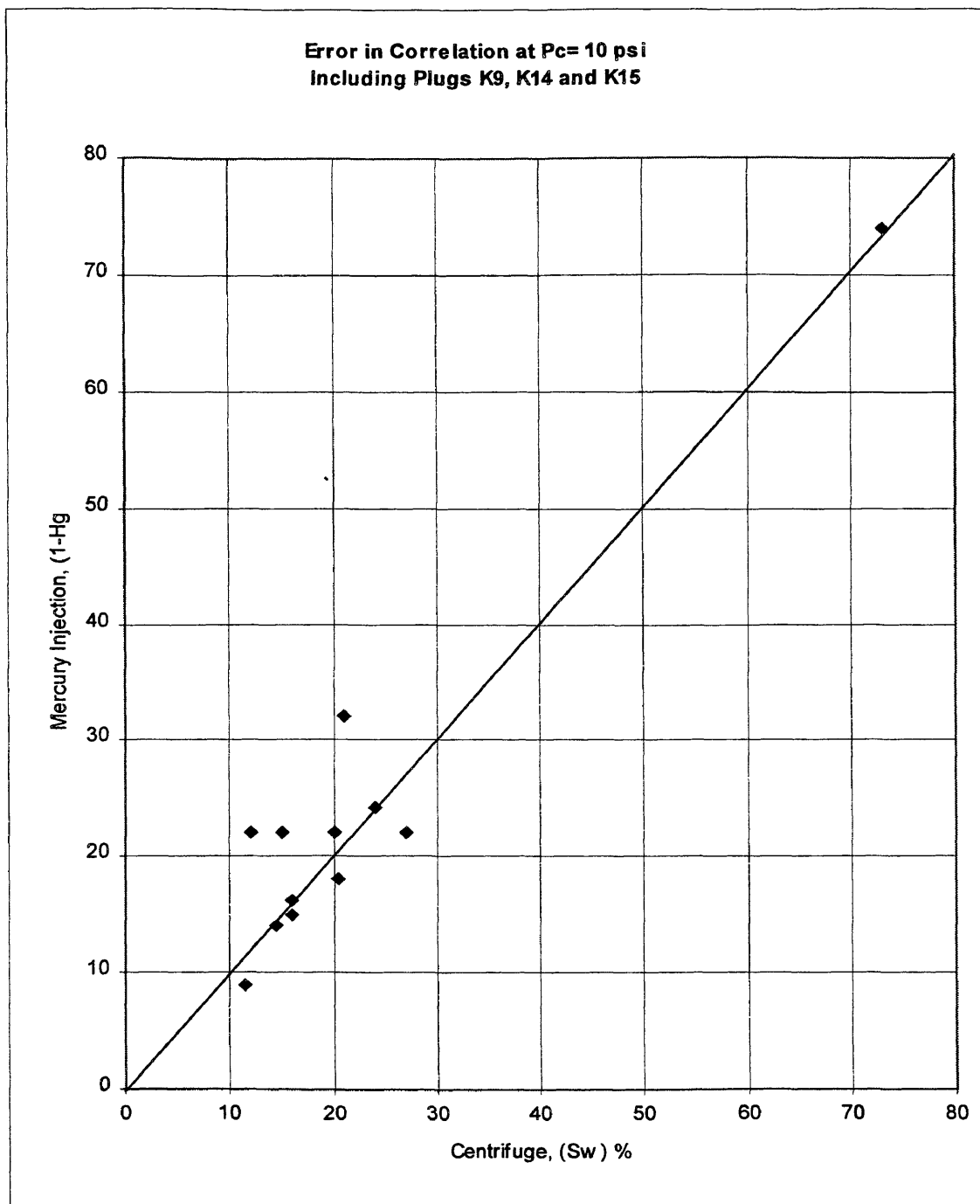


Figure E-8 Accuracy Plot at 10 psi

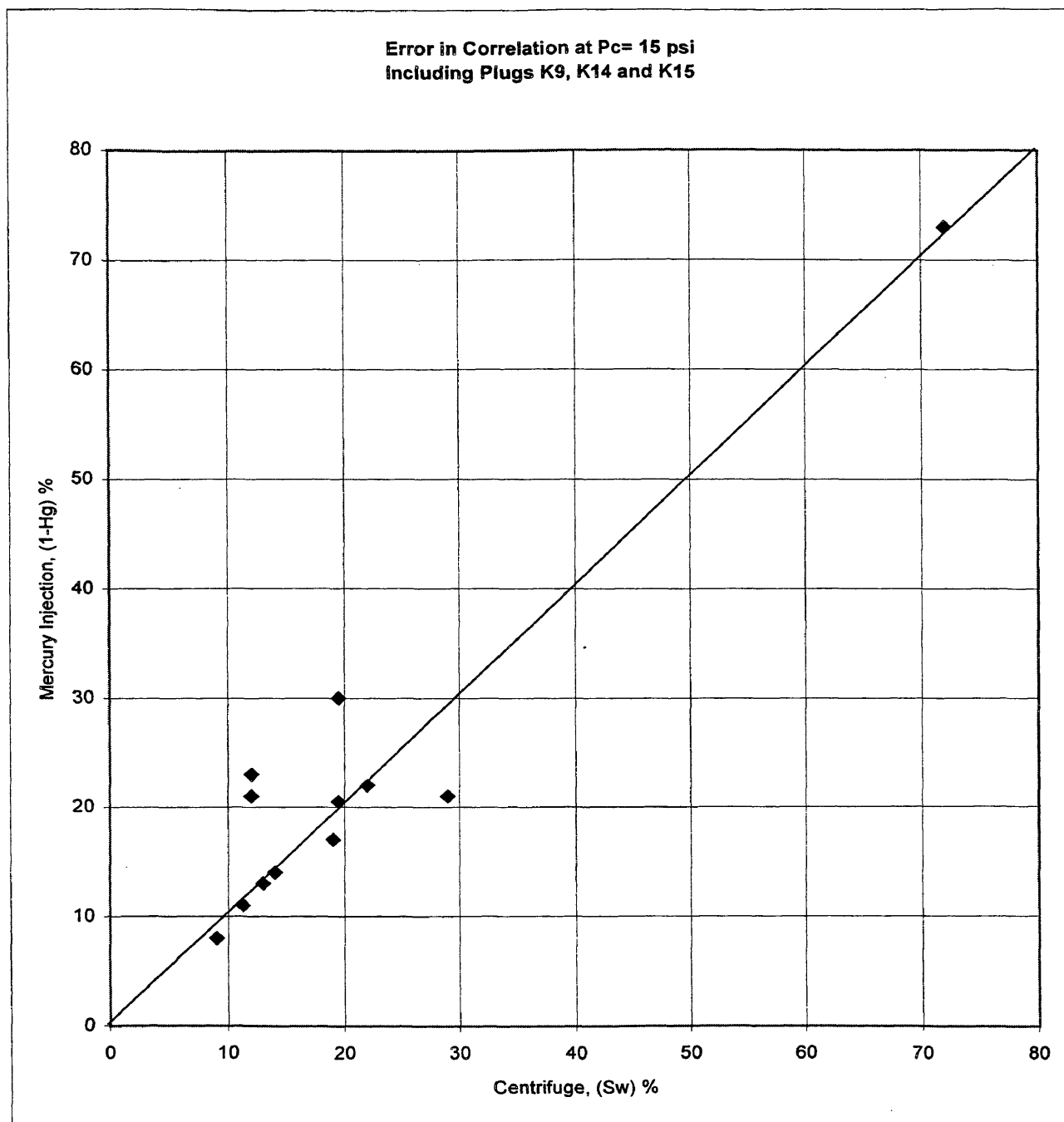


Figure E-9 Accuracy Plot at 15 psi

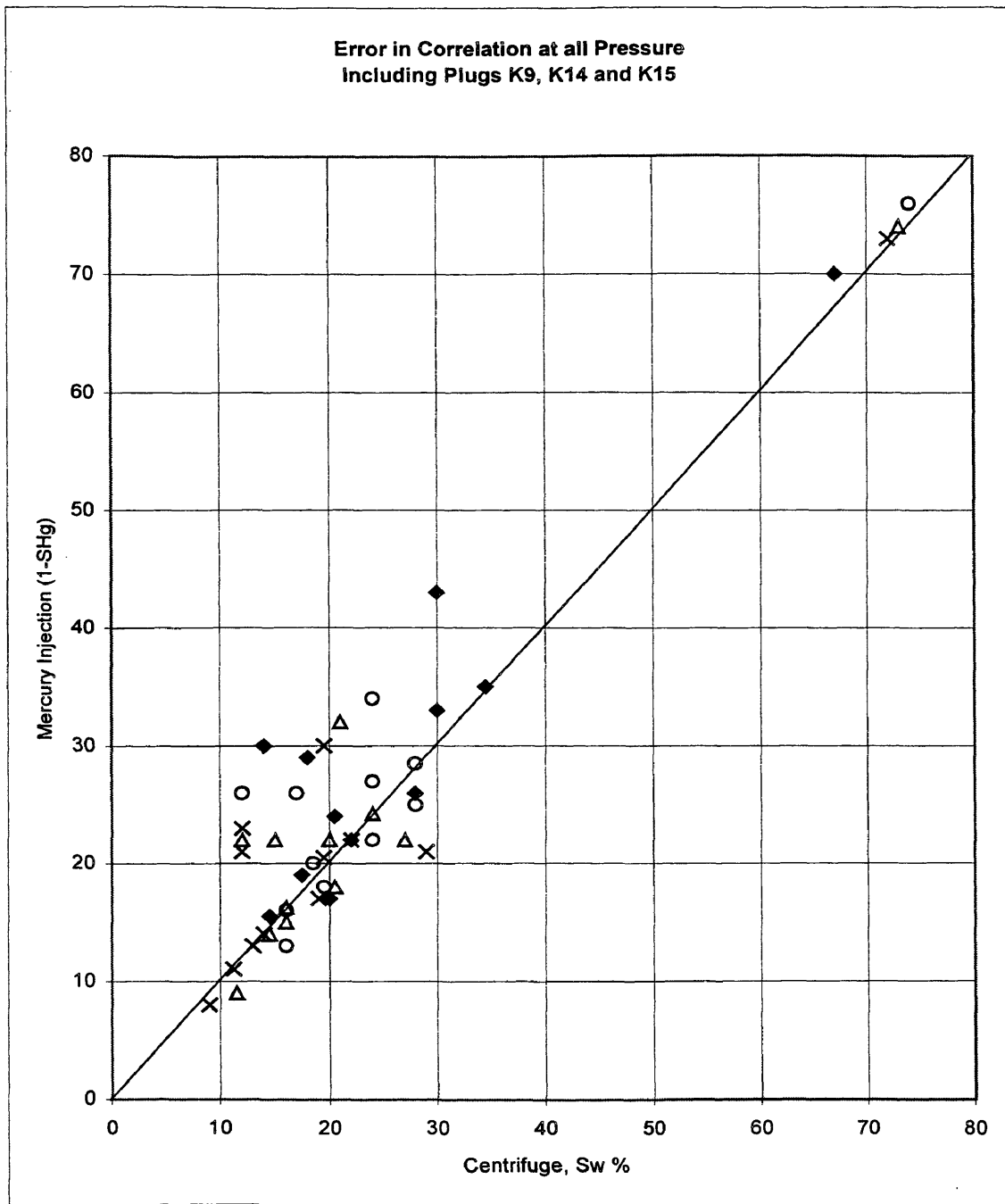


Figure E-10 Accuracy Plot at All Pressure